The author of the Ph.D. dissertation: **Mateusz Olszewski**

Scientific discipline: **Chemistry**

DOCTORAL DISSERTATION

Title of Ph.D. dissertation: Selected symmetrically substituted carbazoles: Investigation of anticancer activity and mechanisms of action at the cellular and molecular levels

Title of Ph.D. dissertation (in Polish): Wybrane symetrycznie podstawione karbazole: Badanie aktywności przeciwnowotworowej oraz mechanizmów działania na poziomie komórkowym i molekularnym

Supervisor
signature
Prof. Dr Eng. Maciej Bagiński

Gdańsk, year 2024

GDAŃSK UNIVERSITY OF TECHNOLOGY

FACULTY OF CHEMISTRY

STATEMENT

The author of the Ph.D dissertation: Mateusz Olszewski

I, the undersigned, agree that my Ph.D dissertation entitled:

Selected symmetrically substituted carbazoles: Investigation of anticancer activity and mechanisms of action at the cellular and molecular levels
may be used for scientific or didactic purposes.[1]

Gdańsk, 15.02.2024 ....

signature of the PhD student

Aware of criminal liability for violations of the Act of 4th February 1994 on Copyright and Related Rights (Journal of Laws 2006, No. 90, item 631) and disciplinary actions set out in the Law on Higher Education (Journal of Laws 2012, item 572 with later amendments)[2], as well as civil liability, I declare, that the submitted PhD dissertation is my own work.

I declare, that the submitted PhD dissertation is my own work performed under and in cooperation with the supervision of Professor Maciej Bagiński.

This submitted PhD dissertation has never before been the basis of an official procedure associated with the awarding of a PhD degree.

All the information contained in the above thesis which is derived from written and electronic sources is documented in a list of relevant literature in accordance with art. 34 of the Copyright and Related Rights Act.

I confirm that this PhD dissertation is identical to the attached electronic version.

Gdańsk, 15.02.2024 ....

signature of the PhD student

I, the undersigned, agree to include an electronic version of the above PhD dissertation in the open, institutional, digital repository of Gdańsk University of Technology, Pomeranian Digital Library, and for it to be submitted to the processes of verification and protection against misappropriation of authorship.

Gdańsk, 15.02.2024 ....

signature of the PhD student

---

[1] Decree of Rector of Gdansk University of Technology No. 34/2009 of 9th November 2009, TUG archive instruction addendum No. 8.

[2] Act of 27th July 2005, Law on Higher Education: Chapter 7, Criminal responsibility of PhD students, Article 226.

GDAŃSK UNIVERSITY OF TECHNOLOGY

FACULTY OF CHEMISTRY

DESCRIPTION OF DOCTORAL DISSERTATION

The Author of the Ph.D dissertation: Mateusz Olszewski

Title of PhD dissertation: Selected symmetrically substituted carbazoles: Investigation of anticancer activity and mechanisms of action at the cellular and molecular levels

Title of Ph.D dissertation in Polish: Wybrane symetrycznie podstawione karbazole: Badanie aktywności przeciwnowotworowej oraz mechanizmów działania na poziomie komórkowym i molekularnym

Language of PhD dissertation: English

Supervision: Maciej Bagiński

Date of doctoral defence:

Keywords of PhD dissertation in Polish: karbazole, leki, nowotwór, topoizomerazy

Keywords of PhD dissertation in English: carbazoles, cancer, drugs, topoisomerases

Summary of Ph.D dissertation in Polish:

Topoizomerazy DNA odgrywają kluczową rolę jako niezbędne enzymy kontrolujące zmiany w topologii DNA. Osiągają to, kierując zorganizowanym procesem przerywania i ponownego łączenia nici DNA, co jest istotne dla utrzymania właściwej struktury DNA podczas regularnego rozwoju komórek.

Poszukiwanie i rozwijanie nowych potencjalnych leków przeciwnowotworowych jest trudnym, ale niezwykle istotnym obszarem badań, który może przyczynić się do znaczącego postępu w leczeniu i zwalczaniu chorób nowotworowych. W zakresie mojej pracy doktorskiej przeprowadzono badania nad trzema heterocyklicznymi związkami będącymi pochodnymi karbazolu, celem zidentyfikowania ich przeciwnowotworowego mechanizmu działania. Badania wykazały, że te związki działają jako nieinterkalujące z DNA inhibitory ludzkiej topoizomerazy I i IIα. Stwierdzono, że spośród trzech badanych związków, **36a** wykazywał znacznie wyższą aktywność hamującą wobec izoformy topoizomerazy IIα niż IIβ. Dodatkowo, określono ich właściwości cytotoksyczne i antyproliferacyjne, zdolność do hamowania białkowych kinaz tyrozynowych oraz zidentyfikowano rodzaj indukowanej śmierci komórkowej. Przeprowadzone eksperymenty umożliwiły wyodrębnienie głównych mechanizmów działania tych przeciwnowotworowych związków, co może w przyszłości przyczynić się do projektowania i syntezowania nowych potencjalnych kandydatów na leki.

Summary of PhD dissertation in English:

DNA topoisomerases play a critical role as essential enzymes in controlling alterations in the topology of DNA. They achieve this by orchestrating the coordinated process of breaking and rejoining DNA strands, which is crucial for maintaining the proper structure of DNA during regular cellular development.

The search for and development of new potential anticancer drugs is a challenging yet immensely important area of research that can contribute significantly to advancements in the treatment and combat of cancer-related diseases. In the scope of my doctoral work, research was conducted on three heterocyclic compounds derived from carbazole, aiming to identify their anticancer mechanism of action. The studies demonstrated that these compounds act as non-intercalating DNA inhibitors of human topoisomerase I and IIα. Among the three investigated compounds, **36a** exhibited notably higher inhibitory activity against the IIα isoform compared to IIβ. Additionally, their cytotoxic and antiproliferative properties were determined, along with their ability to inhibit tyrosine protein kinases and induce cell death. The conducted experiments allowed to determine the main mechanisms of action of these anticancer compounds, which could in the future contribute to the design and synthesis of new potential drug candidates.

I would like to express my sincere gratitude to everyone who provided support throughout my entire PhD journey.

TABLE OF CONTENTS

ABBREVIATIONS

7-AAD	-7-aminoactinomycin D
AIF	-Apoptotic inducing factor
AML	-Acute myeloid leukaemia
ATP	-Adenosine triphosphate
BAX	-BCL-2-associated X protein
BAK	-BCL-2 antagonist killer
BCL-2	-B-cell lymphoma *2*
BID	-BH3 interacting-domain death agonist
BrdU	-Bromodeoxyuridine
CADD	-Computer-aided drug design
CDKs	-Cyclin-dependent kinases
COX-1	-Cyclooxygenase-1
COX-2	-Cyclooxygenase-2
CPT	-Camptothecin
DDR	-DNA damage response
DOXO	-Doxorubicin
EMA	-European Medicines Agency
ETP	-Etoposide
FDA	-Food and Drug Administration
FBDD	-Fragment-based drug design

MOST WIEDZY Downloaded from mostwiedzy.pl

G-segment -	-DNA Gate-segment
GyrA	-A-subunit of DNA gyrase
GyrB	-B-subunit of DNA gyrase
HIV	-Human Immunodeficiency Virus
HDAC	-Histone deacetylases
HPV	-Human papillomavirus
HMEC	-Human mammary epithelial cells
HTS	-High-Throughput Screening
IC_{50}	-50% inhibitory concentration
m-Amsa	-m-Amsacrine
mPTP	-Mitochondrial permeability transition pore
MOMP	-Mitochondrial outer membrane potential
NAC	-N-acetylcysteine
NAD+	-Nicotinamide adenine dinucleotide
NADH	-Nicotinamide adenine dinucleotide + Hydrogen
NSAID	-Non-steroidal anti-inflammatory drug
NSCLC -	-Non-small cell lung cancer
NHBE	-Normal human bronchial epithelial cells
PFA	-Paraformaldehyde
PDGFR	-Platelet-derived growth factor receptor
PI	-Propidium iodide

PKC   -Protein kinase C

PTKs   -Protein tyrosine kinases

PTKI   -Protein tyrosine kinase inhibitor

QSAR   -Quantitative structure-activity relationship

ROS   -Reactive oxygen species

rDNA   -Ribosomal DNA

SAR   -Structure-activity relationship

SD   -Standard deviation

SDS   - Sodium dodecyl sulphate

TBE   -Tris/Borate/EDTA

T-segment   -Transport-segment

Topo   -Topoisomerase

Topo cc   -Topoisomerase cleavage complex

TUNEL   -Terminal deoxynucleotidyl transferase dUTP nick end labelling

UFB   -Ultra-fine anaphase bridge

VEGF   -Vascular endothelial growth factor

VEGFR2   -Vascular endothelial growth factor receptor 2

ΔΨM   -Mitochondrial membrane potential

1. INTRODUCTION

1.1 Confronting cancer: a global challenge and methods of treatment

Cancer, one of the most devastating diseases known to humanity, continues to present a significant challenge to societies worldwide. Its impact is profound, affecting individuals, families, and healthcare systems, demanding relentless efforts to understand its complex nature and develop effective strategies for prevention, diagnosis, and treatment [1,2]. As shown in **Figure 1**, cancer exhibits various features, including the anomalous and unregulated proliferation of cells within the body. This disease can impact almost any organ or tissue and possess the capacity to invade neighbouring structures or metastasize to distant parts of the body [3]. The development of cancer is attributed to a combination of genetic and environmental factors usually related with age. Genetic mutations or changes in DNA can disrupt the normal cell cycle, leading to uncontrolled cell growth. Risk factors for developing cancer can be heightened by environmental elements such as tobacco smoke, exposure to specific chemicals or toxins, radiation, infections, as well as lifestyle factors including an unhealthy diet, insufficient physical activity, and excessive alcohol consumption [4,5]. The manifestations of cancer may differ based on the specific type and stage of the condition. Typical signs encompass inexplicable weight loss, fatigue, discomfort, alterations in the skin, persistent cough or hoarseness, and abnormal lumps or growths [6].
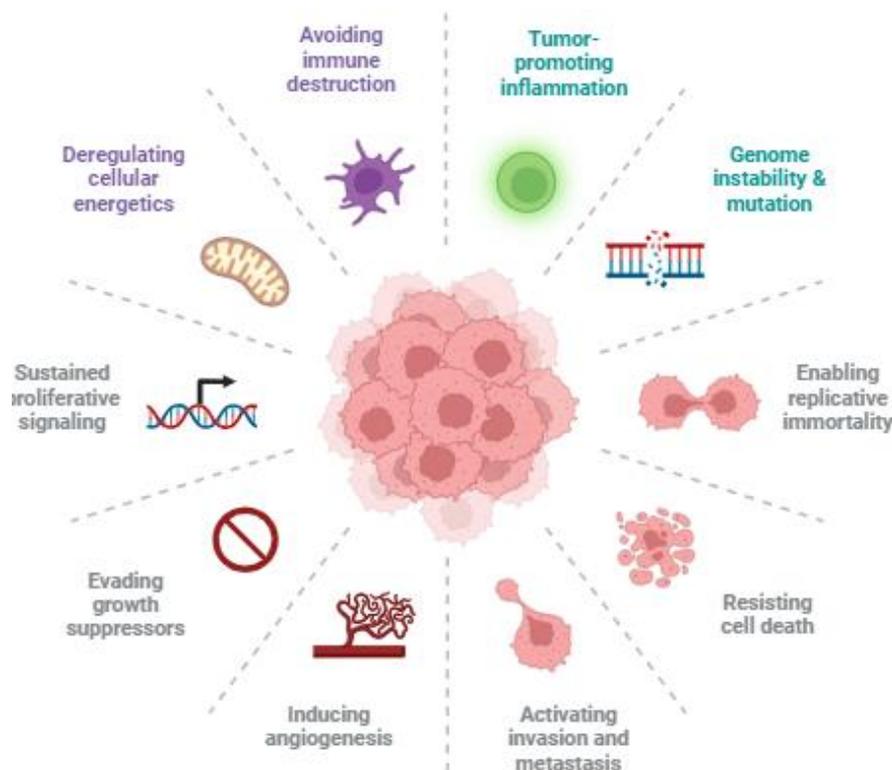
Figure 1 Characteristics of cancer cell [5].

As a global health concern, cancer affects millions of lives, requiring interdisciplinary research and innovation to address its multifaceted aspects. The global burden of cancer is staggering, with an ever-increasing incidence and mortality rate. According to the Globocan (a database prepared by the International Agency for Research on Cancer, Global Cancer Observatory) report of 2020, an estimated 19.3 million new cancer cases and about 10 million cancer-related deaths occurred worldwide in that year alone [7]. According to the data presented in **Figure 2**, the projected number of cancer cases and deaths indicates a significant increase in incidence, estimated to be over 30 million cases, and a high rate of over 16 million deaths by the year 2040 [7]. While breast cancer, lung cancer, colorectal cancer, prostate cancer, and skin cancer are among the most common forms, numerous other types can affect various organs and systems in the body. These alarming statistics highlight the urgent need for effective prevention, early detection, and treatment strategies to address this escalating global health crisis [7–9].

The economic and social consequences of cancer are far-reaching, exerting significant strain on healthcare resources, impairing productivity, and impacting the overall well-being of individuals and communities. Addressing the challenges posed by cancer requires a comprehensive and collaborative approach, with continued research, innovation, and international cooperation. By striving for improved prevention, early diagnosis, and effective treatments, we can make progress in reducing the burden of cancer and improving outcomes for those affected by this devastating disease [10].
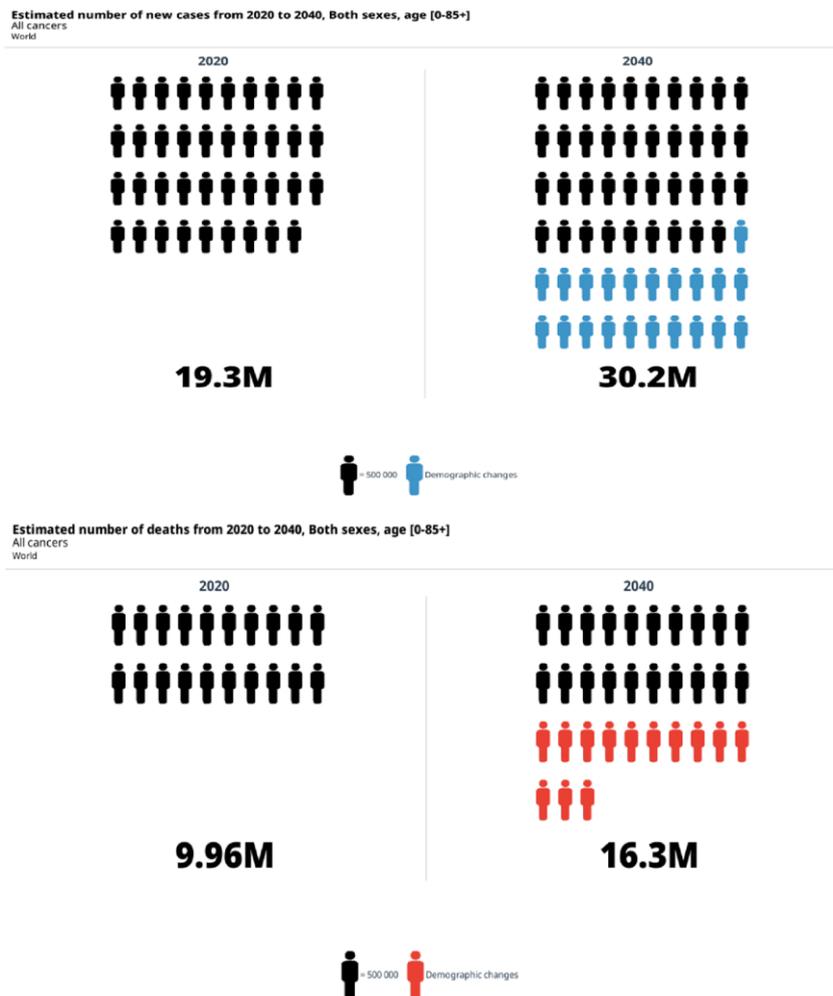
Figure 2 Estimated number of new cases and deaths from 2020 to 2040 in accordance with GLOBOCAN 2020 report [7].

Early detection of cancer is crucial for better treatment outcomes, as it allows for timely intervention and management. The choice of cancer treatment strategies relies on diverse factors, encompassing the type and stage of cancer, along with individual patient characteristics. Common therapeutic methods comprise surgery, chemotherapy, radiation therapy, targeted therapy, immunotherapy, and hormone therapy. Recent advancements in precision medicine and personalized therapies have revolutionized cancer treatment, enabling more tailored approaches based on specific molecular characteristics of tumours [11]. Nevertheless, prevention plays a crucial role in reducing the burden of cancer. Embracing a health-conscious lifestyle, which involves consistent exercise, a well-balanced diet, refraining from tobacco and excessive alcohol intake, and taking precautions against excessive sun exposure, can markedly reduce the likelihood of developing specific types of cancer [12]. Additionally, vaccination against cancer-associated viruses, such as human papillomavirus (HPV) and hepatitis B virus (HBV), can prevent infection and reduce the risk of related cancers

[13,14]. Cancer research continues to drive progress in understanding the underlying mechanisms of cancer, developing new treatment strategies, and improving early detection and prevention methods. Collaboration between researchers, healthcare professionals, policymakers, and patients is essential in the ongoing fight against cancer, aiming for better outcomes for those affected by this disease.

1.2 Unveiling novel anticancer agents

The search for new anticancer agents remains a significant challenge for many scientists. Nevertheless, new strategies, such as immunotherapy and hormone therapies, are very promising [11]. While their development is progressing, their cost is still too high for broader applications and not applicable to all types of cancer. Therefore, classical chemotherapy, based on small molecules and typically used after surgical interventions, remains a valuable approach [15]. However, the development of new anticancer agents is a complex and critical research area focused on improving cancer treatment outcomes and addressing the challenges posed by this devastating disease. Anticancer agents are substances or compounds that target and inhibit the growth of cancer cells, aiming to destroy them or prevent further proliferation [15]. The process of developing new anticancer drugs involves several key stages. It begins with the identification of specific molecular targets that play a crucial role in cancer cell growth and survival. These targets can be proteins, enzymes, receptors, or signalling pathways that are abnormally activated or dysregulated in cancer cells. Once the targets are identified, researchers employ various approaches to discover or design compounds that can interact with and modulate these targets. This includes screening large libraries of chemical compounds, utilizing computer-aided drug design, and exploring natural sources such as plants, marine organisms, or microorganisms for potential lead compounds [16]. Promising lead compounds then undergo extensive preclinical testing in laboratory settings and in animal models. These tests evaluate their efficacy, safety, pharmacokinetics (absorption, distribution, metabolism, and excretion - ADME), and toxicology profiles [16]. The results help researchers select the most promising candidates for further development. If a lead compound demonstrates favourable preclinical results, it progresses to clinical trials, where it is tested in human subjects [17,18].

Clinical trials are conducted in multiple phases, involving increasing numbers of patients to assess safety, efficacy, optimal dosage, and potential side effects [19]. Regulatory authorities closely monitor these trials to ensure patient safety and ethical considerations. Upon successful completion of clinical trials, comprehensive data is submitted to regulatory authorities such as the FDA or EMA for review [19]. If the authorities are satisfied with the efficacy and safety profiles, they approve the new anticancer agent to be marketed and used in clinical

practice [20]. Once approved, the new anticancer agent undergoes post-marketing surveillance in real-world settings. This surveillance aims to identify any additional side effects or long-term safety concerns that may not have been apparent during clinical trials [21]. Ongoing monitoring ensures that the benefits of the drug outweigh any potential risks. Developing new anticancer agents is a complex, time-consuming process that requires significant financial investment. Not all candidate compounds successfully progress through each stage of development, with many failing to meet the desired efficacy or safety criteria [22]. However, despite these challenges, the development of new anticancer agents remains crucial. It offers the potential for more effective and targeted therapies, improved treatment outcomes, and a better quality of life for cancer patients. Continued efforts in this field are essential to meet the evolving needs of cancer treatment and ultimately reduce the global burden of this devastating disease.

1.2.1 Drug development strategies

The first phase in the process of drug development involves either discovering or designing a small, bioactive molecule that will be further developed [23]. The search for new drugs can be conducted through various diverse methods. Practically, each research team develops its own strategy over time for drug discovery. Such a strategy typically involves the sequential application of several standard techniques. The individual strategies primarily differ in the emphasis placed on specific techniques [24]. Moreover, some drugs have been discovered through "blind luck" [25].

Screening

Screening in drug discovery refers to the process of testing a large number of chemical compounds or biological substances to identify potential candidates with therapeutic activity against a specific target. It is a crucial early stage in the drug development pipeline and involves various techniques and approaches to identify promising hit compounds for further optimization and development into potential drugs [26].
There are two main types of screening methods used in drug discovery:

<u>High-Throughput Screening</u>

High-Throughput Screening (HTS) is a drug discovery experimental technique that rapidly tests thousands of chemical compounds against biological targets [27]. It allows for the identification of potential drug candidates from large compound libraries in a time-efficient and cost-effective manner [28] HTS plays a crucial role in the early stages of drug development by quickly identifying compounds with promising interactions with specific targets, which can then be further optimized and tested for their therapeutic potential [28].

14

Phenotypic Screening

Unlike HTS, which focuses on a specific target, phenotypic screening assesses the compounds' effects on whole cells or organisms. In this approach, compounds are tested for their ability to induce a desired therapeutic effect or correct a disease phenotype [29]. Phenotypic screening is especially valuable when the exact molecular target is unknown or when the disease is complex and involves multiple factors [30]. It allows researchers to identify compounds with desirable biological activity, even if the mode of action is not fully understood yet [30].

Computer-aided drug design

Computer-aided drug design (CADD) is a pivotal strategy in modern drug design and development process. Currently, applied in most cases when the target is known [31]. It utilizes computational techniques to model and analyse interactions between potential drugs and their targets, such as proteins or nucleic acids [32]. CADD encompasses molecular docking, virtual screening (virtual HTS screening), QSAR analysis, pharmacophore modelling, and molecular dynamic simulations [33]. By accelerating the identification of promising drug candidates and streamlining the drug development process, CADD plays a vital role in advancing medicine and reducing costs [34]. *In silico* approaches in general two methods are applied.

Structure-based drug design

Structure-based drug design (SBDD) involves screening a library of small, low-molecular-weight compounds for their ability to bind to a target of interest [35]. The molecular structure of the target is known. These structures of ligands are typically simple chemical entities. The goal is to find small molecule that binds specifically to a target and forms the basis (a hit molecule) for the development of more complex drug-like molecules [36]. These structures/ligands in SBDD can be design using fragment based drug design or virtual HTS technology [37].

Ligand-based drug design

Ligand-based drug design relies on the knowledge of known ligands (compounds that bind to a target) and their structure-activity relationships (SAR) [38]. It doesn't require prior knowledge of the target's structure [39]. Usually the molecular structure of the target is not known. It focuses on optimizing and designing new compounds based on the properties and characteristics of existing ligands known to interact with the target [39].

In practice, these approaches are often used in combination. SBDD can identify initial hits, and then ligand-based methods can be used to optimize these hits into more potent lead

compounds [40]. Ligand-based methods can also be used when there's an abundance of ligand data but limited structural information about the target [41]. The ultimate goal of both approaches is to design small molecules with desired pharmacological properties for use as potential drugs [42].

<u>Scaffold hopping strategy</u>

The goal of the "scaffold hopping" approach is to discover new structurally related compounds (usually related isosterically) starting from the active scaffold of known compounds [43]. The term "scaffold" plays a crucial role in medicinal chemistry and drug design, serving as a tool for creating, analyzing, and comparing the central structures of active compounds and analog series [44]. In computational analysis, a prevalent approach involves a hierarchical definition of scaffolds, which entails deriving scaffolds from compounds by eliminating substituents [45]. This allows the retention of the core structure, usually ring systems and linker fragments between the rings. As a result, any compound containing a ring can convey its scaffold, and adding a ring to a compound (which can be considered a substituent group) always generates a new scaffold [46,47]. Scaffold hopping originates from computational and virtual compound selection in chemistry and refers to the search for compounds that exhibit similar activity but contain different core structures [48]. In addition to activity, other molecular properties can also be considered when searching for new compounds. Therefore, the main goal of scaffold hopping is to identify structurally diverse compounds that are similar to each other in terms of 3D structure and activity or properties [49]. Modifications or replacements of the core structure for specific groups of compounds can be made based on chemical knowledge, but finding scaffold cores requires performing calculations using molecular modelling techniques [50].

1.3 Harnessing the potential of carbazole scaffold-based compounds

Carbazole scaffold, similar to the acridine, anthraquinone, thiazole, or quinolone groups, functions as a central core for modification, enabling the synthesis of a diverse array of biologically active compounds [51–53]. The carbazole scaffold has emerged as a focal point in anticancer research, thanks to its remarkable biological potential and promising anticancer properties [54]. Marked by a tricyclic structure composed of two fused benzene rings and a nitrogen-substituted five-membered ring (**Figure 3**), the carbazole scaffold assumes a pivotal role in the creation of a diverse array of biologically active compounds. This includes both natural and synthetic anticancer agents [55,56]. The main reason is that planar rings can effectively serve as a scaffold and platform for attaching various substituents.

16
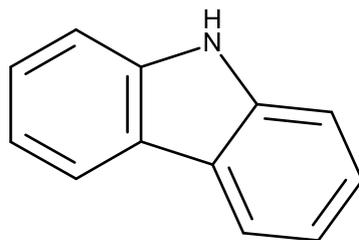
Figure 3 Chemical structure of carbazole scaffold [55].

Numerous studies have unveiled the anticancer potential of carbazole-based compounds, revealing a multitude of mechanisms through which they exert their effects. Foremost among these is the induction of apoptosis in cancer cells. Carbazoles can activate various apoptotic pathways, such as the activation of caspases [57], disruption of mitochondrial function [58], and modulation of Bcl-2 family proteins [59], ultimately leading to the death of cancer cells. Furthermore, carbazole-based compounds demonstrate antiproliferative effects by impeding cell cycle progression. By interfering with the activity of cyclin-dependent kinases (CDKs), which play a pivotal role in regulating the cell cycle, carbazoles prompt cell cycle arrest, effectively impeding the proliferation and division of cancer cells [60]. Intriguingly, carbazoles have also shown potential as potent anti-angiogenic agents. As angiogenesis, the formation of new blood vessels to supply tumours is a critical process for tumour growth and metastasis, the ability of carbazole-based compounds to disrupt angiogenesis holds immense therapeutic value [61]. By targeting key molecular pathways involved in blood vessel formation, such as vascular endothelial growth factor (VEGF) signalling, carbazoles exhibit the ability to inhibit angiogenesis, depriving tumours of their necessary blood supply [61,62]. Moreover, carbazole derivatives have emerged as promising inhibitors of vital enzymes implicated in cancer progression, including topoisomerases [63], protein kinases [64], and histone deacetylases (HDACs) [37]. By inhibiting these enzymes, carbazole derivatives effectively modulate cellular signalling pathways and epigenetic regulation, ultimately suppressing cancer cell growth and survival [66].

The biological potential of the carbazole scaffold in anticancer research is undoubtedly promising. Its ability to induce apoptosis, inhibit cell proliferation, disrupt angiogenesis, and target key enzymes involved in cancer progression positions it as an exciting avenue for the development of novel anticancer agents [67]. However, further research is imperative to fully comprehend the specific mechanisms of action and optimize the therapeutic potential of new carbazole-based compounds for effective anticancer treatments.

1.4 Scaffold hopping employing a carbazole moiety

Carvedilol, primarily employed in the treatment of hypertension (high blood pressure) and heart failure, is a drug derived from carbazole [68] (**Figure 4**). It falls within the category of medications known as beta-blockers. Its mechanism involves inhibiting the effects of specific naturally occurring substances in the body, such as epinephrine, particularly on the heart and blood vessels. This helps to lower blood pressure, reduce the workload on the heart, and improve its ability to pump blood effectively [69]. Carvedilol exhibits also anti-apoptotic, anti-inflammatory, and antioxidant properties within the heart [70,71]. When combined with thyroid hormones following an acute myocardial infarction, it effectively reduces oxidative stress and can be employed to modify cardiac function [72]. A noteworthy aspect of carvedilol is its antibacterial activity, particularly against strains such as *Staphylococcus aureus* and *Staphylococcus epidermidis* [73]. Additionally, carvedilol, when administered alongside venlafaxine, is utilized to address testicular impairment in patients with longstanding rheumatoid arthritis [74].
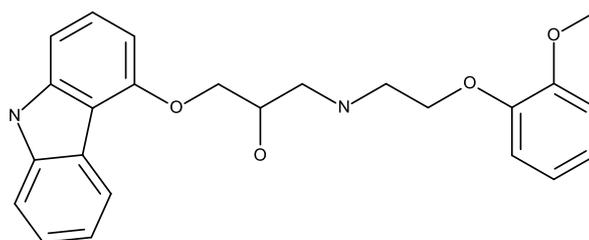
Figure 4 Chemical structure of carvedilol [75].

BMVC (3,6-bis(1-methyl-4-vinylpyridinium)carbazole diiodide), illustrated in **Figure 5**, serves as an exemplary telomerase inhibitor derived from carbazole. Its mechanism of action involves the suppression of telomerase activity, inducing senescence in cancer cells, ultimately leading to tumour degradation [76]. Most of the research focuses on BMVC's role as a G-quadruplex interacting ligand, facilitating interactions with various nucleic acid forms and stabilizing the G-quadruplex structure [77]. Distinguishing itself from other telomerase inhibitors, BMVC led to a notable acceleration in telomere shortening within tumour cells, resulting in a reduction in growth rate before entering the aging phase [78]. Furthermore, BMVC effectively suppressed the neoplastic characteristics of cancer cells, including cell migration, colony formation, and anchorage-independent growth [79,80].
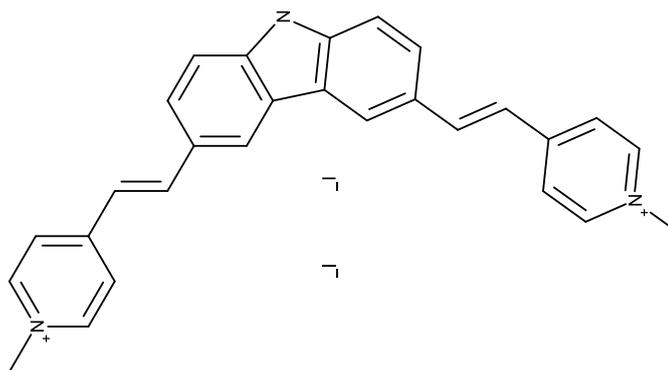
Figure 5 Chemical structure of BMVC [76].

Carprofen (**Figure 6**), classified as a non-steroidal anti-inflammatory drug (NSAID) belonging to the carbazole and propionic acid class, was initially approved for both human and animal use [81]. However, it is now exclusively prescribed by veterinarians as a supportive treatment for various animal-specific conditions [82]. This agent functions by reducing inflammation through the inhibition of COX-1 and COX-2 enzymes, although its selectivity for COX-2 can vary among different species [81]. Carprofen is available under numerous brand names globally and serves as a routine treatment for managing pain and inflammation related to various forms of joint discomfort, as well as post-operative pain in animals [83].
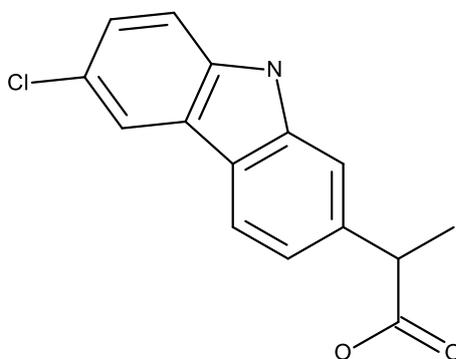
Figure 6 Chemical structure of carprofen [84].

Staurosporine (**Figure 7**), first isolated from *Streptomyces staurosporeus*, had its precise molecular structure unveiled through crystallography in 1994 [85]. This compound belongs to the indolocarbazole class and exhibits a bi-indole structure. Currently, staurosporine and its derivatives continue to be subjects of ongoing research and development in the quest to discover new drugs and therapies for various diseases, including cancer [86]. Staurosporine, as a representative indolocarbazole, functions as a multikinase inhibitor [87]. It competes with ATP for binding to relevant kinases [88]. However, a notable limitation of staurosporine is its lack of specificity. Therefore, there is a need to modify staurosporine to enhance its selectivity [85,89].
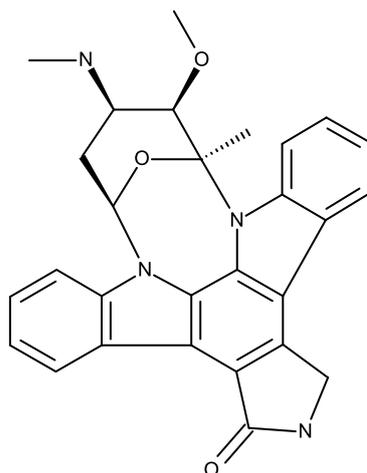
Figure 7 Chemical structure of staurosporine [85].

1.5 Carbazoles applied in the field of cancer treatment

The exploration of carbazoles' potential antitumour activity commenced with the discovery of ellipticin, isolated from the leaves of the tropical tree *Ochrosia elliptica Labill* in 1959 [90]. Subsequently, three carbazole-derivative anticancer drugs have made their way into the pharmaceutical market: celiptium, alecensa, and rydapt [56].

Celiptium (**Figure 8**) (N-methyl-9-hydroxyelipticin acetate) stands as the pioneering synthesized ellipticin analogue to secure approval as an anticancer drug [91]. Its mode of action involves stabilizing the topoisomerase II complex, leading to DNA breaks and subsequent inhibition of DNA, RNA replication, and protein synthesis [92]. Its anticancer properties have been reported as far back as the 1970s, and since then, it has been extensively studied, proving to be beneficial in treating metastatic breast cancer [93]. The low haematological toxicity of celiptium has rendered it a promising component in combination therapy for breast cancer, particularly in conjunction with vinblastine [94].
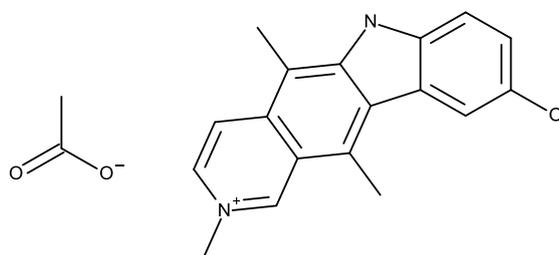
Figure 8 Chemical structure of celiptium [95].

Alectinib (**Figure 9**), commercially known as alecensa, represents the second approved carbazole derivative for cancer treatment [56]. The FDA granted its approval in 2015, followed by the EMA's approval in 2017 [96]. This drug is specifically used for treating advanced ALK-

MOST WIEDZY Downloaded from mostwiedzy.pl

positive (ALK-anaplastic lymphoma kinase) non-small cell lung cancer (NSCLC) [96]. Alecensa's mechanism of action involves blocking the activity of the ALK tyrosine kinase [96]. Abnormal forms of this enzyme, resulting from a defective gene, contribute to the proliferation of cancer cells. By inhibiting this enzyme, alecensa can slow down or halt tumour growth and even reduce its size [97].
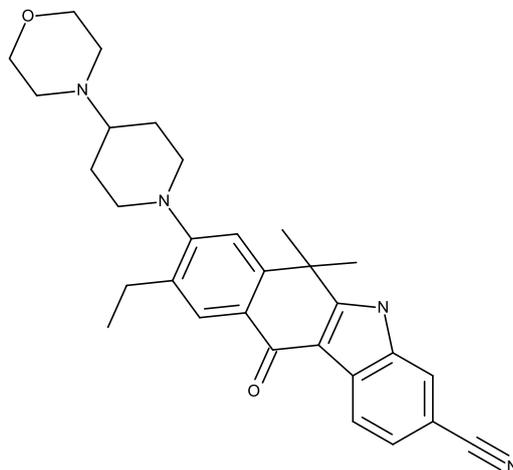
Figure 9 Chemical structure of alectinib [98].

Midostaurin (**Figure 10**), marketed as rydapt, is a third carbazole derivative recently approved by the FDA in 2017 and the EMA in 2018 [56]. It serves as a treatment for acute myeloid leukaemia (AML) with FLT3 gene mutation, aggressive systemic mastocytosis, systemic mastocytosis with associated haematological neoplasm or mast cell leukaemia [99]. The pharmacological action of midostaurin involves inhibiting various receptors with tyrosine kinase activity, notably FLT3 and KIT kinases [100]. By inhibiting the FLT3 receptor signalling pathway, it induces cell cycle arrest and apoptosis in leukemic cells expressing mutant FLT3 ITD or TKD receptors, as well as those overexpressing wild-type FLT3 receptors [99]. Additionally, midostaurin can block KIT signalling, leading to the suppression of mast cell multiplication, survival, and histamine release [100]. Furthermore, midostaurin exhibits inhibitory effects on other receptors with tyrosine kinase activity, including platelet-derived growth factor receptor (PDGFR) and vascular endothelial growth factor receptor 2 (VEGFR2), as well as certain members of the protein kinase C (PKC) family that belong to the serine-threonine kinases [100–102].

21
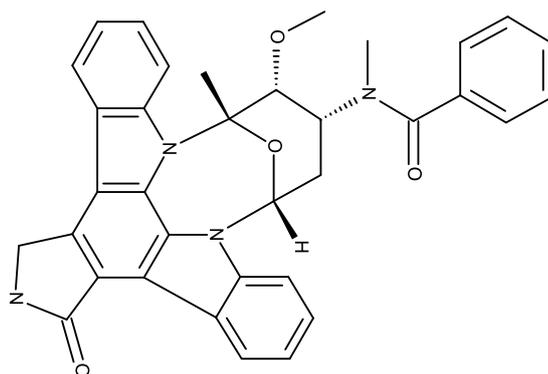
Figure 10 Chemical structure of midostaurin [101].

1.6 DNA topology

In light of the cellular effects elicited by the compounds under investigation in this doctoral thesis, following section of the introduction clarifies the information about the enzymes responsible for changes in DNA topology, along with their roles and functions in cancer cells.

The double-helical configuration of DNA involves the intertwining of two polynucleotide strands around each other, potentially giving rise to topological challenges. DNA topology pertains to the interweaving of the two DNA strands, altering the twist of the double helix and resulting in tertiary DNA conformations like supercoils, knots, and catenanes [103].

The consequences of topological disruptions in DNA become apparent during DNA replication, particularly when the two strands of the double helix are undergoing separation [104]. This strand separation results in the creation of positive supercoils, characterized by DNA overwinding or overtwisting, ahead of the replication fork. Simultaneously, the daughter strands become intertwined, forming structures known as precatenanes, behind the replication process [105]. Failure to relax positive supercoils hinders the progression of the replication fork, while the failure to unlink daughter strands prevents genome segregation necessary for cell division [106,107].

Transcription by RNA polymerase also induces positive supercoiling ahead of and negative supercoiling behind the transcriptional complex, a phenomenon known as the twin-supercoiled domain mode [108]. Resolving these topological perturbations is crucial for DNA metabolism to proceed, enabling the cell to efficiently replicate, transcribe, and partition the genome, facilitating cellular division and vitality [109]. Knots in DNA are encountered in bacteriophages and result from recombination reactions In general, DNA knots are detrimental and require removal by topoisomerases [110]. DNA catenanes form during the replication of circular molecules and need to be resolved by DNA enzymes to ensure the proper separation of daughter molecules during cell division [111].

22

To regulate torsional stress levels (underwinding or overwinding) in DNA or eliminate knots and tangles from the genetic material, it is necessary to break the DNA backbone [112,113]. Torsional stress can be managed through either DNA rotation or strand passage, allowing modulation of supercoiling levels by cleaving one or both strands of the double helix [114]. On the contrary, unraveling knots and tangles necessitates the generation of double-stranded DNA ends. These topological structures can only be resolved by inducing double-stranded breaks in the DNA backbone [115]. Topoisomerases are key enzymes that enable cells to address issues related to DNA topology [116].

1.7 Human topoisomerases

Topoisomerases constitute a highly conserved family of essential enzymes found in both prokaryotic and eukaryotic cells [117]. These enzymes have a crucial function in modifying the three-dimensional structure of DNA by engaging in processes such as relaxation, supercoiling, and decatenation, all of which are connected to the unwinding of complementary DNA strands (**Figure 11**) [118]. The human genome encodes six distinct topoisomerase (Topo) types (Topo 1, Topo1mt, Topo IIα, Topo IIβ, Topo IIIα, and Topo IIIβ), pivotal in inducing structural changes in both nuclear and mitochondrial DNA [115,119]. Their primary function is to relieve unwanted torsional stress that arises during processes like DNA replication or transcription [120]. Two discernible types of topoisomerases can be categorized based on the number of phosphodiester bonds they cleave [121].
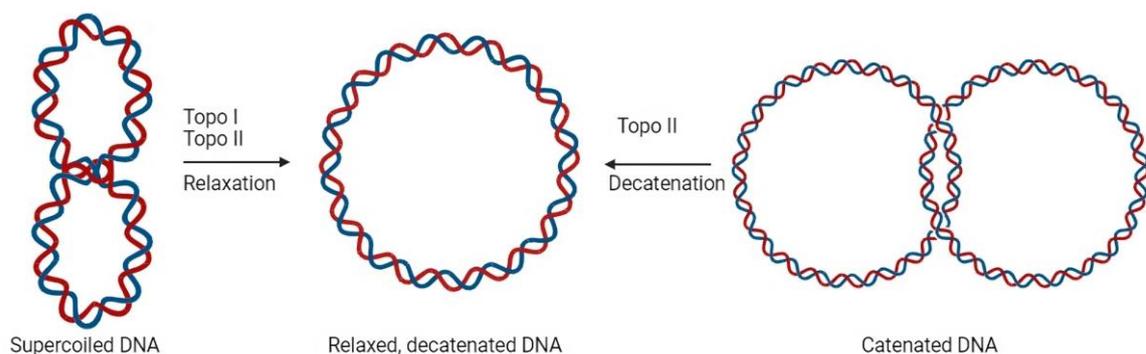
Figure 11 Processes involving DNA that are facilitated by Topo I and Topo II [122].

Type I topoisomerases facilitate the unwinding of DNA strands by temporarily cleaving the single-stranded DNA backbone and rotating it [123]. Topo I positively and negatively coil the DNA, forming a covalent bond with the 3'-phosphate to generate transient single-stranded breaks. In contrast, type II topoisomerases induce double-stranded breaks in the DNA double helix [124]. Topo I, initially identified in 1971, is a 100-kDa protein belonging to the type-I enzyme group

(type IB). It functions as an ATP-independent DNA single-strand endonuclease and ligase (**Table 1**), primarily involved in transcription but also participating in DNA replication [123,125].

On the other hand, Topo II belongs to the type-II enzyme category and is present in two highly similar isoforms in humans, α (170 kDa) and β (180 kDa) [126]. Unlike Topo I, both Topo II isoforms are ATP-dependent double-strand endonucleases and ligases (**Table 1**). While Topo I and the β-form of Topo II are expressed independently of cell proliferation, Topo IIα is regulated throughout the cell cycle [127].

Table 1 Key distinctions between human DNA Topo I and II.

Topo I	Topo II
100 kDa	170,180 kDa
ATP-independent	ATP-dependent
Genes located on chromosome 20q12	Genes located on chromosomes 17q21 and 3p24
Induces single-strand DNA breaks	Induces double-strand DNA breaks
One isoform	Two isoforms, α and β

In both cases, a transient connection forms between the enzyme and DNA, is named the Topo cleavage complex (Topo cc) [128]. These complexes are crucial for condensing chromatin, maintaining its structure, and assisting in the separation of sister chromatids [128]. Additionally, topoisomerases have the capability to detect pathological alterations in DNA structure, whether internal or external [129]. Due to the rapid proliferation of cancer cells, topoisomerases, taking into their function, have become significant targets for various anticancer drugs. These drugs aim to disrupt the essential functions of topoisomerases and have shown promise in cancer therapy [130].

1.7.1 Inhibitors of human Topo I

1.7.1.1 Camptothecins

Camptothecin (CPT) (**Figure 12**) was originally extracted from the bark of the Chinese tree, *Camptotheca acuminata*. Initial clinical trials in the mid-1970s exhibited anticancer potential for camptothecin carboxylate, but its use was halted due to side effects [131]. The

24

discovery that Topo I was the target of CPT led to the successful creation of water-soluble derivatives: topotecan and irinotecan (**Figure 12**) [132]. The unique pharmacological aspects of camptothecins are noteworthy [133]. Several drugs, including CPT, have the capability to transform Topo I into a poison that can harm cells by obstructing the religation process. This, in turn, amplifies the occurrence of enduring DNA fractures that are responsible for causing cell death [134].

The sole target of camptothecins is Topo I, confirmed in yeast cells rendered resistant to CPT when Topo I is removed [135]. Rapid penetration into vertebrate cells allows camptothecins to promptly target Topo I upon exposure [132]. The reversible binding of CPT to Topo I ccs enables precise control over drug exposure and trapping of Topo I ccs [136]. Despite these advantages, CPT and its derivatives have limitations [132]. Maintaining Topo I ccs long enough for conversion into DNA damage requires extended infusion due to the rapid diffusion of camptothecins from the complexes [137]. Moreover, side effects like leucopoenia restrict the safe dose of CPTs and consequently the effectiveness against tumours [135,138,139].
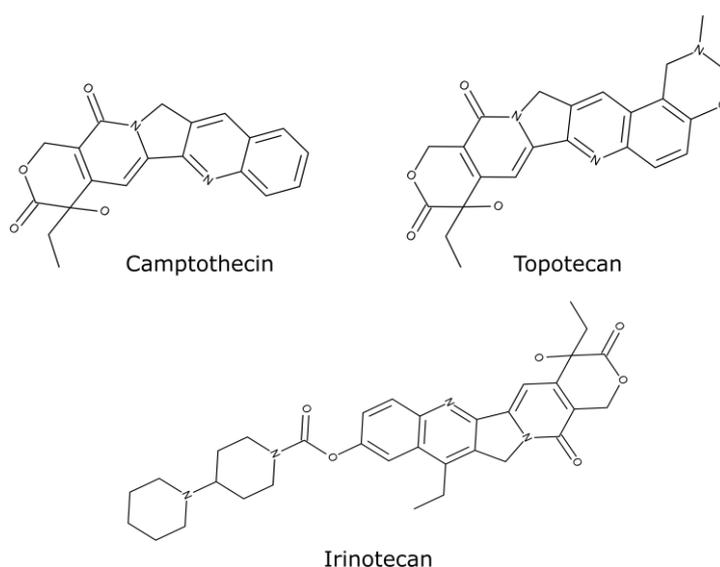
Figure 12 Chemical structures of camptothecin, topotecan and irinotecan [140].

1.7.1.2 Non-camptothecins

Despite the clinical achievements of numerous derivatives of CPT, they come with significant drawbacks such as the need for prolonged infusions, poor water solubility, and a range of adverse effects including temporary liver dysfunction, severe diarrhoea, and bone marrow damage [131]. Furthermore, there has been a concerning increase in single-point mutations that confer resistance to Topo I against camptothecin (CPT) [141]. The inaugural compound of the indolocarbazole family of Topo inhibitors, BE-13793C, was discovered in

1991 [142]. It originated from Streptomycetaceae closely related to *Streptoverticillium mobaraense*, and DNA relaxation assays confirmed its ability to inhibit both Topo I and Topo II [142]. Consequently, the FDA is currently evaluating three non-CPT inhibitors of Topo I: indenoisoquinoline, phenanthridines, and indolocarbazoles (**Figure 13**) as potential chemotherapeutics [137]. Among these alternatives, indolocarbazoles exhibit the most promise. They offer unique advantages compared to CPT: they possess greater chemical stability due to the absence of the lactone E-ring, can attach to different sections of DNA-bound Topo I, and display less reversibility of Topo I/DNA cleavage complex in drug treated cells, than CPT, reducing the likelihood of inhibitor complex dissociation [143,144]. As a result, indolocarbazoles necessitate shorter infusion times [145]. In addition to indolocarbazoles, topovale (ARC-111) is one of the most advanced clinically developed phenanthridines [146]. While it has shown promise in combating colon cancer, its effectiveness against breast cancer is limited [146]. LMP-744 stands as a noteworthy instance of indenoisoquinoline derivatives undergoing clinical trials, utilized in patients with recurrent solid tumours and lymphomas [147].
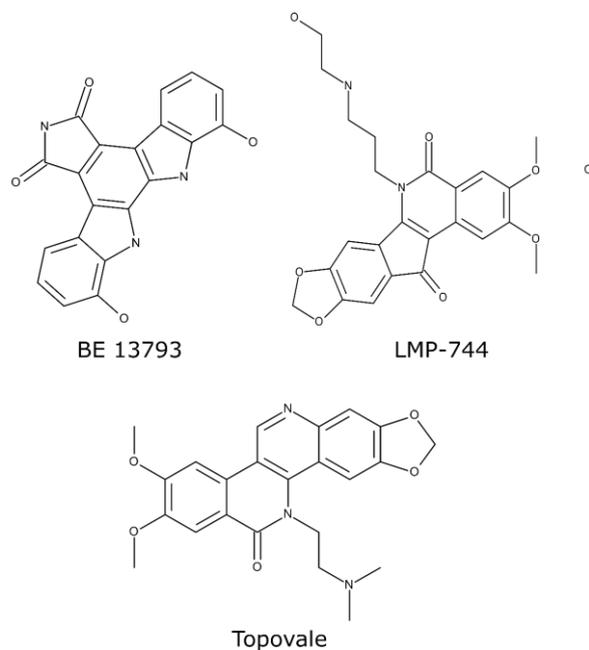
Figure 13 Chemical structures of non-camptothecin inhibitors [142,147,148].

1.7.2 Human Topo II

In vertebrates, two isoforms of Topo II exist: IIα and IIβ. Both of these isoforms require the presence of Mg^{2+} ions and ATP hydrolysis to perform their functions [109]. Topo IIα is vital for cellular viability, playing key roles in DNA replication and mitosis, with its expression pattern regulated throughout the cell cycle [149]. While Topo IIα's significance in chromosome condensation is well-established, recent findings contradict previous results, revealing its importance in maintaining chromosome structure [116,]. Chromatin compaction appears to result

partly from the interplay between Topo IIα and structural maintenance of chromosome complexes, like condensin [150,151].

Topo IIα is also essential for chromosome segregation. It resolves catenanes along chromosome arms before metaphase and, subsequently, at the centromere after the removal of cohesin by separase during the onset of anaphase [152]. During chromatid separation, intertwined DNA at the centromere forms ultra-fine anaphase bridges (UFBs) bound by Plk1-interacting checkpoint helicase (PICH). This stimulates the decatenation activity of Topo IIα [153]. Moreover, Topo IIα participates in resolving chromatids at ribosomal DNA (rDNA) regions alongside PICH, tankyrase, and condensin II during anaphase [109]. Beyond its intricate protein-protein interaction profile, Topo IIα's C-terminal domain (CTD) holds essential *in vivo* roles. It includes a nuclear localization signal, the chromatin tether domain (critical for mitotic activity), and sites for sumoylation, acetylation, phosphorylation, and ubiquitination. These sites regulate the enzyme's activity in a cell-cycle-dependent manner [154,155].

Topo IIα and IIβ exhibit distinct *in vivo* functions, which are believed to result from the differing characteristics of their C-terminal domains, leading to variations in regulation and activity [156]. While knockout mice lacking Topo IIα are embryonic lethal and display restricted expression primarily in proliferating cells, Topo IIβ knockout mice survive birth but succumb to respiratory failure, and this isoform is found in most adult tissues [109]. Numerous investigations have further associated Topo IIβ activity with processes related to neuronal development and transcription [157,158]. Notably, recent research has connected the activation of early-response genes in neurons, crucial for sensing the external environment, with the formation of double-stranded DNA breaks in gene promoters, a phenomenon likely induced by Topo IIβ [157]. Topo IIβ has also been linked to DNA repair [159], aging [160], HIV infection [161], and cancer [162], and, much like Topo IIα, the understanding of the full range of biological roles played by Topo IIβ is steadily unfolding [163].

In **Figure 14**, the domain structure of human Topo IIα is illustrated. This structure consists of three distinct domains:

1. The N-terminal domain, bears similarity to the B-subunit of DNA gyrase (GyrB) and houses the ATP binding and hydrolysis site.

2. The central domain, which shares homology with the A-subunit of DNA gyrase (GyrA) and contains the crucial active site tyrosine (Y805) responsible for DNA binding, cleavage, and ligation. For human Topo IIα, this tyrosine is present at position 805.

3. The C-terminal domain, which exhibits significant variability among species and between the two human isoforms. It encompasses nuclear localization sequences (NLS) and phosphorylation sites (PO4). Historically, this C-terminal domain was considered unimportant for the enzymatic activity of type II topoisomerases. However, recent research data suggests

27

its involvement in recognizing DNA geometry, potentially conferring unique capabilities such as DNA supercoiling or interaction with replication forks to specific type II enzymes. Notably, there is currently no available structural data for the C-terminal domain of any eukaryotic type II enzyme [150,164].
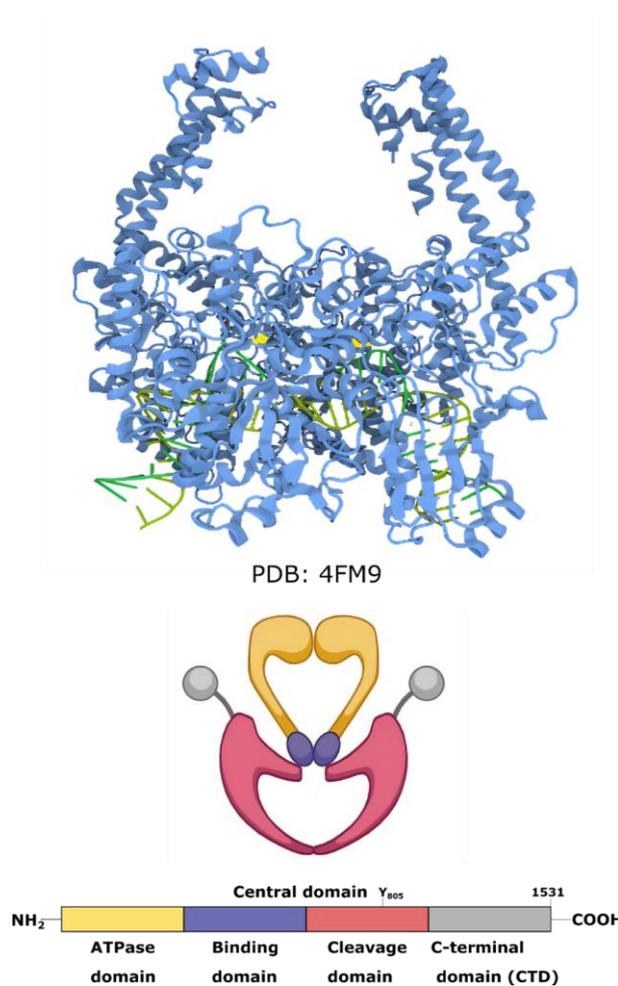
Figure 14 PDB structure and domain organization of human Topo IIα [150]. The colours match particular domains.

1.7.3 Inhibitors of human Topo II

The catalytic cycle of Topo II encompasses a series of steps, as illustrated in the schematic diagram (**Figure 15**) [165]. Initially, the enzyme forms a homodimer and binds to DNA crossovers, designating one of the double helices as the DNA Gate-segment (G-segment) and the other as the Transport-segment (T-segment). The bent G-segment undergoes cleavage through nucleophilic attacks on the DNA backbone catalysed by specific tyrosine residues. This process leads to the formation of a covalent link between the enzyme and the cleaved DNA strands [166]. This intermediate stage is known as the cleavage complex. Subsequently, the ATPase domain of the enzyme binds two ATP molecules, causing the N-gate to close. Hydrolysis of one ATP molecule initiates signal transmission within the enzyme, facilitating the rapid passage of the T-segment through the DNA gate. Once the T-segment has passed through, the previously opened DNA-gate is resealed. The T-segment is then released from the enzyme. Finally, after the hydrolysis of the second ATP molecule, the enzyme releases the G-segment, effectively resetting itself to capture another DNA crossover [165,167,168].

Topo II can be hindered at various stages of its enzyme reaction cycle (**Figure 15**), resulting in diverse biochemical and cellular effects. One straightforward method of inhibition involves targeting an early step in the enzyme reaction cycle. For instance, competitive inhibitors that obstruct ATP binding can impede strand passage without causing enzyme-mediated DNA damage [169].

Agents like novobiocin and coumermycin can inhibit both prokaryotic and eukaryotic Topo II enzymes, but they may either lack potency and specificity (e.g., novobiocin) or face poor uptake by mammalian cells (e.g., coumermycin) [170]. Similar outcomes can be expected from inhibitors that hinder the binding of Topo II to DNA, such as aclarubicin, owing to its targeting beyond Topo II [171]. Agents preventing DNA cleavage by Topo II, like merbarone, would also function as straightforward catalytic inhibitors [172]. An alternative inhibition mechanism involves interrupting the catalytic cycle after DNA cleavage but before DNA religation. Many presently employed Topo II-targeting agents, such as anthracyclines and epipodophyllotoxins (e.g., etoposide (ETP)), as well as agents targeting prokaryotic type II topoisomerases, function through this mode of action [165]. These agents impede enzyme turnover, making them potent inhibitors of catalytic activity [165]. The primary effect of these inhibitors, though, is the generation of substantial levels of Topo II-DNA covalent complexes [166]. Consequently, these inhibitors cause DNA damage and interfere with various DNA metabolic processes like transcription and replication. Due to their ability to convert Topo II into an agent entity that induces cellular damage, these inhibitors are referred to as Topo poisons [166].

Catalytic inhibitors of Topo II can also hinder enzyme activity after strand passage is concluded but before ATP hydrolysis and the dissociation of the amino-terminal dimerization [166,173].

Bisdioxopiperazines, such as dexrazoxane (ICRF-187), hinder both ATP hydrolysis and maintain the Topo II structure in a closed clamp configuration [174]. Similar to Topo II poisons, bisdioxopiperazines mainly inhibit Topo II catalytic activity by blocking enzyme turnover. Although these agents are often termed catalytic inhibitors, they retain Topo II trapped on DNA and may interfere with DNA metabolism in a manner analogous to Topo II poisons [133]. Nonetheless, as bisdioxopiperazines specifically target Topo II, they are the most commonly employed catalytic inhibitors of Topo II in mammalian cells [175,176].
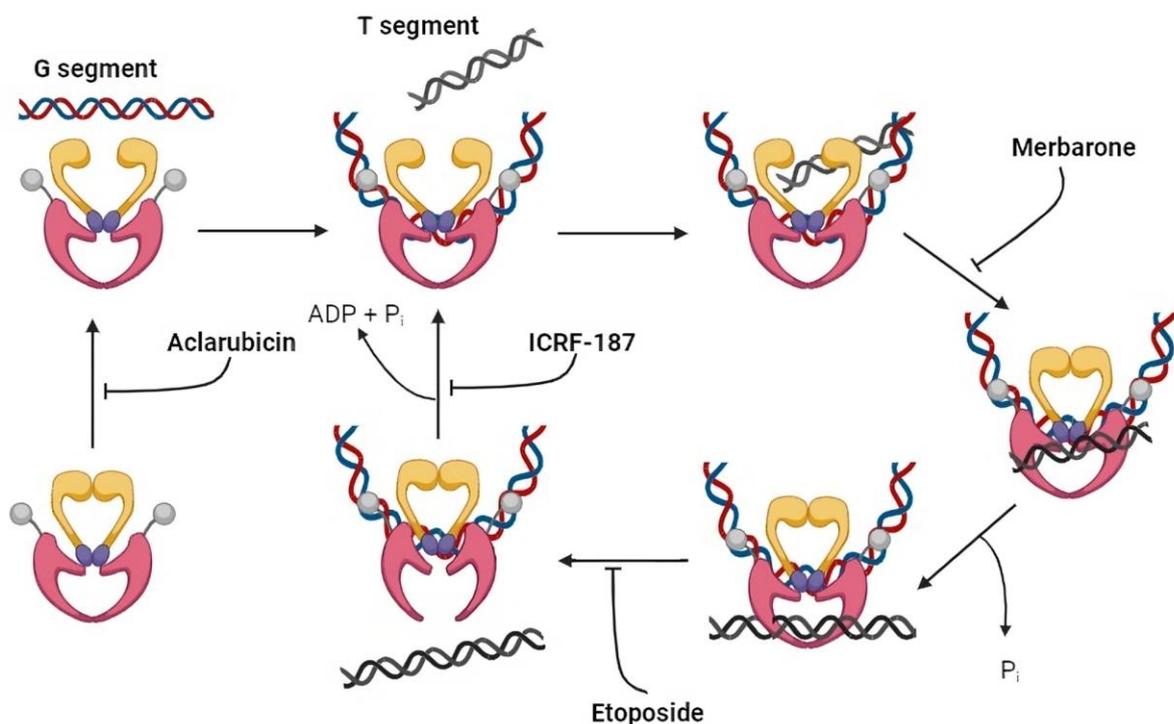
Figure 15 The catalytic cycle and the mechanism of inhibition of Topo II catalytic cycle [165].

1.7.3.1 Topo II poisons

As previously mentioned, compounds that aim to inhibit Topo II can be divided into two main groups based on how they work [177]. The first group includes compounds called Topo II poisons. Topo II poisons constitute a category of extensively prescribed anticancer drugs. These agents encompass a range of naturally occurring and synthetic compounds and are employed in the treatment of various human malignancies. Significantly, frontline therapies for numerous systemic cancers and solid tumours, including leukaemia, lymphomas, sarcomas, breast cancers, lung cancers, neuroblastomas, and germ-cell malignancies, involve ETP, doxorubicin (DOXO), and their derivatives. ETP stands out as the most thoroughly studied

Topo II poison [178,179]. Extensive research on this anticancer agent has yielded foundational knowledge that has paved the path for subsequent drug investigations. ETP was the initial Topo II poison demonstrated to impede the DNA ligation activity of the type II enzyme [180]. Additionally, it was established that the drug primarily enters the binary enzyme-DNA complex through interactions with the protein. Recent data has unveiled structure-function relationships pertaining to ETP's interaction with Topo II, which can guide the design of new drugs [181]. Additionally, mitoxantrone is utilized in the treatment of breast cancer, AML, non-Hodgkin lymphoma, and multiple sclerosis [182,183]. Topo II poisons induce the formation of a covalent complex between Topo II and DNA, resulting in elevated levels of DNA damage within cells. Ultimately, this process activates apoptosis. These poisons can be further classified based on their capability to bind to DNA. Some, like ETP and teniposide (**Figure 16**) do not intercalate into DNA, while others, like DOXO, daunorubicin, amsacrine (m-AMSA), and mitoxantrone, do intercalate into DNA (**Figure 17**) [165,168].

Etoposide   Teniposide
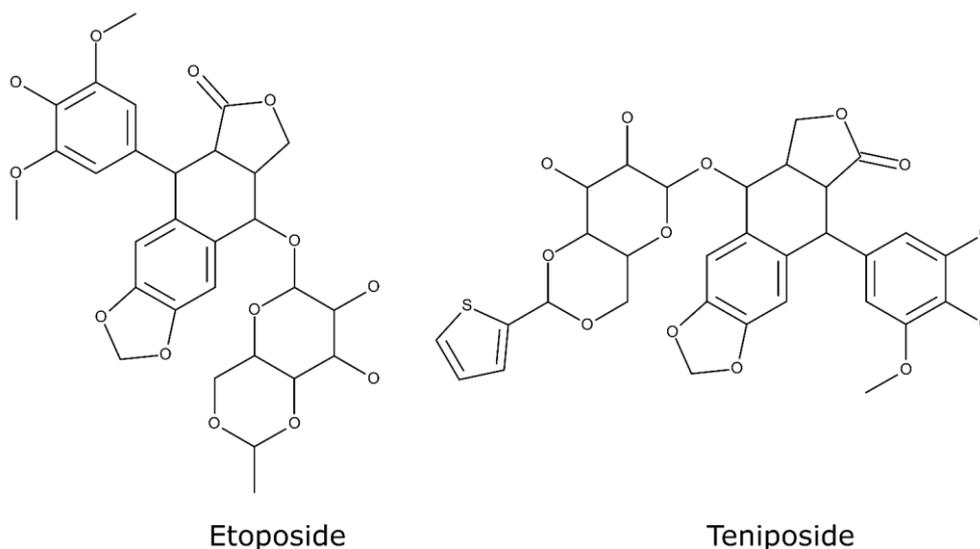
Figure 16 Chemical structures of non-intercalating Topo II poisons [184].
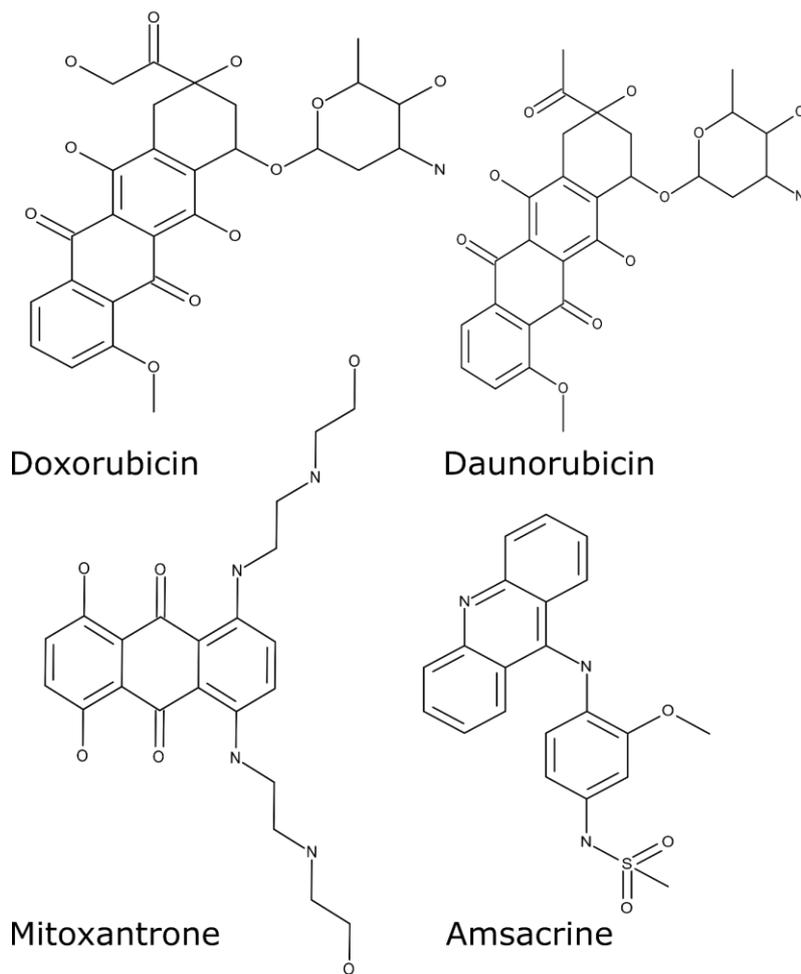
Figure 17 Chemical structures of intercalating Topo II poisons [168].

1.7.3.2 Catalytic inhibitors

The second category encompasses catalytic inhibitors that focus on the essential enzymatic activity of Topo II. These inhibitors elicit cytotoxic effects without substantially increasing DNA damage by stabilizing the Topo II/DNA complex [165]. Catalytic inhibitors operate through diverse mechanisms, such as inhibiting ATP hydrolysis (e.g., ICRF-187, ICRF-193) [185], competing for the ATP binding site (e.g., novobiocin) [186], or preventing DNA cleavage (e.g., merbarone)[187]. Overall, the strategic targeting of the catalytic functions of Topo II presents a systematic approach to oncology therapy, providing potential avenues for the development of effective cancer treatments [172].

Aclarubicin (**Figure 18**), isolated from *Streptomyces galilaeus*, possesses dual properties, acting as both an antibacterial agent and an inhibitor of cell proliferation [188]. It demonstrates a favourable safety profile in animal models [189]. This compound belongs to the anthracycline family and stands out for its reduced cardiotoxicity compared to DOXO and daunorubicin [190]. Aclarubicin exerts its multifaceted mechanism of action through various pathways. It includes the insertion of its trisaccharide chain into the minor groove of DNA, functioning as a Topo I poison, inhibiting Topo II, displacing histones from nucleosomes, and acting as an inhibitor of the 20S proteasome [191]. Worth noting is aclarubicin's rapid *in vivo* biotransformation, leading to the formation of inactive metabolites [189]. Consequently, patients with AML require repetitive daily treatments. While aclarubicin's global use in cancer treatment has been discontinued, it remains in use in conjunction with cytarabine in Japan, India, and China [189]. Aclarubicin's capacity to hinder cell proliferation stems from a combination of mechanisms, ultimately prompting apoptosis in cancer cells, as demonstrated by Rogalska et al. in 2010 [192]. These mechanisms primarily revolve around aclarubicin's affinity for DNA binding. In contrast to the actions of DOXO and daunorubicin, which promote the formation of cleavable complexes between DNA and the nuclear enzyme Topo II, leading to DNA double-strand breaks and subsequent apoptosis, aclarubicin takes a distinct approach. Aclarubicin, instead of fostering cleavable complexes, interferes with the noncovalent binding of Topo II to DNA under *in vitro* conditions [193]. Consequently, aclarubicin's interference effectively prevents DNA cleavage, contributing to its unique antiproliferative effect [194].
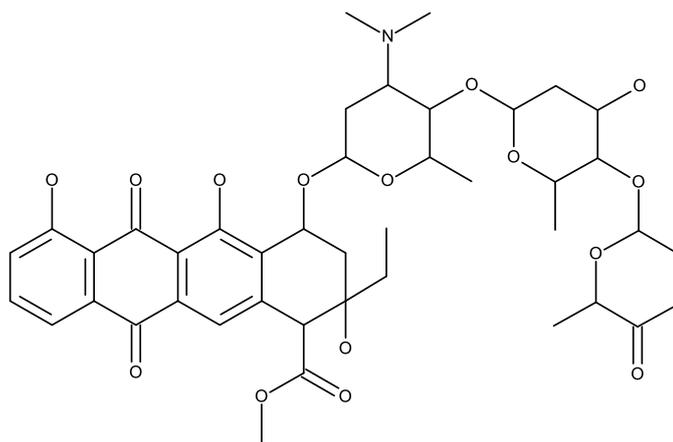
Figure 18 Chemical structure of aclarubicin [168].

Bisdioxopiperazine derivatives inhibit the catalytic activity of Topo II while having no impact on Topo I [172]. Among the most extensively studied bisdioxopiperazines are ICRF-154, the foundational compound, and MST-16 (Sobuzoxane), a clinically utilized prodrug that undergoes metabolism to yield ICRF-154 [185]. Another noteworthy compound is ICRF-159 (Razoxane), initially discovered as an antitumour agent [195]. It represents a monomethyl derivative of ICRF-154 and exhibits comparable antitumour activity. In the clinical setting, ICRF-187 (Dexrazoxane, Cardioxane, Zinecard, and ADR-529) (**Figure 19**) is the (+)-enantiomer of racemic ICRF-159 and is employed to mitigate DOXO-induced cardiotoxicity [172].

Notably, ICRF-193, a dimethyl derivative of ICRF-154, is the most potent among bisdioxopiperazine derivatives in its action against Topo II [196]. ICRF-193 effectively targets various mammalian Topo II forms, including those found in yeast, flies, frogs, plants, and mammals, while having no impact on prokaryotic type II enzymes such as DNA gyrase [197]. A comparison between the two human Topo II isoforms reveals that purified human Topo IIα displays more than tenfold greater sensitivity to ICRF-159 and ICRF-193 compared to the β form of the enzyme [198]. ICRF-193 operates by inhibiting Topo II through the stabilization of a noncovalent form of the enzyme that encircles DNA. The formation of this complex necessitates the presence of both the drug and ATP, ultimately leading to the inhibition of the ATPase activity of the enzyme [199,200].
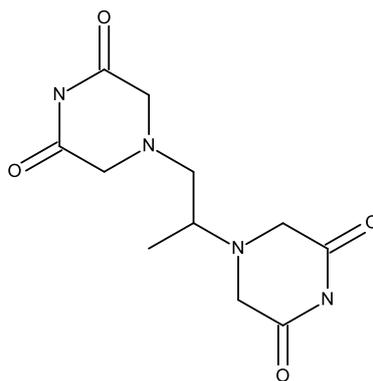
Figure 19 Chemical structure of ICRF-187 [175].

Merbarone (**Figure 20**) is a compound formed by connecting thiobarbituric acid and aniline through an amide linkage [201]. Out of approximately 700 barbituric acid analogues assessed in the National Cancer Institute's screening program in Bethesda, MD, USA, only merbarone displayed activity [202]. Merbarone has been found to possess curative potential against L1210 leukaemia and significant activity against certain other murine tumours [113].

This drug selectively inhibits the catalytic activity of Topo II, particularly the Topo IIα isoform, while showing only weak activity against Topo I [203]. Detailed investigations into the various stages of the catalytic cycle have revealed that merbarone has no effect on DNA binding or ATP hydrolysis but is a potent inhibitor of enzyme-mediated DNA cleavage [203]. Moreover, merbarone can compete with ETP, indicating a potential competition for similar binding sites on Topo II [187,204]. Clinical trials involving merbarone have been conducted for various tumour types. However, these studies were halted due to nephrotoxicity and a general lack of antitumour activity [205].
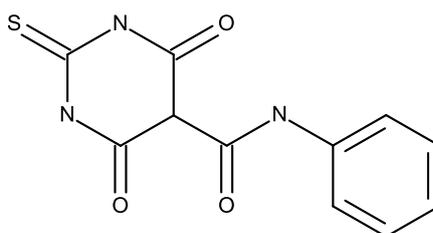
Figure 20 Chemical structure of merbarone [206].

Novobiocin (**Figure 21**), an agent-derived from coumarin, utilizes distinct mechanisms to inhibit DNA topoisomerases [207]. It achieves inhibition by blocking the ATP binding site, effectively targeting bacterial gyrase B and mammalian Topo II [208]. In contrast, novobiocin's interaction with *vaccinia* virus Topo I disrupts the enzyme's ability to engage with DNA [209]. Importantly, leukaemia cells resistant to novobiocin also exhibit notable cross-resistance to ETP and teniposide, with lesser degrees of resistance to m-AMSA and DOXO [209].

35

Novobiocin has been widely employed to modulate cellular responses to alkylating agents and other Topo inhibitors. Many cell lines that have developed resistance to alkylating agents frequently display heightened Topo II activities. Conversely, cells that have become resistant to Topo II inhibitors often demonstrate reduced Topo activities and display collateral sensitivity to alkylating agents. Furthermore, novobiocin has the ability to enhance the cytotoxicity of ETP and teniposide in multiple tumour cell lines. This heightened cytotoxicity does not arise solely from an additive effect of these agents on Topo II but is instead attributed to novobiocin's capacity to inhibit the efflux of ETP and teniposide. This inhibition results in elevated intracellular drug concentrations, leading to an increased formation of covalent DNA Topo complexes [210,211].
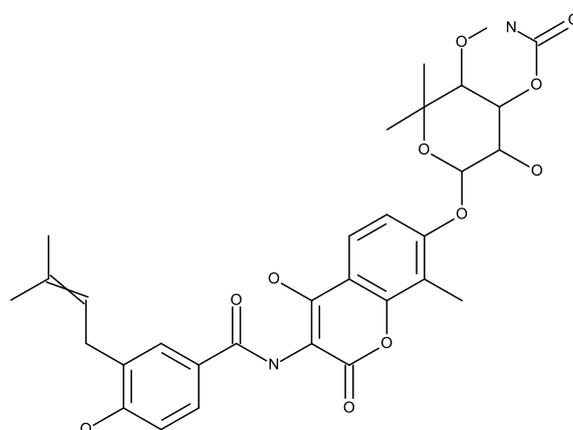
Figure 21 Chemical structure of novobiocin [168].

1.8 Cellular effects

In this study, in addition to assessing the activity of the tested compounds against human topoisomerases, an attempt was made to understand the cellular response to the action of the tested compounds in the context of various processes occurring in cancer cells and to determine whether there are potential unintended targets (off-targets) or possibly alternative mechanism of action.

1.8.1 Cell cycle

The cell cycle is a meticulously orchestrated process composed of two distinct phases. The first phase is mitosis (M), during which a cell undergoes division. The second phase is interphase, which encompasses G1 (pre-DNA synthesis), S (DNA synthesis), and G2 (pre-division) phases (**Figure 22**) [212]. After interphase, the cell reverts to the G0 phase, which signifies a state of quiescence. G0 is typically used to describe cells that are not actively participating in the cell cycle but still retain the potential for division (**Figure 22**). The majority

36

of non-growing or non-proliferating cells fall into the G0 category [213]. Cells can transit from the quiescent state of G0 to the G1 phase if they are stimulated to proliferate or activated by mitogenic signals [214]. The G1 phase marks the initial stage in cell cycle progression [215]. During the S phase, cells synthesize DNA, resulting in a DNA content ranging from 2N to 4N [216]. Upon accurate duplication of chromosomes, cells advance to the G2 phase, during which they prepare for the M phase. In the M phase, the cell undergoes division, resulting in the formation of two separate daughter cells [214,215].

Each stage of the cell cycle is under tight regulation by cyclin-dependent kinases (CDKs), which belong to a highly conserved family of serine/threonine protein kinases, and their regulatory partners, known as cyclins (**Figure 22**) [217]. Conversely, cell cycle progression is inhibited by cyclin-dependent kinase inhibitors (CKIs) [218]. A complex of cyclin-dependent kinase (CDK) and cyclin (CDK-cyclin) is created through the binding of an inactive catalytic subunit of the protein kinase (CDK) with a regulatory subunit (cyclin) [219]. Cyclin-CDK complexes serve as central regulators of cell cycle progression, transducing external signals such as growth factors and nutrient availability to the cell [220]. Distinct cyclins are required at different phases of the cell cycle. D-type cyclins (D1, D2, and D3) associate with CDK4/6 are crucial for entry into the G1 phase [221]. Cyclin E is also pivotal during G1, forming a complex with CDK2 to regulate the late G1 phase and initiate DNA synthesis in the early S phase [222]. The cyclin E/CDK2 complex plays a vital role in facilitating the transition from the G1 to S phase [223]. As the cell cycle advances, cyclin A takes the place of cyclin E as the binding partner for CDK2. Cyclin A is responsible for overseeing DNA synthesis and replication during the S phase [224]. Subsequently, cyclin A associates with CDK1 to drive entry into the M phase. CDK1 collaborates with other kinases, such as polo-like kinases and Aurora, to facilitate the transition from G2 to M phase, thus contributing to mitotic progression during cell division. In the G2 phase, cyclin B replaces cyclin A, and the cyclin B/CDK1 complex plays a pivotal role in triggering mitosis [225,226].

In cancer cells, cell cycle proteins often display increased activity, leading to uncontrolled cell proliferation. Notably, when individual cyclins or CDKs are genetically removed or when the function of cyclin-CDK kinase complexes is suppressed in mice-bearing tumours, it effectively hinders the onset and progression of specific cancer types driven by particular oncogenic triggers [227]. What's striking is that this intervention has minimal effects on normal tissues[159]. This observation suggests that cancer cells have a reliance to specific CDKs, depending on the genetic mutations they carry. Consequently, targeting CDKs through inhibition emerges as a precise strategy for addressing cancer cells while safeguarding the integrity of normal tissues [225,228].
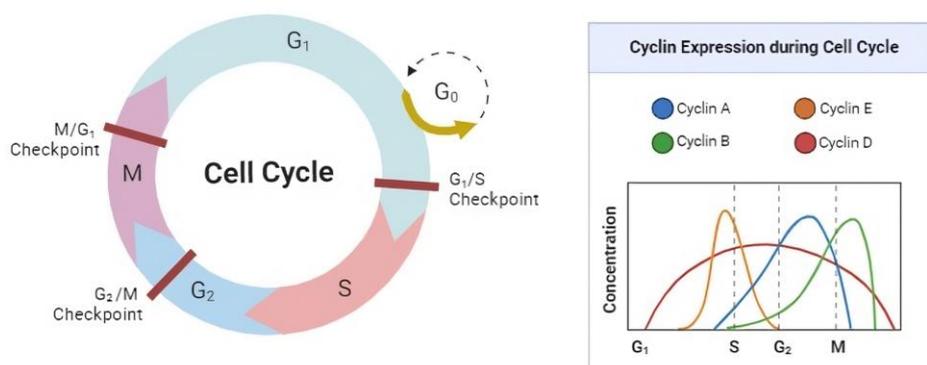
Figure 22 Cell cycle and its regulation [212].

1.8.2 DNA damage

Double-strand breaks (DSBs) represent the most harmful DNA lesions. If left unpaired, they can have serious repercussions on cell survival, giving rise to chromosome abnormalities, genomic instability, or even cell death [229,230]. DSB induction involves various physical, chemical, and biological factors. Cells respond to DNA damage through the activation of the DNA damage response (DDR), a complex molecular mechanism designed to detect and repair DNA damage [231]. The occurrence of DSBs initiates the activation of numerous factors, including the phosphorylation of the histone variant H2AX, resulting in the formation of γ-H2AX [232]. H2AX phosphorylation plays a pivotal role in DDR, essential for recruiting DNA repair proteins to damaged chromatin sites and for the activation of checkpoint proteins that halt cell cycle progression. In essence, the analysis of γ-H2AX expression can be employed to detect the genotoxic effects of various toxic substances [233]. When employed with clinical samples from cancer patients, evaluating γ-H2AX levels can not only facilitate the monitoring of the effectiveness of anticancer treatments but also predict the sensitivity of tumour cells to DNA-damaging anticancer agents and assess the toxicity of such treatments on normal cells [234,235].

1.8.3 Reactive oxygen species

Reactive oxygen species (ROS), a category of highly active molecules, have been extensively investigated in various cancer types [236]. These ROS are typically considered natural byproducts of numerous cellular processes. In general, cancer cells tend to exhibit elevated baseline levels of ROS in comparison to normal cells due to an imbalance between oxidants and antioxidants [237]. ROS play a dual role in cellular metabolism [238]: When present at low to moderate levels, they serve as signal transmitters, activating processes such as cell proliferation, migration, invasion, and angiogenesis. Conversely, when ROS levels are high,

they cause damage to proteins, nucleic acids, lipids, membranes, and cellular organelles, ultimately resulting in cell death [239]. In-depth investigations have revealed that anticancer treatments, which regulate levels of ROS, including immunotherapies, demonstrate encouraging outcomes in both laboratory experiments *in vitro* and *in vivo* [236,240].

1.8.4 Calcium efflux

Calcium serves as a versatile and dynamic second messenger crucial for the survival of higher organisms [241]. In cells undergoing activation or excitation, calcium is discharged from the endoplasmic/sarcoplasmic reticulum to activate calcium-dependent kinases and phosphatases, thus governing a wide array of cellular processes, including apoptosis and autophagy. In the context of apoptosis, either endogenous ligands or pharmacological agents induce a sustained increase in cytosolic calcium, leading to cell death [242,243].

1.8.5 Protein tyrosine kinases

Protein tyrosine kinases (PTKs) are a group of enzymes that play a pivotal role in regulating numerous cellular processes such as cell growth, differentiation, and survival [244]. The dysregulation of PTKs has been implicated in the initiation and progression of various cancer types. Consequently, PTKs have emerged as crucial targets in the quest to develop anticancer therapies [245,246]. For instance, imatinib, a protein tyrosine kinase inhibitor (PTKI), has been approved for treating chronic myeloid leukaemia and gastrointestinal stromal tumours. Imatinib specifically targets the BCR-ABL PTK, which is overexpressed in these cancer cell types, leading to uncontrolled proliferation. By inhibiting BCR-ABL activity, imatinib effectively eradicates cancer cells and induces remission [247,248]. Another notable PTKI is dasatinib, which targets multiple PTKs, including BCR-ABL, SRC, and c-KIT. Dasatinib has demonstrated promising outcomes in the treatment of various cancers, such as chronic myeloid leukaemia, acute lymphoblastic leukaemia, and non-small cell lung cancer [249]. Beyond imatinib and dasatinib, several other PTKIs are currently under development or undergoing clinical trials for the treatment of diverse cancer types [250]. These medications hold significant promise in enhancing the outcomes of cancer treatment and diminishing the toxicity associated with traditional chemotherapy [251]. However, it is known that PTKIs quite often cause resistance; therefore, the development of new compounds from this group is still needed [252].

1.8.6 Apoptosis

Apoptosis, the natural mechanism for cell death, holds significant promise as a target for anticancer therapy [253]. Both the intrinsic and extrinsic pathways utilize caspases to execute apoptosis by cleaving hundreds of proteins. In cancer, the apoptotic pathway is typically hindered through various means, such as the overexpression of antiapoptotic proteins and the

under expression of proapoptotic proteins. Numerous conditions can activate the apoptotic pathway, including DNA damage and uncontrolled cell proliferation [254]. This pathway responds to signals from both, inside and outside the cell. Two distinct pathways, the intrinsic (or mitochondrial) and extrinsic (or death receptor) pathways, correlate with the type of signal. Intracellular signals include DNA damage, deprivation of growth factors, and cytokines [253,255]. When apoptosis is initiated, the cell undergoes a series of changes, including the activation of caspases, which cleave vital cellular components, including cytoskeletal and nuclear proteins. As a result of caspase activity, apoptotic cells shrink and exhibit changes in the plasma membrane, signalling a response from macrophages [256]. The activity of caspase proteases is crucial for successful apoptosis, as they cleave numerous proteins. There are four initiator caspases (caspase-2, -8, -9, 10) and three executioner caspases (caspase-3, -6, -7) [257]. The executioner caspases cleave target proteins, ultimately leading to cell death [258,259]. These pathways are tightly regulated, ensuring that apoptosis only occurs when appropriately signalled. The intrinsic pathway is particularly regulated by the B-cell lymphoma-2 (BCL-2) protein family, which includes proapoptotic effector proteins, proapoptotic BH3-only proteins, and antiapoptotic BCL-2 proteins [260]. Antiapoptotic BCL-2 proteins inhibit apoptosis by counteracting proapoptotic BCL-2 proteins, such as BCL-2-associated X protein (BAX) and BCL-2 antagonist killer (BAK). BH3-only proteins also play a role in inhibiting antiapoptotic BCL-2 proteins [261,262].

Another significant protein involved in the apoptosis process is Poly(ADP-ribose) polymerase (PARP1 [263]. Its primary function is to recognize and bind to DNA strand breaks induced by various genotoxic agents [264]. Upon the occurrence of DNA breaks, PARP1 becomes activated and subsequently promotes the synthesis of poly(ADP-ribose) using its substrate, the coenzyme NAD+, directly at the break site [265]. It has been observed that during both drug-induced and spontaneous apoptosis, PARP1 undergoes proteolytic cleavage, resulting in the generation of 89-kDa and 24 kDa fragments. These fragments respectively contain the enzyme's active site and DNA-binding domain. In the execution of the apoptotic program, caspase-3 assumes a central role and is responsible for cleaving PARP1 during the cell death process [266,267].

One approach to cancer treatment involves gaining control over, or possibly terminating, the uncontrolled growth of cancer cells by harnessing the cell's own mechanism for programmed cell death. Targeting apoptosis is an effective method and has proven to be the most successful non-surgical treatment for various types of cancer [253]. This approach is effective across all types of cancer, as evasion of apoptosis is a common hallmark of cancer and is not specific to the cause or type of cancer. Numerous anticancer drugs target various stages in both the intrinsic and extrinsic pathways [268].

2. AIM OF STUDY

Cancer is a highly intricate and multifaceted disease, stemming from a complex interplay of physiological and biochemical changes. Recent years have illuminated a concerning trend: cancer cells are demonstrating an alarming ability to develop resistance to numerous traditional anticancer drugs, resulting in the recurrence of tumours. Contemporary cancer management encompasses a diverse array of therapeutic modalities, including surgery, radiotherapy, immunotherapy, and the frequently employed chemotherapy. Despite the rising incidence of cancer and the emergence of drug resistance, chemotherapy remains the predominant strategy for combatting this ailment. In the forthcoming decades, the exploration and innovation of novel cancer treatments will prove indispensable in effectively addressing these challenges. Consequently, the imperative to develop alternative approaches to cancer treatment becomes increasingly significant in our quest for enhanced outcomes. As we move forward, the quest for discovering new and potent anticancer medications remains a pressing and unrelenting mission [269,270].

The subject of the conducted research was three symmetrically substituted carbazole derivatives: 2,7-Di(2-furyl)-9*H*-carbazole (**27a**), 3,6-Di(2-furyl)-9*H*-carbazole (**36a**), and 3,6-Di(2-thienyl)-9*H*-carbazole (**36b**) (**Figure 23**), designed based on the asymmetrically substituted carbazole proposed within the OPUS project titled 'New inhibitors of the telomerase catalytic unit' [271]. The project was conducted by prof. Baginski's group several years ago. These compounds were initially designed by Dr. Eng. Umesh Kalathiya through high-throughput screening techniques with the intention of serving as potential inhibitors of telomerase catalytic activity. They were subsequently synthesized by Prof. Makowski's group at the University of Gdansk for further investigation within the TARGETTELO project (STRATEGMED). However, after being tested by Dr. Eng. Natalia Maciejewska using the TRAP assay, these compounds did not show an impact on telomerase activity. Apparently, despite their lack of telomerase activity, the compounds **27a**, **36a**, and **36b** exhibited promising cytotoxicity against cancer cell lines in preliminary screenings. Therefore, the aim of my project was to perform biological studies to determine their molecular mechanism of action.

Within this study it was planned to assess the biological anticancer properties of carbazole derivatives with symmetrical substitutions, incorporating either furan or thiophene. Especially to determine the target and mode of action. My working hypothesis was that these compounds can target other DNA operating proteins, namely topoisomerase. The novelty of this approach lies in the symmetrical substitutions of these compounds and their exploration of potential anticancer properties. The primary focus of this assessment revolves around the molecular pharmacology of three specific derivatives. It includes a thorough examination of their inhibitory effects on human Topo I and II and an investigation into their potential as anticancer agents

41

across various cancer cell lines. This comprehensive analysis encompasses the assessment of their cytotoxicity, antiproliferative effects, induction of DNA damage, prooxidative properties, and proapoptotic effects. Moreover, it also included assessment of their effects on the activity of other potential targets. Notably, the investigation also delved into the inhibition of protein tyrosine kinase activity. **Thus**, **through numerous studies employing molecular biology techniques, the goal of my doctoral thesis was to elucidate the anticancer mechanism responsible for the high cytotoxic properties of carbazole derivatives**.
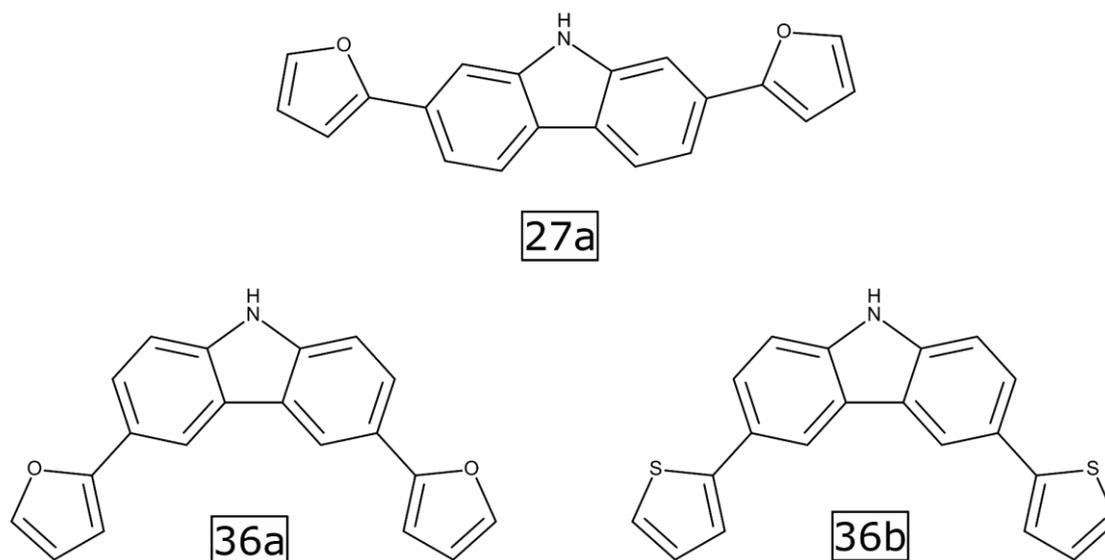
Figure 23 Chemical structure of the investigated compounds.

3. MATERIALS AND METHODS

All reagents and materials were purchased from Sigma-Aldrich (Saint Louis, United States) unless otherwise stated. **Tables 2** and **3** displayed the inventory of antibodies that were employed.

Table 2 List of antibodies employed in Western blot analysis.

Antibody	Company	Dilution
anti-Caspase-9 (#9502)	Cell Signaling	1:1000
anti-PARP (#9542)	Cell Signaling	1:1000
anti-BID (#2002)	Cell Signaling	1:1000
anti-Bax (#2772)	Cell Signaling	1:1000
anti-Actin, (sc-1616)	Santa Cruz Biotechnology	1:1000
anti-AIF(#5318S)	Cell Signaling	1:1000
anti-mouse-HRP, 715-035-150	Jackson ImmunoResearch Labs	1:10000
anti-rabbit-HRP, 711-035-152	Jackson ImmunoResearch Labs	1:10000
anti-goat-HRP, 705-036-147	Jackson ImmunoResearch Labs	1:10000

Table 3 List of antibodies employed in immunofluorescence or flow cytometry assessments.

Antibody	Company	Dilution
Alexa Fluor 488-conjugated anti-H2AX (pS139), (#560445)	BD Pharmingen	1:100
anti-β-tubulin, #T8328	Sigma-Aldrich	1:250
anti AIF(5318S)	Cell Signaling	1:100
anti-Cytochrome c (#11940S)	Cell signaling	1:100
anti-mouse Alexa Fluor 488,(#SA5-10166)	Invitrogen	1:500
anti-rabbit Alexa Fluor 594, (sc-516250)	Santa Cruz Biotechnology	1:500
anti-BrdU (#ab6326)	Abcam	1:200
anti-Phospho-tyrosine (P-Tyr-100), (#9411)	Cell Signaling	1:200

<u>Protocols</u>

All protocols for the employed methods were devised in the Department of Pharmaceutical Technology and Biochemistry at Gdańsk University of Technology, unless specified otherwise.

3.1 Cell culture

A549 (CCL-185), H226 (CRL-5826), H460 (HTB-177), GLC4 (CVCL-0279), MCF-7 (HTB-22), HCT-116 (CCL-247), HT-29 (HTB-38), U-2 OS (HTB-96), U87-MG (HTB-14), HaCat (CRL-2404), HEK293 (CRL-1573) cells were obtained from the American Type Culture Collection (ATCC). Normal human bronchial epithelial cells (NHBE) and human mammary epithelial cells (HMEC) were acquired from Lonza (Walkersville, USA). All cell lines were cultured in a humidified environment at 37°C with either 5% or 10% CO_2 and regularly screened for *Mycoplasma* contamination. The culture medium for each cell line (**Table 4**) consisted of 10% foetal bovine serum (Corning, New York, USA), 2 mM L-glutamine, and antibiotics (62.6 µg/ml penicillin and 40 µg/ml streptomycin). The culture media for normal cell lines was supplemented with appropriate growth factors and additives as per the manufacturer's instructions.

Table 4 A summary of the cell lines used for the conducted research

Cell line	Type	Medium	CO_2
A549	lung cancer cell line	RPMI-1640	5%
H226	lung cancer cell line	RPMI-1640	5%
H460	lung cancer cell line	RPMI-1640	5%
GLC4	lung cancer cell line	RPMI-1640	5%
HCT-116	colon cancer cell line	McCoy's 5A	5%
HT-29	colon cancer cell line	McCoy's 5A	5%
MCF-7	breast cancer cell line	RPMI-1640	5%
U-2 OS	bone cancer cell line	McCoy's 5A	5%
U87-MG	brain cancer cell line	MEM	5%
HaCat	noncancerous skin cell line	RPMI-1640	5%
HEK293	noncancerous kidney cell line	DMEM	10%
NHBE	lung normal cell line	BEGM	5%
HMEC	breast normal cell line	MEGM	5%

3.2 Drug sensitivity

Cell viability was assessed via the MTT (3-(4,5-dimethylthiazol-2-yl)-2,5-diphenyl-2*H*-tetrazolium bromide) assay. Initially, cells were seeded into 96-well plates and exposed to varying concentrations of the investigational compounds, ranging from 0 to 50 µM, for a duration of 72 h. Reference compounds, ETP and m-AMSA, were included for comparative analysis. Subsequent to treatment, the cells were subjected to a 3 h incubation period with an MTT solution (0.4 mg/ml in PBS) at 37°C. Following this incubation, the culture medium was carefully aspirated, and the formazan crystals formed during the reaction were solubilized in 100 µl of DMSO. The absorbance of the resulting solution was quantified at 540 nm, employing an ASYS UVM340 microplate reader from Biochrom Ltd. To ensure robustness and accuracy, the experiment was independently conducted in triplicate. The 50% inhibitory concentration (IC_{50}) was characterized as the concentration at which the absorbance of the DMSO-treated cells was reduced by 50% compared to the control. Calculations of IC_{50} values were carried out using GraphPad Prism software (GraphPad Prism version 9.0.0 for Windows, GraphPad Software, San Diego, USA) by constructing survival curves based on data obtained from a minimum of three independent biological experiments.

Concentrations employed in subsequent assays

To monitor alterations in cellular responses caused by the **27a**, **36a**, and **36b**, further assays were carried out using the IC_{90} concentration established for each compound relative to each cell line after 72 h of treatment, unless stated otherwise.

3.3 Clonogenic assay

In 6-well plates, A549 and HCT-116 cells were initially seeded at a density of 400 cells per well. Subsequently, the cells underwent treatment with varying concentrations of carbazole derivatives under investigation for a duration of 24 h. After this treatment period, the cells were subjected to a thorough wash and were allowed to continue culturing for an additional 8 days. To stabilize the cells, methanol was employed as a fixing agent. This was followed by staining with 0.5% crystal violet. Visible colonies resulting from the culture were quantified using ImageJ 1.53n software (National Institutes of Health, Bethesda, USA). The viability of the cells was then determined relative to the control conditions.

3.4 Flow cytometry

In preparation for each flow cytometry experiment, A549, HCT-116, MCF-7, and U-2 OS cells were initially seeded onto tissue culture plates and given 24 h to adhere. Subsequently, the

cells were incubated with the compounds under investigation, each at its respective IC_{90} concentration, for the specified duration for each individual experiment. The analysis involved examining 10,000 events using the Guava easyCyte 8 cell sorter from Merck Millipore, and the data were processed using FlowJo v10 software. To ensure the reliability of the results, each experiment was independently replicated three times.

3.5 Cell cycle analysis

To conduct cell cycle analysis, A549, HCT-116, MCF-7, and U-2 OS cells were subjected to treatment with carbazole derivatives for either 24 or 48 h. Following this treatment period, the cells were carefully collected, fixed using ice-cold 75% ethanol, and stored overnight at a temperature of -20°C. In the subsequent phase, after centrifugation, the cells underwent a thorough rinse with PBS. They were then stained with a solution comprising 20 µg/µl of propidium iodide (PI) and 100 µg/µl of RNaseA (Thermo Fisher Scientific), all dissolved in PBS. This staining procedure was carried out for a duration of 20 min at RT.

3.6 BrdU assay

To assess DNA synthesis, A549, HCT-116, MCF-7, and U-2 OS cells were first exposed to 20 µM BrdU (5-bromo-2'-deoxyuridine) for a duration of 1 h, just prior to the conclusion of their respective treatments. Subsequently, the cell samples were harvested using a trypsin solution and then fixed in 75% ethanol. The fixation was carried out overnight or for an extended period at -20°C. Following fixation, the samples underwent a 10 min rehydration step with PBS. To facilitate the denaturation process, the samples were treated with 2 M HCl for 45 min at RT. The suspension was then neutralized using 0.1 M sodium tetraborate with a pH of 8.5 for 10 min at RT. To minimize nonspecific binding, a solution consisting of 1% w/v bovine serum albumin (BSA) in PBS was used for blocking for 30 min at RT. Following this blocking step, the samples were subjected to a sequence of antibody incubations. Initially, they were incubated with rat anti-BrdU antibody (at a 1:100 dilution) from Abcam (#ab6326) (**Table 3**) for 1 h at 37°C. Subsequently, the samples were treated with goat anti-rat conjugated antibody (at a 1:200 dilution) from Abcam (#ab150157) for 30 min at 37°C. Finally, the DNA was stained using a solution composed of 20 µg/µl propidium iodide (PI) and 100 µg/µl RNaseA in PBS for 20 min at RT.

3.7 DNA damage

Cells were initially plated onto tissue culture plates and given time to adhere overnight. On the following day, all cells received treatment with either 10 µM of compounds or 1% (v/v) DMSO for durations of 24 and 48 h. Following incubation, the cells were collected via trypsinization,

then fixed in ice-cold 75% ethanol and stored at -20°C until further analysis. The subsequent steps involved rehydrating the cells with PBS on ice for a duration of 10 min, followed by permeabilization in 0.2% Triton X-100 in PBS at RT for 5 min. After centrifugation, the cells were washed with 1% BSA in PBS and subsequently incubated with Alexa Fluor™ 488-conjugated mouse anti-γ-H2AX (Ser139) antibody at a 1:100 dilution (#613406; BioLegend, San Diego, USA) (**Table 3**) for 1.5 h at 37°C. Following another round of washing with 1% BSA in PBS, the cells were stained with 20 µg/µl PI and 100 µg/µl RNaseA in PBS for 30 min at RT.

3.8 Calcium efflux staining

Cells were initially plated onto tissue culture plates and given the opportunity to adhere overnight. On the following day, the cells underwent treatment with either 1% (v/v) DMSO, the test compounds, or ETP for 24 and 48 h. Subsequently, the cells were subjected to staining with Fluo-4 AM (#F14201; Thermo Fisher Scientific) for 1 h at 37ºC, followed by a 30-minute washing step in Hank's Balanced Salt Solution (Thermo Fisher Scientific). The next phase involved cell collection through trypsinization.

3.9 JC-1 staining

Following the completion of the treatment period, the A549 and HCT-116 cell culture medium was exchanged with fresh medium supplemented with 5 µg/ml JC-1 dye. Subsequently, the cells were incubated in the absence of light for an additional 20 min at 37°C. After this incubation, the cells underwent two washes with PBS before measurement. As a reference, 50 µM FCCP was introduced 15 min before concluding the drug treatment incubation.

3.10 Assessment of apoptosis and caspase 3/7 activation

In a nutshell, subsequent to exposure to the test compounds and ETP, A549, and HCT-116 cells were collected via trypsinization, underwent two PBS rinses, and were then subjected to staining. For apoptosis analysis, they were stained with Annexin V FITC conjugate (Thermo Fisher Scientific, #A13199), following the manufacturer's guidelines. Additionally, for the evaluation of caspase-3/7 activation, cells were stained utilizing the CellEvent™ Caspase-3/7 Green Flow Cytometry Assay Kit (Thermo Fisher Scientific, #C10427), following the manufacturer's recommended procedures. ETP was employed as a comparative reference in these experiments.

3.11 DNA fragmentation

A549 and HCT-116 cells were subjected to examination using the Terminal deoxynucleotidyl transferase dUTP nick end labeling (TUNEL) assay (Abcam, #ab66108). Post-drug treatment,

47

the procedure involved the following consecutive steps. Initially, cell samples were harvested using a trypsin solution. Subsequently, these samples were meticulously washed with PBS to remove any residual components. To stabilize their condition, the cells were then fixed using a 1% formaldehyde solution. The entirety of this experiment was executed meticulously, strictly adhering to the manufacturer's prescribed protocol, which ensured the highest level of precision and consistency. Additionally, ETP was employed as a point of reference in this study.

3.12 Relaxation of human Topo I

The assessment of inhibitory activity for the investigated compounds closely adhered to the manufacturer's protocol (Inspiralis; #HTR102). In summary, the procedure encompassed the following steps: A mixture was prepared, combining 250 ng of supercoiled pBR322 (Thermo Fisher; #SD0041), the test compounds, and a reaction buffer. The reaction was initiated by introducing diluted Human Topo I in assay buffer to the mixture. Subsequently, the samples underwent a 30 min incubation at 37°C. To halt the reaction, a loading buffer (New England BioLabs; #B7024S) was added. The samples were then loaded onto a 1% (w/v) agarose gel and subjected to electrophoresis in 1xTBE at a voltage of 20 V for an extended period of 18 h. Following electrophoresis, the gel was stained with ethidium bromide, underwent destaining in H_2O, and was subsequently photographed using the ChemiDoc Imaging System from Biorad.

3.13 Relaxation/Decatenation of human Topo IIα/IIβ

The assessment of inhibitory activity for the investigated compounds followed the manufacturer's guidelines (Inspiralis; #HT205). Here's a concise overview of the procedure: A mixture comprising 250 ng of supercoiled pBR322 (Thermo Fisher; #SD0041), the test compounds, and a reaction buffer was prepared. The reaction was initiated by the addition of diluted human Topo IIα or IIβ in assay buffer, and the samples were subsequently incubated for 30 min at 37°C. To conclude the reaction, a loading buffer (New England BioLabs; #B7024S) was introduced. The samples were loaded onto a 1% (w/v) agarose gel and subjected to electrophoresis in 1xTBE at 20 V for an extensive duration of 18 h. Following electrophoresis, the gel was stained with ethidium bromide and then destained in H_2O. The results were captured using a ChemiDoc Imaging System (Biorad). For the decatenation assay, 250 ng of kDNA (Inspiralis, #K1002) was employed. As reference points for comparison, ETP and ICRF-187 (Cayman Chemical) were utilized in this study.

3.14 Formation of cleavable complexes

The composition of the mixture paralleled that used for the relaxation of the human Topo IIα assay, with one exception: a fivefold greater amount of enzyme was employed. The sequence of events unfolded as follows. The reaction was set in motion by introducing the enzyme to the samples, initiating a 10-min incubation period at 37°C. Subsequently, 0.35% SDS and 0.3 mg/ml proteinase K from A&A Biotechnology were added, and the samples were subjected to an additional incubation at 56°C for a duration of 1 h. Following this incubation, a loading buffer (New England BioLabs, #B7024S) and chloroform: isoamyl alcohol (in a ratio of 24:1 v/v) were introduced. In this study, ETP and ICRF-187 served as reference compounds for comparative analysis. The procedure for detecting Topo I-nicked DNA remained consistent, with the exception of excluding the addition of proteinase K. The electrophoresis was conducted in the presence of EtBr at a concentration of 1 µg/ml in TBEx1.

3.15 Intercalation into DNA

The unwinding assay was executed following the manufacturer's guidelines (Inspiralis, #DUKSR002) to assess the intercalating potential of the carbazole derivatives under investigation, with ETP and DOXO serving as reference compounds. Here's a comprehensive description of the procedure: Wheat germ Topo I, pre-diluted in assay buffer, was introduced into a mixture consisting of assay buffer, the tested carbazole derivatives, and relaxed pBR322 DNA. This mixture underwent a 30 min incubation at 37°C. To halt the reaction, 50 µl of butanol and 20 µL of H_2O were added. Subsequently, the samples were vigorously vortexed, followed by centrifugation. The aqueous layer was then combined with a solution of chloroform and isoamyl alcohol in a 24:1 v/v ratio, along with a loading buffer (New England BioLabs, #B7024S).

3.16 Measurement of intracellular ROS

Cells were initially seeded onto tissue culture plates and allowed to adhere overnight. The following day, the cells were subjected to treatment with compounds at their IC_{90} concentration, 1% (v/v) DMSO, or 250 µM H_2O_2 for the specified duration. In the case of carbazole derivatives, the study also explored the effects of combined treatment with 2 mM NAC. Approximately 30 min before concluding the treatment, the cells were stained with 1 µM CM-H2DCFDA (#C6827; Thermo Fisher Scientific). Subsequently, the cells were detached through trypsinization and stained with 10 µg/ml 7-Aminoactinomycin D (7-AAD; Thermo Fisher Scientific).

3.17 Immunofluorescence

Cells (2×10^5) were initially seeded onto tissue culture plates, with a glass slide included, to allow for overnight attachment. The following day, the cells were exposed to the tested compounds or 1% (v/v) DMSO for the specified duration. After treatment, the cells underwent a series of steps: they were washed with PBS, fixed for 15 min at RT using 4% paraformaldehyde (PFA) in PBS and then permeabilized for 15 min with 0.25% Triton-X100 in PBS. Subsequently, the cells were blocked with 3% BSA in PBS-T (PBS containing 0.1% Tween-20) for 1 h at RT and incubated with primary antibodies for 1.5 h at 37°C in a humidified chamber. After the primary antibody incubation, the cells were washed three times with PBS-T and then subjected to incubation with appropriate peroxidase-conjugated secondary antibodies for 1 h in a humidified chamber at 37°C. Following this secondary antibody incubation, the cells were washed three times for 10 min each with PBS-T, stained with 0.25 µg/ml DAPI for 15 min, and finally mounted onto slides using PBS-glycerol (90%) containing 2.5% (w/v) DABCO. Image acquisition was performed utilizing an LSM 800 inverted laser-scanning confocal microscope from Carl Zeiss, which featured an airyscan detector and utilized a ×63 1.4 NA Plan Apochromat objective. During image acquisition, parameters such as laser intensity, exposure times, and gain settings were kept consistent for both the cells treated with compounds and those treated with DMSO. The specific antibodies used are detailed in **Table 3**.

3.18 Universal Tyrosine Kinase Assay Kit

Protein tyrosine kinase activity in A549 cell extract was assessed utilizing the Universal Tyrosine Kinase Assay Kit (#MK410; TaKaRa, Shiga, Japan), following the manufacturer's provided instructions. In brief, A549 cells were first collected using an extraction buffer and then subjected to centrifugation (10000 g, 10 min, 4°C). Subsequently, each sample was mixed with a solution containing 40 mM ATP-2Na and incubated for 30 min at 37°C. Following incubation, the sample solution was removed, washed four times with a washing solution, and subsequently blocked with a blocking solution for 30 min at 37°C. Next, an anti-phosphotyrosine (PY20)-HRP solution was added to each well and incubated for 30 min at 37°C. After this incubation, the wells were washed four times and incubated with HRP substrate solution for 20 min at 37°C, followed by halting the reaction using a stop solution. The absorbance at 450 nm was then measured using an ASYS UVM340 microplate reader from Biochrom Ltd. The calculation of PTK activity was carried out employing the PTK standard curve supplied within the kit.

50

3.19 Phospho-flow cytometry

Cells were initially seeded onto tissue culture plates and allowed to adhere overnight. Following this, the complete medium was replaced with a medium containing 1% FBS, and cells were left to incubate for 12 h prior to any stimulation. Subsequently, the cells were pretreated with compounds for 45 min, washed, and exposed to the same compounds in the presence of 20% FBS for an additional 75 min. The cells were then gently detached using 1 mM EDTA in PBS, washed 2-3 times with PBS, and harvested through centrifugation (1100 rpm, 5 min, 4°C). After this, the cells were fixed with 4% PFA in PBS for 15 min at 4°C, followed by another round of centrifugation (1100 rpm, 5 min, 4°C). Following fixation, the cells were permeabilized by slowly adding 4.5 ml of ice-cold 100% methanol to the pre-chilled cells suspended in 0.5 ml of PBS, gently vortexing to reach a final concentration of 90% methanol. The samples were then left to incubate for 45 min on ice. Next, the cells were washed with incubation buffer (0.5% BSA in PBS), subjected to centrifugation (1100 rpm, 5 min, 4°C), and subsequently blocked with blocking buffer at RT for 30 min. The cells were then exposed to anti-p-Tyr-100 (1:1500 dilution; #9411; Cell Signaling, Danvers, USA) antibody (**Table 3**) at RT for 1 h, followed by incubation with anti-mouse IgG cross-adsorbed secondary antibody conjugated to DyLight 488 (1:200 dilution; #SA5-10166; Thermo Fisher Scientific) for 30 min at RT. Subsequently, the cells underwent two PBS-T washes and were stained with 7-AAD and RNaseA (50 µg/ml) in the dark at RT for 15 min.

3.20 Live-cell imaging

For live-cell imaging of A549 and HCT-116 cells, JC-1 and Annexin V-FITC staining procedures were employed. These cells were initially seeded into glass-bottom 24-well plates. The drug-treated samples were subjected to the same staining processes as utilized in flow cytometry analysis. To visualize cell nuclei, Hoechst33342 was utilized. The acquisition of images was accomplished using an LSM 800 inverted laser-scanning confocal microscope from Carl Zeiss, equipped with a ×63 1.4-NA Plan Apochromat objective (Carl Zeiss) and an airyscan detector, which facilitated high-resolution confocal scanning. Throughout the analysis, an incubation chamber was maintained at 37°C with a 5% CO_2 atmosphere. In this study, ETP served as a reference standard for comparative purposes.

3.21 *In situ* assay for cellular senescence using β-Galactosidase

The β-Galactosidase assay followed a protocol based on Dimri et al. with minor adjustments [272]. Briefly, cells were treated with either 1% (v/v) DMSO or test compounds for 72 h at 37°C in a 5% CO_2 atmosphere. Afterward, the medium was replaced with fresh medium, and cells were further cultured for 48 h. Next, the cells underwent two rounds of PBS washing and were

fixed with a solution containing 2% formaldehyde and 0.2% glutaraldehyde for 5 min at RT. After fixing, the cells were washed twice with PBS and incubated with β-Gal staining buffer (comprising 5 mM Potassium Ferricyanide, 5 mM Potassium Ferrocyanide, 2 mM $MgCl_2$, 6 M NaCl, and 1 mg/ml X-Gal in a citrate/sodium phosphate buffer of 40 mM pH 6) for 16 h at 37°C without CO_2. Following staining, the cells were washed with citric acid and phosphate buffer (40 mM, pH 4). Subsequently, the slides were washed twice in PBS and mounted using a mounting medium (composed of 90% glycerol and 2.5 mg DABCO). Image acquisition was performed using a fluorescence microscope (Olympus BX60; Tokyo, Japan) equipped with an appropriate filter.

3.22 Western blot

Cells were seeded onto tissue culture plates with a glass slide to attach overnight. The following day, cells were treated with compounds at their IC_{90} concentration for 24 and 48 h. Negative control cells were treated with 1% (v/v) DMSO. Total protein content was extracted from the cells using NP-40 cell lysis buffer (containing 10 mM Tris-HCl pH 7.4, 10 mM NaCl, 3 mM $MgCl_2$, 0.5% Nonidet P-40, and cOmplete Mini EDTA-free Protease Inhibitor Cocktail). Subsequently, 30 μg of protein extract was separated by 4-15% sodium dodecyl sulfate-polyacrylamide gel electrophoresis, followed by transfer onto microporous polyvinylidene difluoride membranes (Bio-Rad). The membranes were then blocked with 5% (w/v) non-fat dry milk or bovine serum albumin in TBST (Tris-buffered saline with 0.1% [v/v] Tween 20) buffer (comprising 0.2 M Tris-base, 0.137 M NaCl, and 0.1% Tween 20) for 1 h at RT. They were subsequently incubated overnight with primary antibodies at 4°C. Afterward, the membranes underwent three washes with TBST, followed by incubation with appropriate peroxidase-conjugated secondary antibodies for 1 h at RT, and another round of washing. Proteins were then detected using an enhanced chemiluminescence detection reagent kit (Thermo Fisher Scientific) and a ChemiDoc XRS+ Imaging System (Bio-Rad). Band intensity was quantified using Image Lab 5.2 software (Bio-Rad). Details of all antibodies used are provided in **Table 2**.

3.23 Statistical analyses

Statistical analysis was carried out using GraphPad Prism 9 software. A consistent set of significance levels was applied across the entire manuscript, with the following conventions: ns for non-significant ($p > 0.01$); * for $p < 0.01$; ** for $p < 0.001$; *** for $p < 0.0001$; and **** for $p < 0.00001$. The determination of statistical significance was made in comparison to the DMSO-treated control (1% v/v) using either one or two-way ANOVA methods.

4. RESULTS

4.1 Carbazoles exhibit a strong cytotoxic effect

The primary objective of this study was to investigate the potential cytotoxic effects of carbazole derivatives which is further important for study of cellular mechanisms. This investigation involved performing the MTT assay following a 72 h incubation period with these compounds. To assess their cytotoxicity, a total of 10 cell lines were utilized. These encompassed various cancer cell lines, including A549, H226, H460, GLC4 (lung), HCT-116, HT-29 (colorectal), MCF-7 (breast), U-2 OS (bone), U-87 MG (brain), and HepG2 (liver). Additionally, two non-cancer cell lines, namely HEK293 (human embryonic kidney cells) and HaCat (human keratinocytes), were employed. These two cell lines are commonly used as *in vitro* cell models to assess the toxicity of both drugs and natural products [273,274]. Furthermore, normal cell lines NHBE (human bronchial epithelial cells) and human breast epithelial cells were incorporated into the study.

The results obtained demonstrated that all three tested carbazole derivatives exhibited significant cytotoxic activity in the nanomolar range against most of the cancer cell lines. These findings were quantified in terms of IC_{50} values and are presented in **Table 5**. Among these compounds, **27a** emerged as the most potent, with an IC_{50} below 1 μM for all the investigated cell lines, including HEK293. Similarly, **36b** demonstrated growth inhibition activity similar to that of **27a** for the majority of the tested cell lines, except for U-87 MG and GLC4 cells, where the IC_{50} values were 1.40±0.24 μM and 1.07±0.44 μM, respectively. In contrast, compound **36a** exhibited varying levels of cytotoxicity, with the highest activity against HCT-116 cells (IC_{50} = 0.48±0.06 μM) and the lowest against U87-MG cells (IC_{50} = 2.19±0.30 μM). Notably, the impact of **36a** on HEK293 cells was comparable to the IC_{50} value of etoposide (ETP), which was employed as a reference. The cytotoxic activity observed against normal cell lines (NHBE, HMEC) suggests that these compounds are non-selective and may have different mechanisms of action. The IC_{90} concentration, determined after a 72 h incubation with the compounds, was selected for the subsequent experiments based on the results obtained from the MTT test.

Table 5 *In vitro* assessment of anticancer activity examined compounds after 72 h of treatment, with IC_{50} values expressed as mean ± standard error (SD) in micromoles (μM). The IC_{50} value signifies the concentration at which 50% of cell growth is inhibited. ETP was used as a control.

Cell line	27a	36a	36b	ETP
A549	0.26±0.12	0.93±0.15	0.60±0.10	0.54±0.21
HCT-116	0.22±0.04	0.48±0.06	0.27±0.11	0.39±0.01
MCF-7	0.79±0.21	1.39±0.29	0.83±0.21	0.83±0.15
U-2 OS	0.37±0.05	0.99±0.18	0.71±0.06	0.61±0.04
U-87 MG	0.45±0.15	2.19±0.30	1.40±0.24	11.86±1.31
H226	0.46±0.04	0.96±0.09	0.67±0.12	1.03±0.16
H460	0.29±0.02	0.98±0.18	0.62±0.05	0.05±0.01
GLC4	0.38±0.13	1.14±0.49	1.07±0.44	ND
HT-29	0.39±0.21	0.72±0.19	0.45±0.06	2.12±0.21
HepG2	0.63±0.17	1.17±0.23	1.62±0.21	7.12±0.16
HaCat	0.53±0.13	0.93±0.21	0.84±0.17	0.46±0.08
HEK293	0.19±0.07	1.65±0.13	0.32±0.11	1.91±0.97
NHBE	0.11±0.1	0.08±0.12	0.78±0.06	4.21±0.23
HMEC	0.36±0.14	0.82±0.23	0.55±0.27	ND

For further investigations aimed at determining and comparing the antiproliferative properties of **27a**, **36a**, and **36b** against various cancer cell lines, A549, HCT-116, MCF-7, and U-2 OS were selected. The selection of cell lines was justified by comparing the cellular effects induced by carbazole derivatives on cell lines derived from different tissues: lungs, colon, breast, and bone. Additionally, their cytotoxic activity was assessed after 24 h and 48 h. As indicated in **Table 6**, the metabolic activity of the examined cancer cells consistently decreased over time when exposed to all the compounds.

Table 6 *In vitro* assessment of anticancer activity examined compounds after 24 h, 48 h, and 72 h of treatment, with IC_{50} values expressed as mean ± standard error (SD) in micromoles (μM).

A549			
Compound	**24h**	**48h**	**72h**
27a	0.98±0.14	0.75±0.22	0.26±0.12
36a	1.96±0.21	1.20±0.16	0.93±0.15
36b	1.39±0.21	0.98±0.12	0.60±0.10

HCT-116			
Compound	**24h**	**48h**	**72h**
27a	2.19±0.26	0.85±0.20	0.22±0.04
36a	4.47±0.32	1.59±0.27	0.48±0.06
36b	3.39±0.37	0.99±0.13	0.27±0.11

MCF-7			
Compound	**24h**	**48h**	**72h**
27a	2.54±0.54	1.21±0.43	0.79±0.21
36a	4.25±1.21	2.31±0.24	1.39±0.29
36b	3.67±0.65	1.95±0.32	0.83±0.21

U-2 OS			
Compound	**24h**	**48h**	**72h**
27a	1.81±0.28	0.95±0.14	0.37±0.05±
36a	3.99±0.81	2.05±0.45	0.99±0.18±
36b	2.86±0.54	1.54±0.31	0.71±0.06±

4.2 Carbazole derivatives demonstrate significant antiproliferative potency

The BrdU assay is a method that involves replacing thymidine with BrdU, a thymidine analogue, in the DNA of actively dividing cells. Once BrdU is integrated into the DNA, it is then detected using an immunoassay. As a result, the BrdU assay is frequently employed to assess the antiproliferative effects of potential anticancer compounds [275].

Carbazole derivatives demonstrate robust antiproliferative activity. To further illustrate this, the BrdU incorporation assay was employed to assess their effects on selected cancer cells *in vitro*. Treatment with equitoxic concentrations of these compounds resulted in a time-dependent reduction in DNA synthesis across nearly all of the examined cell lines (**Figure 24**). Notably, the U-2 OS cell line displayed the least pronounced antiproliferative effect, whereas HCT-116 cells exhibited the most substantial impact (**Figure 24**).

The BrdU incorporation assay provided insights into the inhibition of BrdU incorporation by all tested carbazoles in the A549, HCT-116, and MCF-7 cell lines, with **36b** demonstrating the highest potency. This particular compound displayed its most significant antiproliferative effects on the A549 and HCT-116 cell lines, leading to an approximate 4-fold and 3.5-fold decrease in BrdU-positive cells, respectively (**Figure 24**). Collectively, these findings suggest that carbazole derivatives hold the potential to inhibit cancer cell proliferation in an *in vitro* setting.
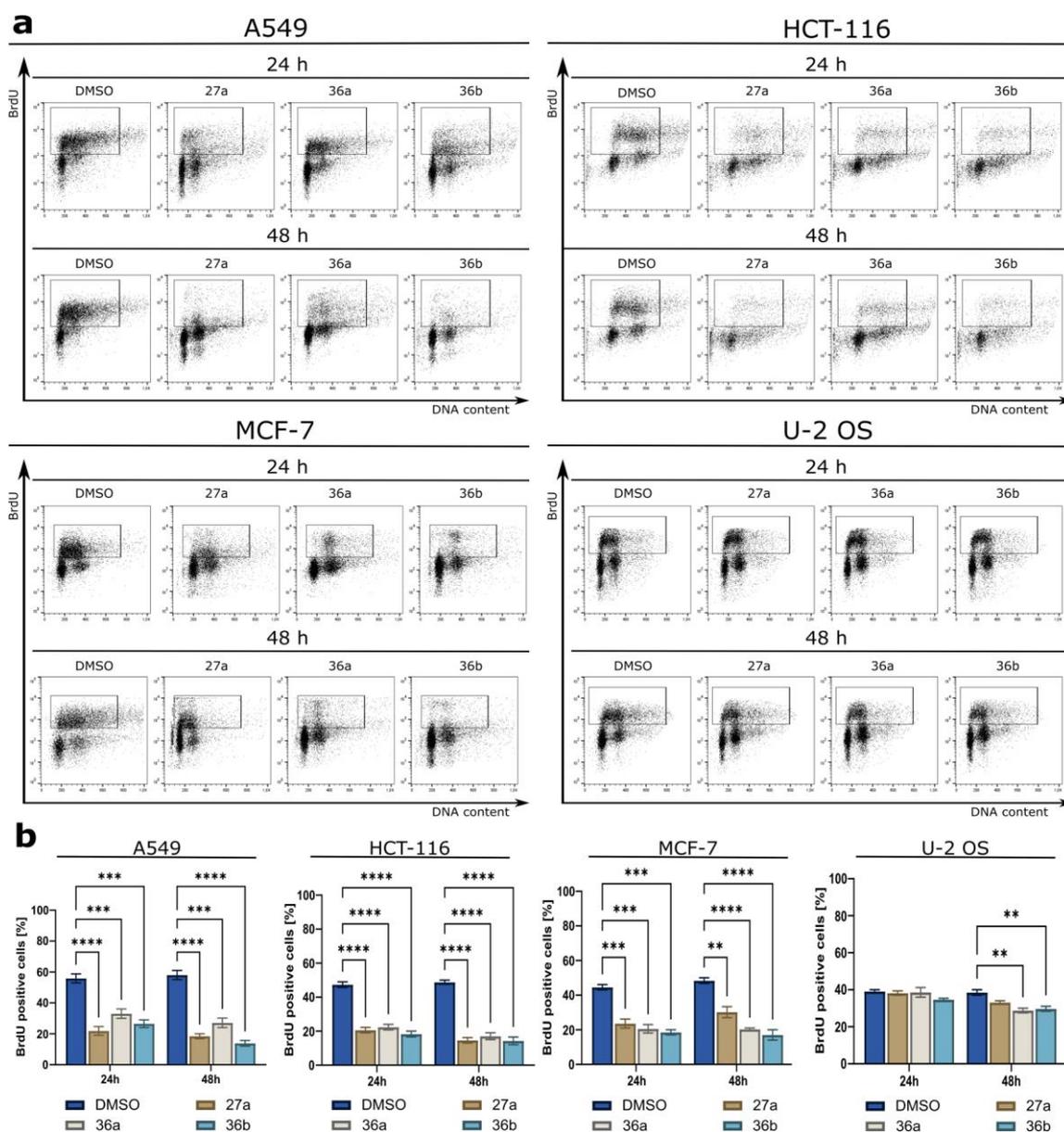
Figure 24 Analysis of BrdU incorporation through cytometry was conducted on A549, HCT-116, MCF-7, and U-2 OS cells following treatment with compounds **27a**, **36a**, and **36b** for either 24 or 48 h. Representative histograms and subsequent statistical assessments were performed after DNA staining (a). The quantification analysis results are depicted in bar graphs (b). Error bars represent the mean ± SD of data derived from three independent experiments. Statistical analysis was carried out using the two-way ANOVA test.

4.3 Carbazole derivatives interfere with the progression of the cell cycle

Flow cytometry-based cell cycle analysis primarily relies on assessing DNA content through staining with PI. The precise stoichiometric properties of PI guarantee the reliable quantification of DNA content, enabling the differentiation of cells in the G1, S, and G2 cell cycle phases, as well as the sub-G1 cell death stage, which is marked by DNA fragmentation [276]. Carbazole derivatives were investigated for their impact on cell cycle progression by tracking the phases of A549, HCT-116, MCF-7, and U-2 OS cells following exposure to equitoxic concentrations of the compounds for 24 and 48 h. The cell cycle profiles illustrated in **Figure 25** reveal that all carbazole derivatives induced significant G0/G1 arrest (***p<0.0001) in A549 cells, accompanied by a decrease in the G2/M phase. Among the tested compounds, only **36a** demonstrated a time-dependent increase in the number of HCT-116 cells in the G0/G1 phase (**Figure 25**). In MCF-7 cells, all carbazole derivatives led to a notable, time-dependent rise in the G0/G1 phase, along with a concurrent reduction in the S phase compared to cells treated with DMSO alone. The most potent cell cycle blockade was observed after 48 h of exposure to **36b**, resulting in a substantial increase in the G0/G1 phase (59.85±2.15%; ****p<0.00001) (**Figure 25**). The time-dependent treatment of U-2 OS cells caused a ~1.7-fold increase in the number of cells in the G2/M phase compared to DMSO-treated cells, accompanied by a reduction in the G0/G1 phase (**Figure 25**). These findings suggest that carbazole derivatives have the potential to induce G0/G1 arrest in A549 and MCF-7 cells while increasing the number of cells in the G2/M phase in U-2 OS cells. The divergent responses of these cells to carbazole treatment may be attributed to their distinct genetic profiles and variability in sensitivity to these compounds. Alternatively, carbazole derivatives may target different biological processes in the two types of cell lines.
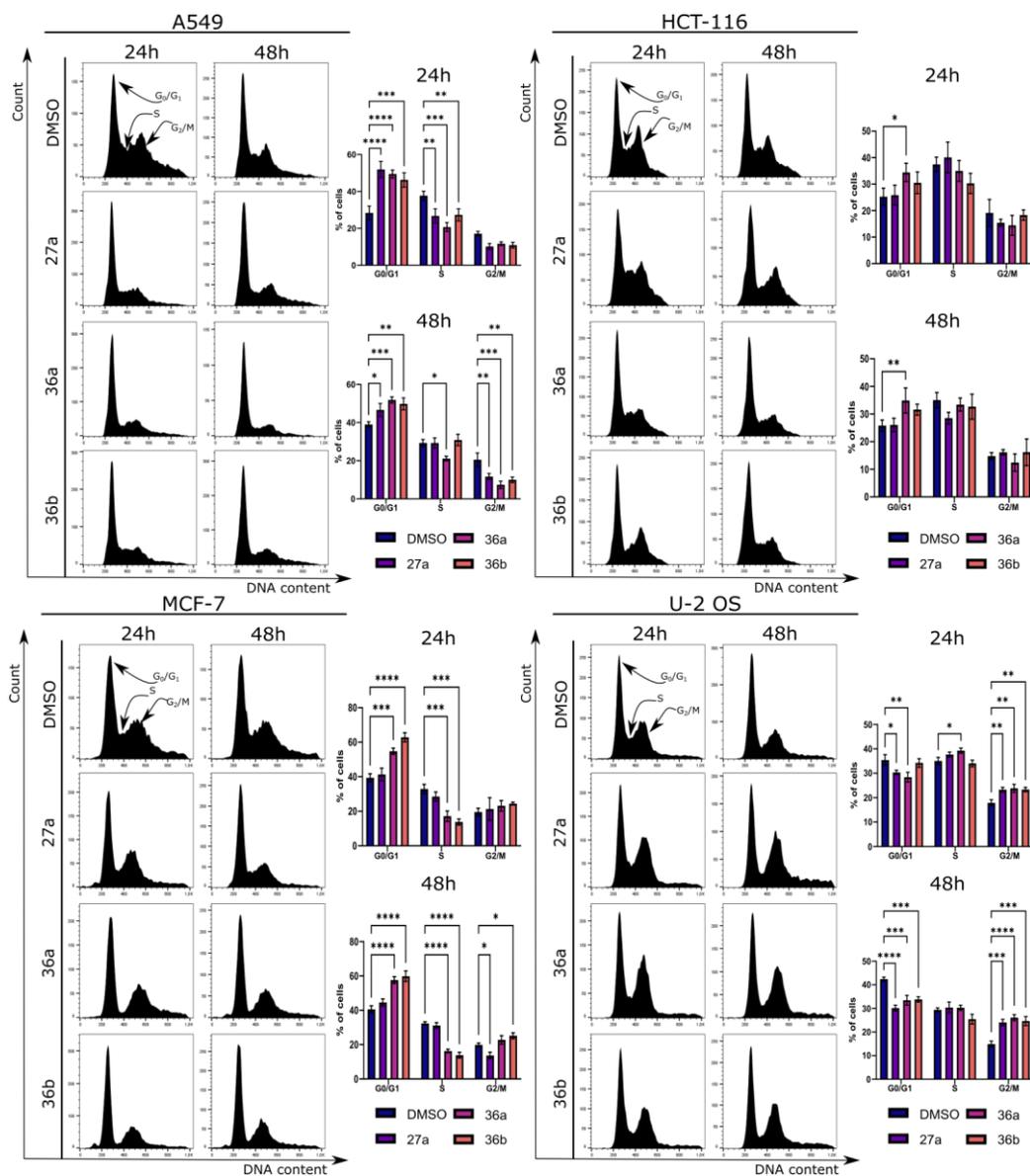
Figure 25 The cell cycle characteristics of A549, HCT-116, MCF-7, and U-2 OS cells following exposure to **36a**, **36b**, and **27a** are depicted. Representative histograms derived from propidium iodide staining and their respective quantification are displayed in the bar charts. Error bars denote the mean ± SD of data gathered from three independent experiments. Statistical analysis was carried out using the two-way ANOVA test.

4.4 Carbazole derivatives inhibit the capability to form colonies

Expanding on the most promising cytotoxicity and antiproliferative effects observed with **27a**, **36a**, and **36b** on A549 and HCT-116, these two cell lines were selected for more comprehensive biological investigations. To delve deeper into the impact of carbazole derivatives on cancer cell growth, A549, and HCT-116 cells underwent a clonogenic assay. The findings from this assay revealed that treatment with carbazole derivatives led to a significant reduction in the number of colony-forming cells in comparison to control cells treated with DMSO (**Figure 26**). Specifically, the administration of compounds **27a** and **36a** resulted in a concentration-dependent decrease in colony formation in both tested cell lines. However, compound **36b** exhibited relatively lower inhibitory activity against the A549 cell line ($p > 0.01$).
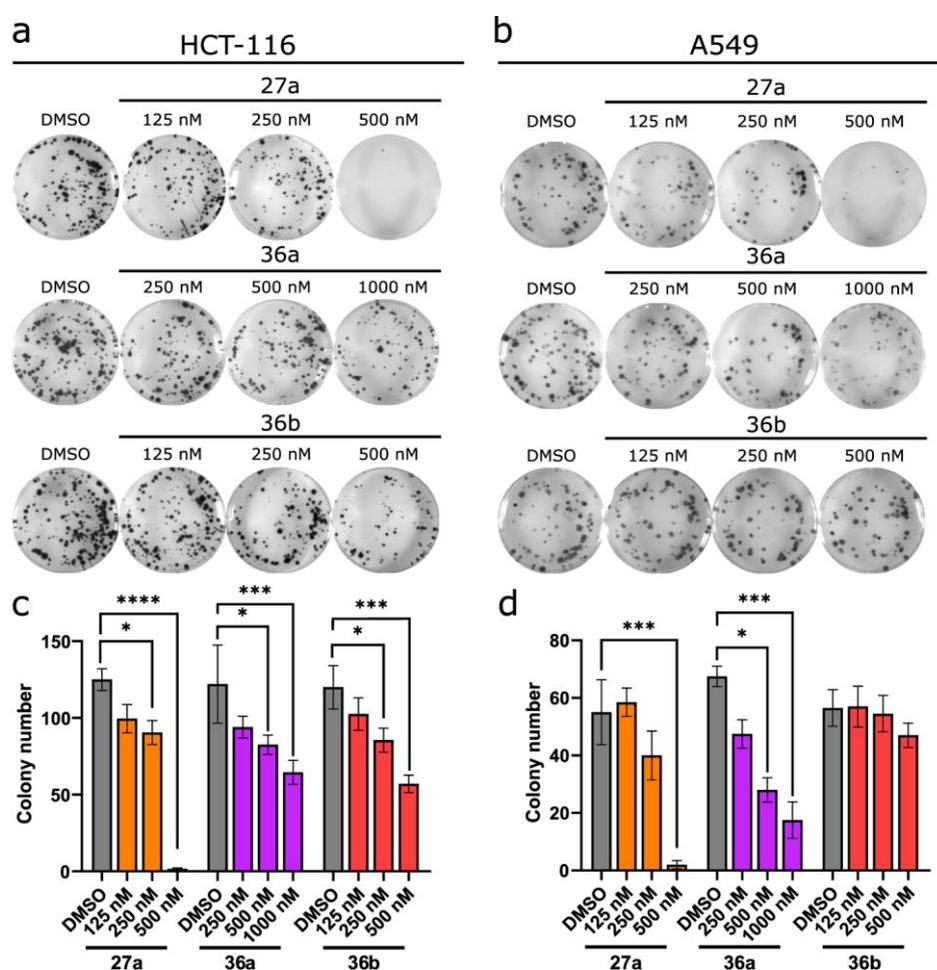
Figure 26 The colony-forming capability of HCT-116 and A549 cells following exposure to **27a**, **36a**, and **36b** was assessed. Representative images from the clonogenic assay for HCT-116 and A549 cell lines (a, b) and their quantification (c, d) are presented. The data presented here represent the mean ± SD of results obtained from three independent experiments. Statistical analysis was carried out using the two-way ANOVA test.

4.5 Carbazole derivatives inhibit human Topo II

Human Topo II possesses the capability to alleviate supercoiled DNA. In this particular test, the substrate utilized is supercoiled pBR322, which the enzyme relaxes. These two plasmid forms can be distinguished through agarose gel electrophoresis. This method serves as a means to evaluate the effectiveness of various compounds as Topo II inhibitors.

To explore the potential of carbazole derivatives as inhibitors of Topo II, a pBR322 DNA relaxation assay in the presence of both Topo IIα and Topo IIβ was conducted. As depicted in **Figures 27a** and **27b**, the tested compounds exhibited concentration-dependent activity against both isoforms of Topo II. Notably, compound **36a** fully inhibited DNA relaxation in the presence of Topo IIα at the highest concentrations (20-100 µM) but did not affect the activity of Topo IIβ. These results suggest that compound **36a** selectively inhibits the relaxation activity of Topo IIα. Furthermore, compounds **36b** and **27a** moderately affected the functionality of both Topo IIα and Topo IIβ, inhibiting the relaxation of supercoiled DNA at the highest tested concentrations. In contrast, ETP and ICRF-187 completely inhibited relaxation activity with respect to Topo IIα but exerted relatively weaker inhibitory effects against Topo IIβ compared to the negative control (**Figures 27a** and **27b**).

Intercalators are comprised of flat, typically polycyclic, aromatic structures that have the capacity to insert themselves between the base pairs of the double-stranded DNA molecule [277]. Compounds capable of intercalation into DNA or binding within its grooves can induce localized unwinding of the DNA helix, resulting in a reduction in the DNA's overall twist. In cases where a DNA molecule undergoes nicking and rejoining (e.g., through the action of a Topo) in the presence of such a compound, it leads to the formation of a relaxed, underwound DNA structure. Upon removal of the enzyme and the intercalating compound, this relaxed DNA configuration transitions back to its supercoiled state. The formation of supercoiled DNA under these conditions serves as an indicator of the presence of an intercalating compound [278]. To assess the intercalating properties of the tested compounds, a DNA unwinding assay using Topo I and relaxed pBR322 DNA as substrates was performed. ETP, a non-intercalating agent, and DOXO, an intercalating agent, were used as controls. The results, presented in **Figure 27c**, indicate that the carbazole derivatives were unable to convert relaxed plasmid DNA into the supercoiled form in the presence of Topo I. These findings strongly suggest that compounds **36a**, **36b**, and **27a** act as non-intercalating Topo inhibitors, indicating a distinct mechanism of action from intercalating agents like DOXO.
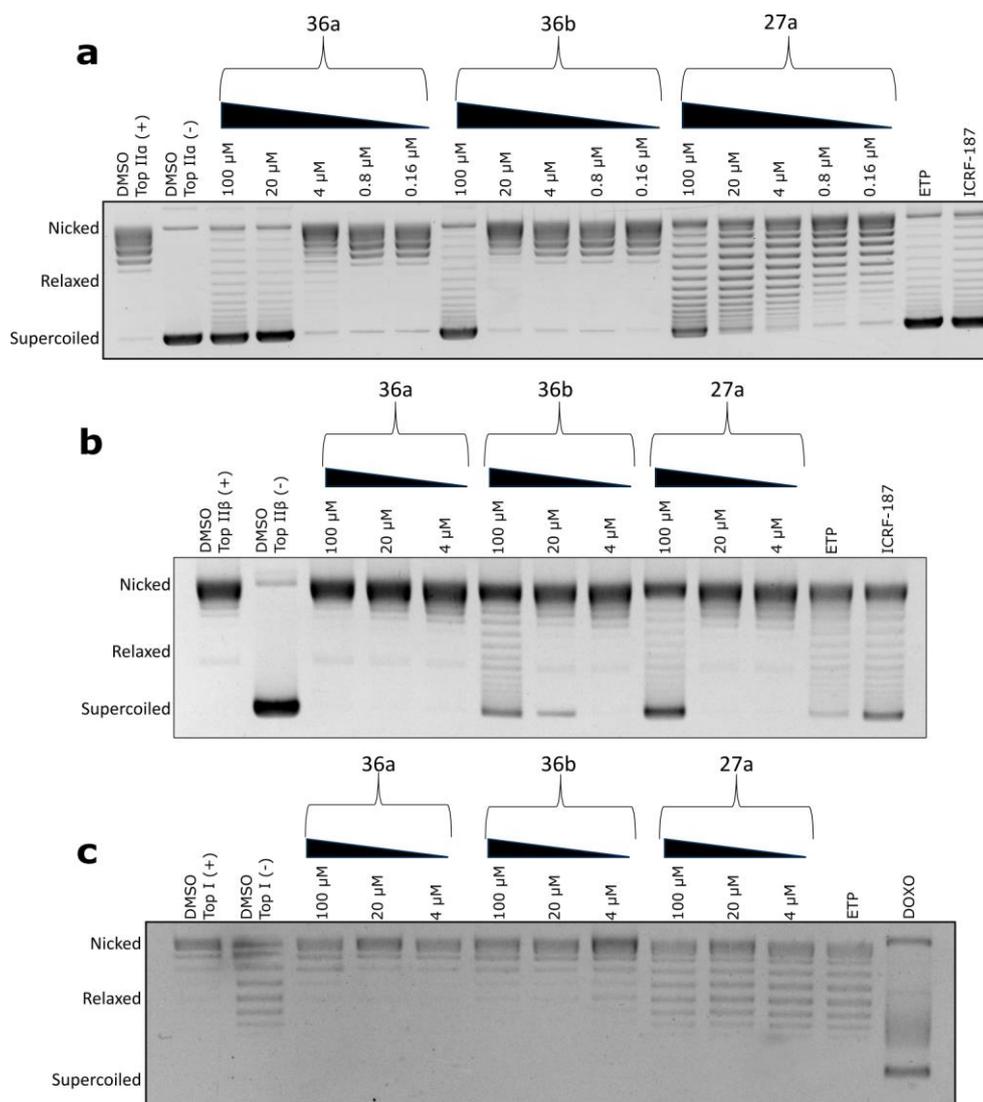
Figure 27 Inhibition of Topo IIα (a) and Topo IIβ (b) mediated pBR322 relaxation. The experiment was conducted with either Topo IIα/IIβ in the presence of the solvent (DMSO Top IIα/IIβ (+)) or with varying concentrations of carbazole derivatives. ETP (100 μM) and ICRF-187 (100 μM) served as reference compounds. (c) Unwinding assay. Evaluation of the capacity of carbazole derivatives to intercalate into DNA in the presence of Topo I. ETP and DOXO (10 μM) were employed as negative and positive controls, respectively.

4.6 Carbazole derivatives are not Topo IIα poisons

Topo II plays a vital role in decatenation, a process required for the separation of catenated DNA duplexes at the end of replication [122]. To assess the ability of carbazole derivatives to inhibit the catalytic decatenation activity of Topo II, electrophoretic separation experiments using highly knotted circular kDNA and the respective Topo II isoforms were conducted (**Figures 28a** and **28b).**

In the absence of Topo II, the high molecular weight kDNA remained stationary in the well of the negative control. Compound **36a** demonstrated effective and concentration-dependent inhibition of Topo IIα-mediated decatenation across the concentration range of 4-100 μM (**Figure 28a**). Conversely, compounds **36b** and **27a** either completely inhibited decatenation only at the highest concentration tested or partially inhibited the decatenation of higher-order catenates containing two, three, four, or more minicircles (**Figure 28a**). These catenates migrated more slowly through the gel compared to the decatenated kDNA.

To comprehensively assess the inhibitory effects of the compounds on both Topo II isoforms, I conducted a decatenation assay using Topo IIβ. Consistent with the results obtained from the relaxation test (**Figures 27a** and **27b**), **36a** displayed significantly lower inhibitory activity against Topo IIβ (**Figure 28b**), partially inhibiting decatenation only at the highest concentration tested. In comparison, **36b** exhibited similar levels of activity against both Topo IIα and Topo IIβ. Interestingly, compound **27a** completely inhibited decatenation in the presence of Topo IIβ at a concentration of 100 μM (**Figure 28b**). It's noteworthy that ICRF-187, known for reducing the catalytic activity of Topo II, demonstrated a more pronounced effect than ETP, which stabilizes the cleavage complex of DNA/Topo II.

To determine whether carbazole derivatives could be classified as Topo II poisons, a DNA cleavage assay using Topo IIα and pBR322 plasmid was conducted. The results, as seen in **Figure 28c**, demonstrate that only ETP, a well-known Topo II poison, induced a significant amount of linear plasmid visible on the gel. This suggests that compounds **36a**, **36b** and **27a** do not stabilize the covalent cleavage complex formed between Topo II and DNA, unlike the effects of ETP. To further confirm this, I repeated the cleavage assay in the presence of ETP to establish whether **36a** could inhibit Topo IIα similarly to ICRF-187 by stabilizing the non-covalent Topo II/DNA complex after the Topo II/DNA cleavage complex had been induced by ETP treatment (**Figure 28d**). Co-treatment with **36a** reduced the level of linear plasmid compared to ETP and ICRF-187, indicating that **36a** prevented the formation of the ETP-induced DNA cleavage reaction with Topo IIα. Further investigation is necessary to identify the specific step or steps of the Topo II catalytic cycle that **36a** affects.
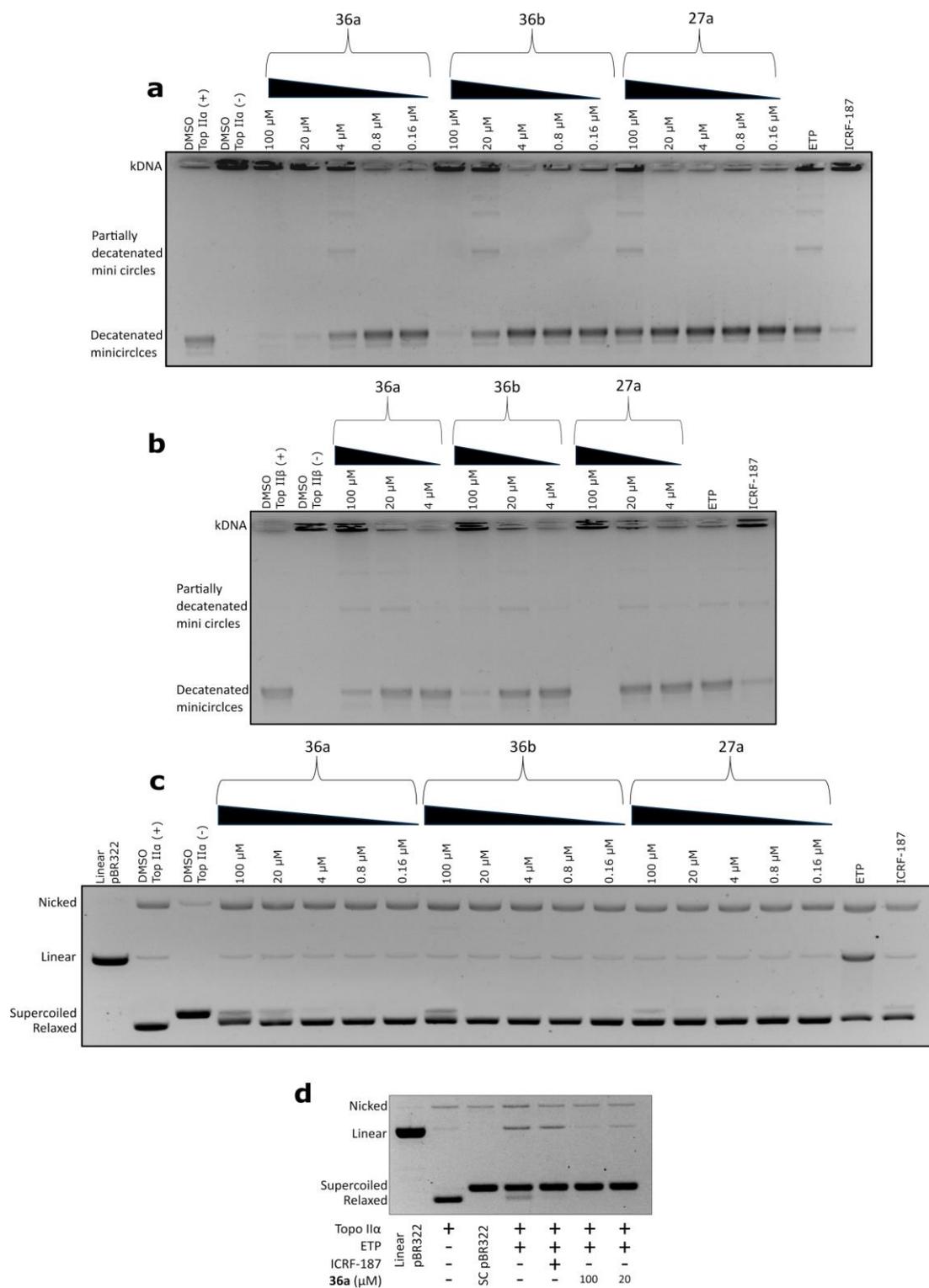
Figure 28 Inhibition of Topo IIα/IIβ-mediated kDNA decatenation by carbazoles. The experiment was conducted with either Topo IIα/IIβ in the presence of the solvent (DMSO Top IIα/IIβ (+)) or with varying concentrations of carbazole derivatives (a, b). DNA cleavage assay was conducted in the presence of **36a**, **36b**, and **27a**, respectively (c). DNA cleavage assay involving the co-treatment of **36a** with ETP (d). ETP (100 µM) and ICRF-187 (100 µM) were employed as reference compounds.

64

4.7 36a acts as a dual inhibitor of both Topo IIα and Topo I

Topo I plays a crucial role in unwinding both positively and negatively supercoiled DNA by creating single-stranded breaks in the DNA molecule. In contrast to Topo II, Topo I does not rely on ATP for its activity. Both Topo I and Topo II are established targets for cancer therapy. These two targets have overlapping functions in DNA metabolism and play essential roles in the normal cell cycle progression. Therefore, simultaneous targeting of both Topo I and Topo II could potentially lead to synergistic anticancer effects [168].

In order to evaluate the inhibitory effects of carbazole derivatives on Topo I activity, a relaxation test was performed. The results displayed in **Figure 29a** demonstrate that compound **36a** displayed the most pronounced inhibitory effects on Topo I, notably restraining the enzyme within the concentration range of 4-100 µM. This outcome is similar to the activity of **36a** against Topo IIα, as shown in **Figure 27a**. Compounds **27a** and **36b** displayed a moderate inhibitory effect on Topo I, with a noticeable reduction in enzyme activity observed only at the highest tested concentration. A 10 µM concentration of CPT was used as a reference. In order to determine if **27a**, **36a**, and **36b** function as a Topo I poison similar to CPT, DNA cleavage in the presence of Topo I was examined by electrophoretically separating nicked monomers from relaxed and supercoiled monomers in the presence of EtBr. As illustrated in **Figure 29b**, a clear, prominent band signifying extensive nicked DNA is observed only in the lane with CPT. This implies that carbazole derivatives employ a different mechanism to inhibit Topo I when compared to CPT. Additional studies are needed to verify and clarify the inhibitory mechanism of **36a** on Topo I.

65
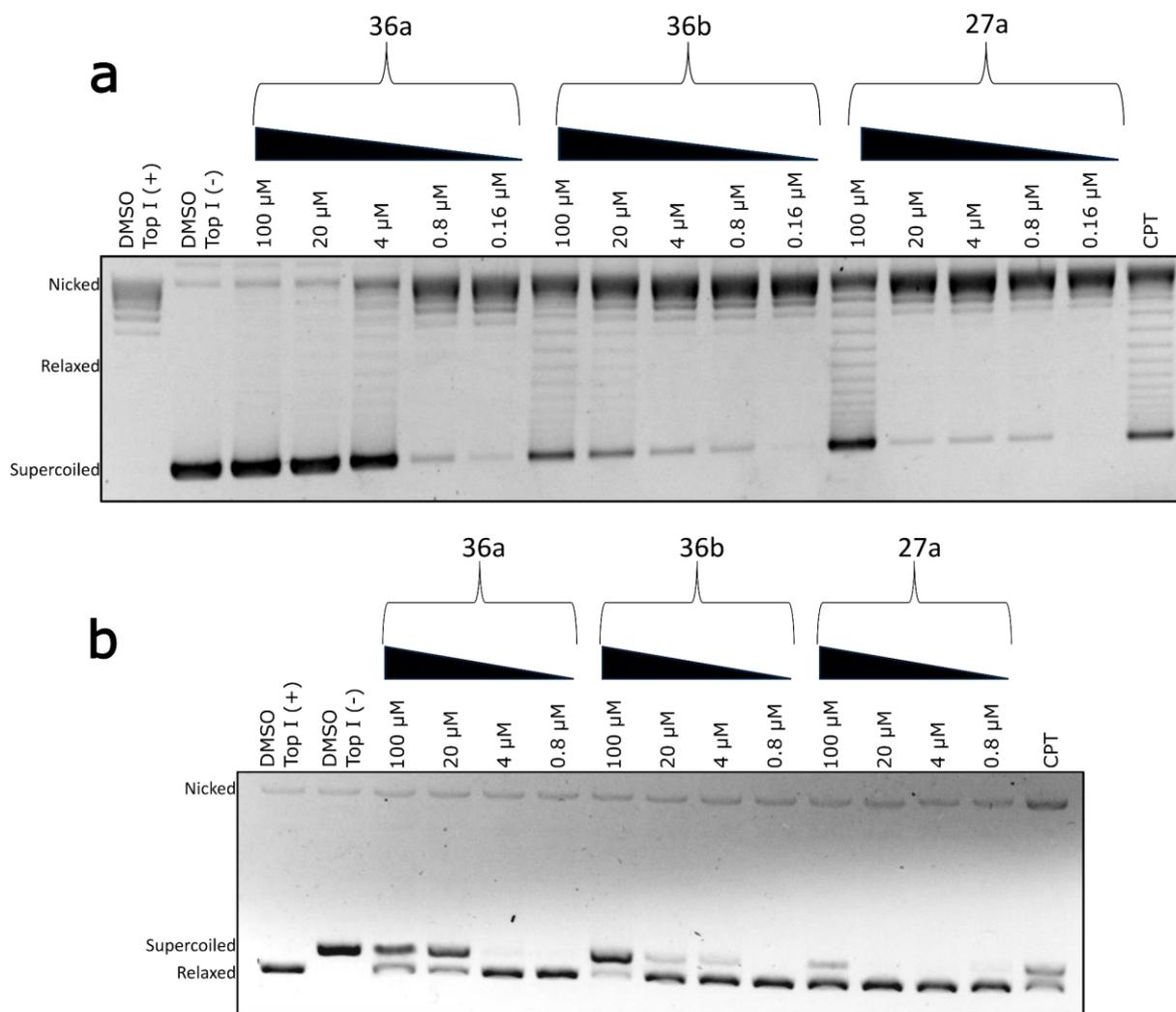
Figure 29 Inhibition of human Topo I mediated pBR322 relaxation. The experiment was conducted with Topo I in the presence of the solvent (DMSO Top I (+)) or with varying concentrations of carbazole derivatives (a). The cleavage of DNA in the presence of Topo I was examined through electrophoretic separation of the nicked monomers from the relaxed and supercoiled monomers in the presence of EtBr (b). CPT (10 μM) served as a reference compound.

66

4.8 Carbazoles trigger alterations in the cancer cell morphology

Evading apoptosis is a fundamental characteristic of tumour transformation. Commonly employed chemotherapeutic agents are designed to stimulate apoptosis, with Topo inhibitors, among others, being the most potent activators of this process [279]. Apoptosis exhibits a distinct set of characteristic morphological changes, including cellular shrinkage, fragmentation into apoptotic bodies enclosed by membranes, and swift engulfment by neighbouring cells [280]. For many years, internucleosomal fragmentation of genomic DNA has served as the biochemical signature of apoptosis. The orchestrated nature of the cell death process underscores the presence of well-preserved molecular pathways [281,282]. To assess alterations in nuclear morphology after a 24 h treatment with these compounds, confocal imaging was conducted using Annexin V-FITC and Hoechst33342 staining on A549 and HCT-116 cell lines. As illustrated in **Figures 30** and **31**, compounds **27a**, **36a**, and **36b** exhibited distinct features associated with cells undergoing apoptosis, including numerous shrunken cells, fragmented nuclei, and the presence of apoptotic bodies. Annexin V is a qualitative tool for identifying cells displaying phosphatidylserine (PS) on their cell surface, a phenomenon observed in apoptosis and various other types of cell death [283]. Furthermore, confocal imaging using Annexin V-FITC staining indicates that the examined carbazole derivatives, similar to the reference compound used, induce the process of apoptotic cell death in A549 and HCT-116 cell lines (**Figures 30** and **31**).
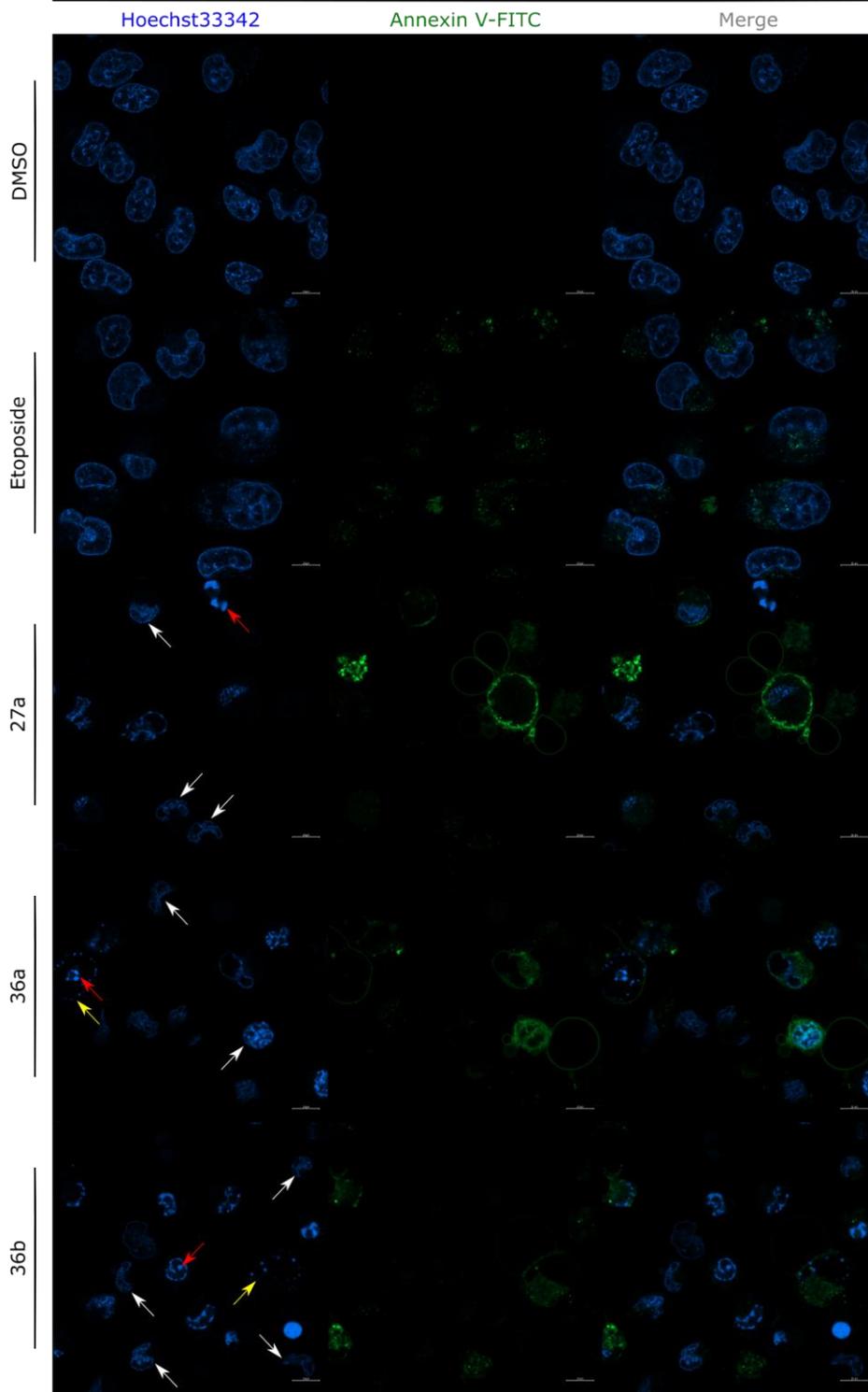
Figure 30 Confocal microscopy was employed to capture images of A549 cells after 24 h of exposure to carbazole derivatives, ETP, or DMSO. These cells were stained with Hoechst33342 and Annexin V-FITC, and the scale bar represents 10 μm. Notably, cell shrinkage (white arrows), fragmented nuclei (red arrows), and the presence of apoptotic bodies (yellow arrows) are observable features.
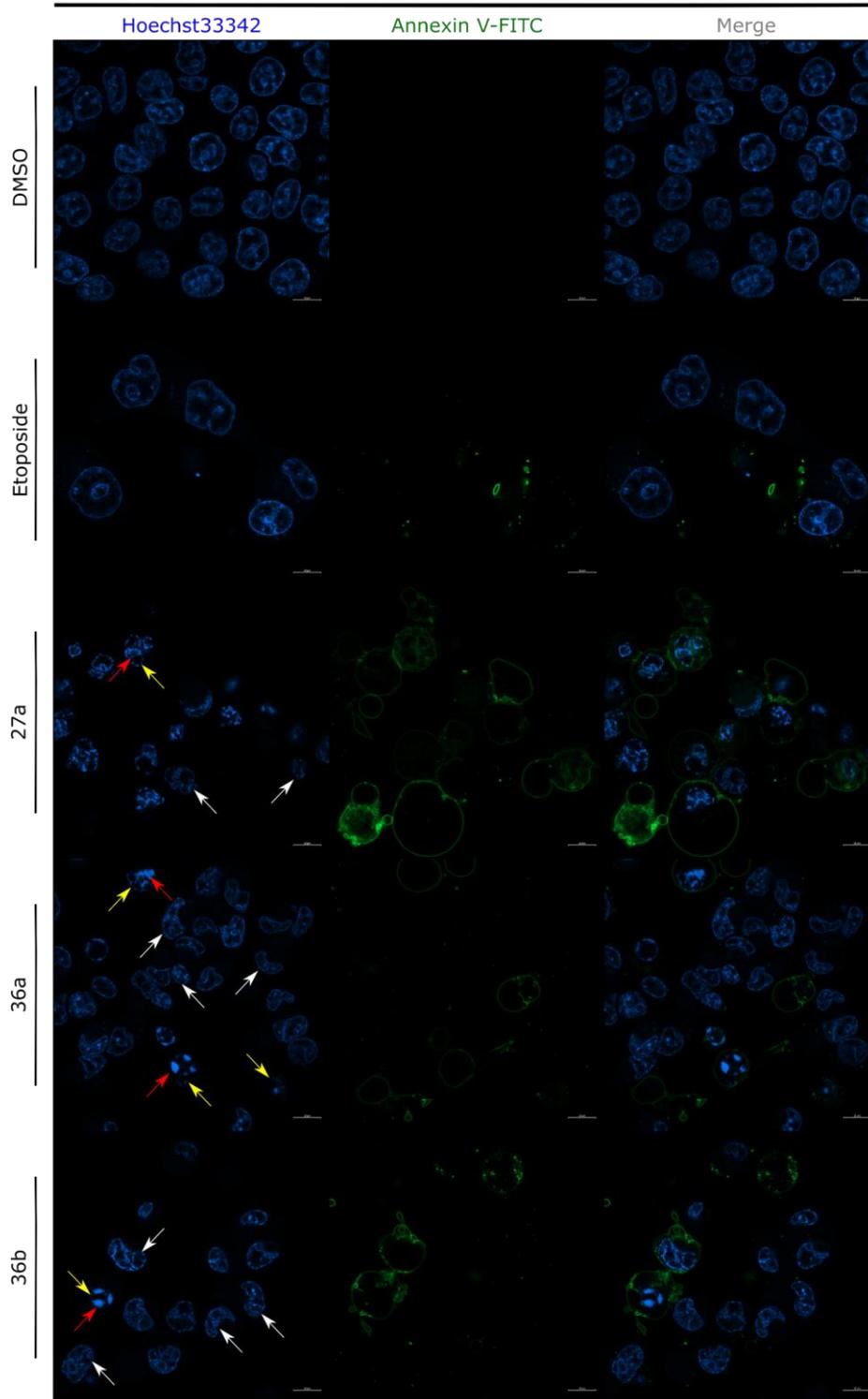
Figure 31 Confocal microscopy was employed to capture images of HCT-116 cells after 24 h of exposure to carbazole derivatives, ETP, or DMSO. These cells were stained with Hoechst33342 and Annexin V-FITC, and the scale bar represents 10 µm. Notably, cell shrinkage (white arrows), fragmented nuclei (red arrows), and the presence of apoptotic bodies (yellow arrows) are observable features.

4.9 Carbazoles induce apoptotic cell death

The apoptotic potential of carbazoles was assessed through flow cytometry using dual staining with Annexin V-FITC and 7-AAD, enabling the distinction of viable (Annexin V-FITC(-)/7-AAD(-)), early apoptotic (EA) (Annexin V-FITC(+)/7-AAD(-)), late apoptotic (LA) (Annexin V-FITC(+)/7-AAD(+)), and necrotic (Annexin V-FITC(-)/7-AAD(+)) cells. As depicted in **Figure 32**, following 24 h of treatment with A549 cells, the tested compounds increased the proportion of apoptotic cells (EA + LA) to over 40%, compared to the control group (8.7 ± 2.3%). Subsequent exposure (48 h) to carbazoles demonstrated a significant increase in the late apoptotic phase, ranging from around 30% to 60%, depending on the specific compound (**Figure 32**). Similar to A549, the treatment of HCT-116 cells with the investigated compounds led to a time-dependent increase in apoptotic cells, with the apoptotic potential of carbazoles being consistent in both cell lines (**Figures 32** and **33**). The most pronounced pro-apoptotic effects were observed with compound **27a**, causing an 8-fold increase in the fraction of apoptotic cells compared to the control in both tested cancer lines. Furthermore, in both tested cell lines, carbazoles also induced a slight degree of necrosis, with this effect being statistically significant only for **27a** and **36b** against HCT-116 (**$p<0.001$) (**Figures 32** and **33**,). Notably, all tested compounds induced apoptosis approximately 2.5 times more effectively than the reference compound ETP, a well-known Topo II inhibitor used in chemotherapies for treating various tumours, including lung cancer.

By employing Annexin V-FITC and 7-AAD staining, I examined the potential of **27a**, **36a**, and **36b** to trigger apoptosis in normal human bronchial epithelial cells, as illustrated in **Figures 34** and **35**. This assessment was conducted following a 72 h incubation period at various concentrations for each of the tested compounds. Compound **27a** exhibited a noteworthy increase in the proportion of early apoptotic cells even at the lowest concentration of 125 nM, underscoring its potent proapoptotic activity. Furthermore, at concentrations of 500 nM and 250 nM, **27a** induced a fraction of necrotic cells (*$p<0.01$). In the case of compound **36b**, a substantial portion of necrotic and late apoptotic cells was observed in NHBE cell lines, albeit only at the highest concentration of 1000 nM. Conversely, **36a** did not significantly induce necrotic cells at either of the tested concentrations.
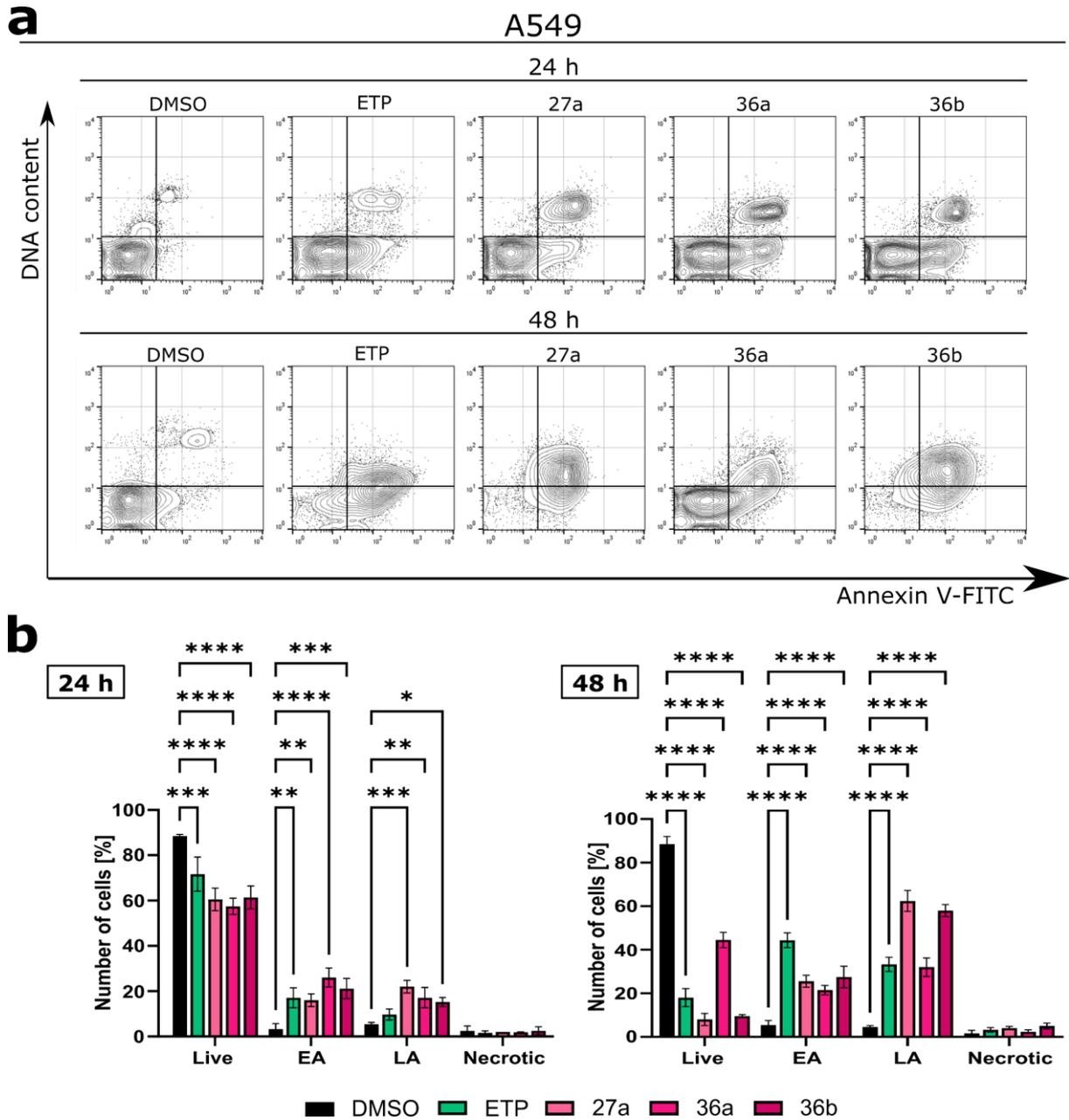
Figure 32 Flow cytometric examination of the A549 cell line was conducted following treatment with compounds for 24, and 48 h. Representative histograms (a) and their quantification (b) are presented. Annexin V-FITC/7-AAD staining was employed for this analysis. DMSO and ETP were utilized as negative and positive controls, respectively. The data presented here represent the mean ± SD of results obtained from three independent experiments. Statistical analysis was carried out using the two-way ANOVA test.
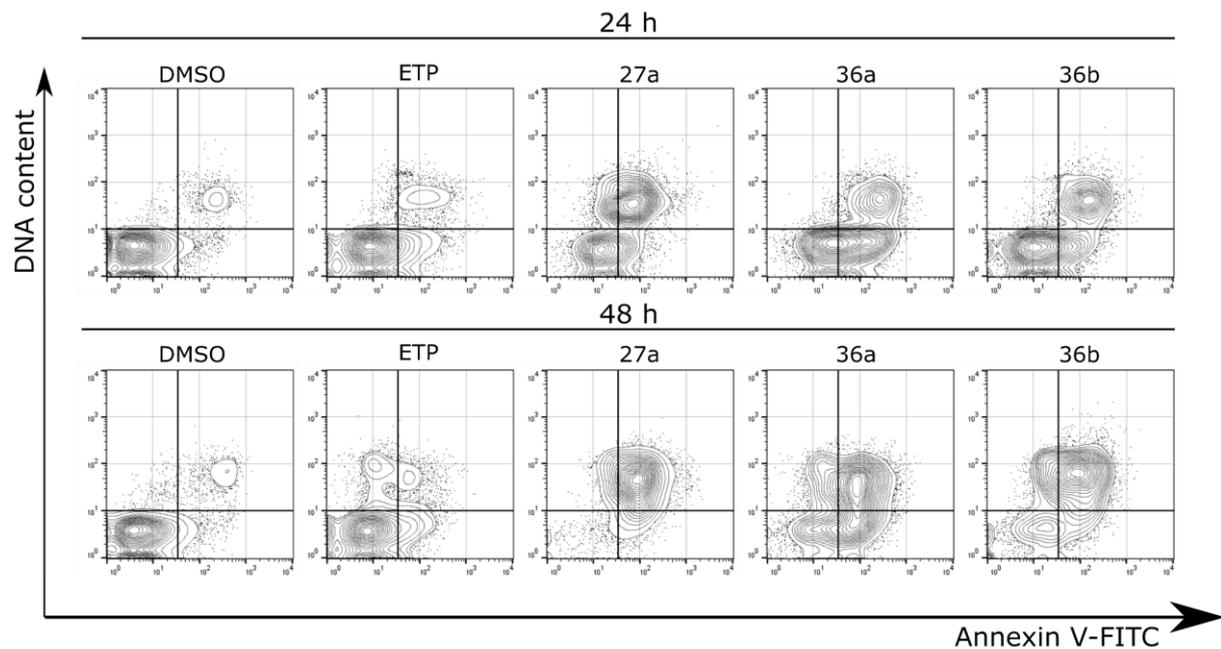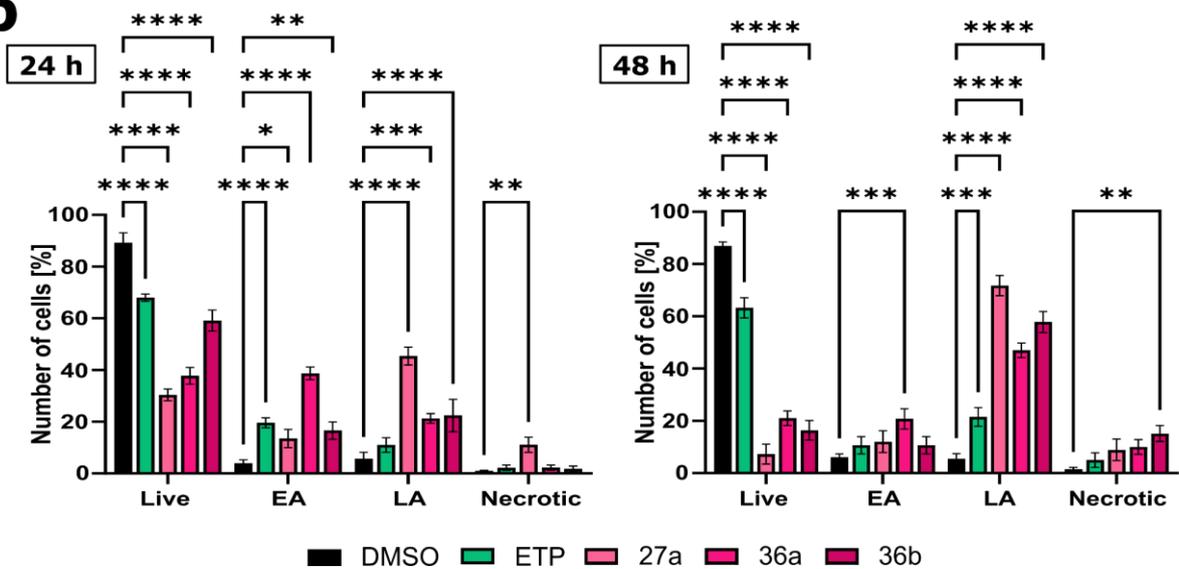
Figure 33 Flow cytometric examination of the HCT-116 cell line was conducted following treatment with compounds for 24, and 48 h. Representative histograms (a) and their quantification (b) are presented. Annexin V-FITC/7-AAD staining was employed for this analysis. DMSO and ETP were utilized as negative and positive controls, respectively. The data presented here represent the mean ± SD of results obtained from three independent experiments. Statistical analysis was carried out using the two-way ANOVA test.
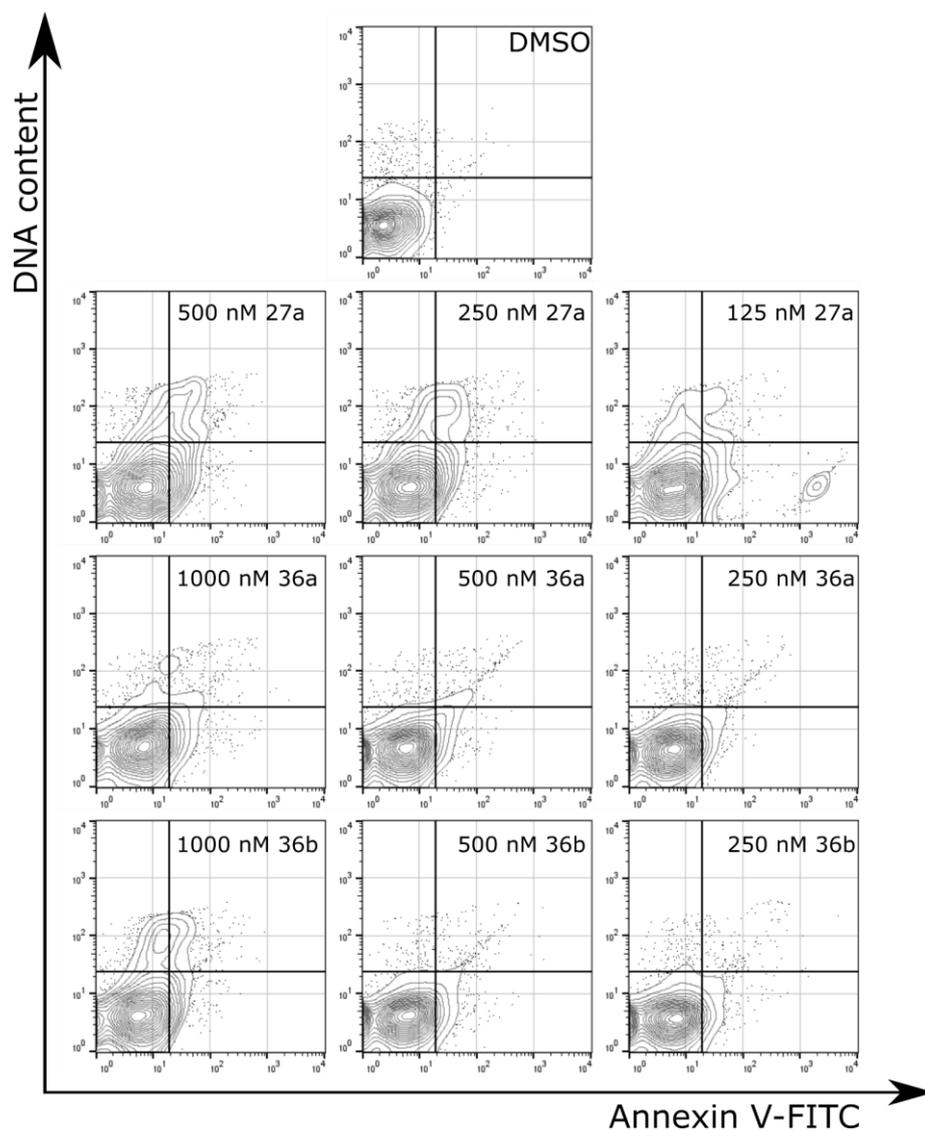
Figure 34 Representative dot plots from flow cytometric analysis of the NHBE cell line after treatment with **27a**, **36a**, and **36b** for 24 and 48 h. Annexin V-FITC/7-AAD staining was used for this assessment, with DMSO and ETP serving as negative and positive controls, respectively. The data presented here represent the mean ± SD of results obtained from three independent experiments.
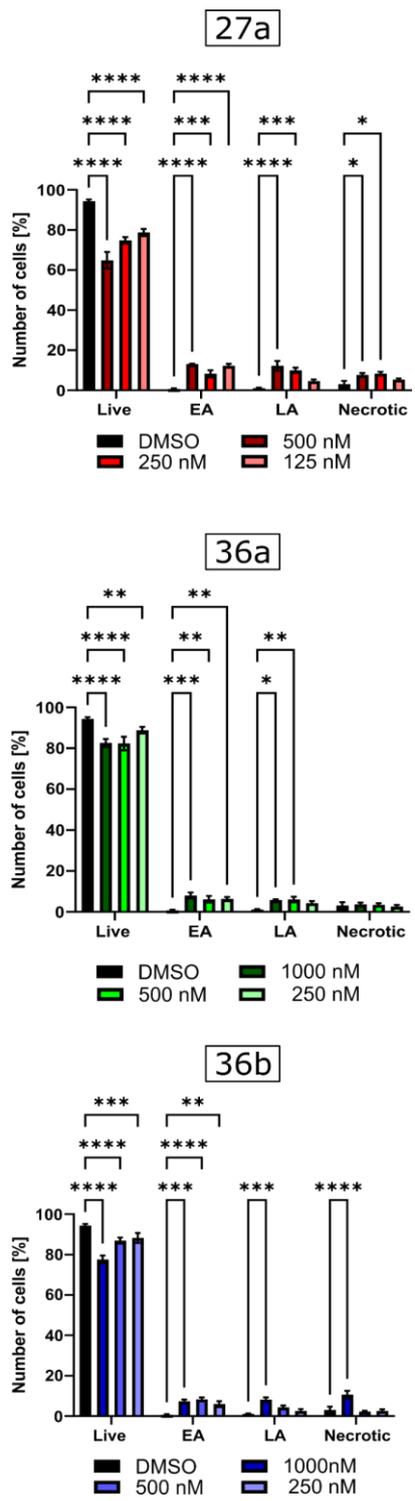
Figure 35 The flow cytometric quantification of the NHBE cell line after treatment with **27a**, **36a**, and **36b** for 24 and 48 h. Annexin V-FITC/7-AAD staining was used for this assessment, with DMSO and ETP serving as negative and positive controls, respectively. The data presented here represent the mean ± SD of results obtained from three independent experiments. Statistical analysis was carried out using the two-way ANOVA test.

74

4.10 Carbazole derivatives cause a loss of mitochondrial transmembrane potential

Mitochondria play a vital role in the process of cell death, and the loss of mitochondrial outer membrane potential (MOMP) is a crucial event for initiating mitochondrial apoptosis [284]. In healthy cells with a typical mitochondrial membrane potential (ΔΨM), JC-1 dye enters the energized and negatively charged mitochondria, resulting in the spontaneous formation of red fluorescent J-aggregates. In contrast, in unhealthy or apoptotic cells, JC-1 enters the mitochondria to a lesser extent because the interior of the mitochondria is less negatively charged due to increased membrane permeability and the subsequent loss of the electrochemical potential [285]. In this scenario, JC-1 does not accumulate in sufficient concentrations to initiate the formation of J-aggregates, thereby retaining its initial green fluorescence [286,287].

Confocal imaging of live cells employing JC-1 (**Figures 36** and **37**) revealed that compounds **27a**, **36a**, and **36b** resulted in a decrease in red fluorescence (JC-1 aggregates) and an elevation in green fluorescence (JC-1 monomers), indicating a loss of mitochondrial outer membrane potential in both A549 and HCT-116 cell lines when compared to cells treated with DMSO. In contrast, the reference compound FCCP induced a substantial increase in green fluorescence in both of the tested cell lines (**Figures 36** and **37**). As illustrated in **Figure 38**, flow cytometry analysis after the treatment of A549 and HCT-116 cells with carbazole derivatives for 24 h resulted in a significant increase in the percentage of cells with dissipated MOMP, as evidenced by an approximately five-fold rise in JC1-monomers when compared to the vehicle (DMSO). In contrast, the reference compound, carbonyl cyanide 4-(trifluoromethoxy)phenylhydrazone (FCCP), led to an 11-fold and 6.3-fold increase in JC-1-monomers for A549 and HCT-116 cells, respectively, compared to the control (**Figure 38**).

A549
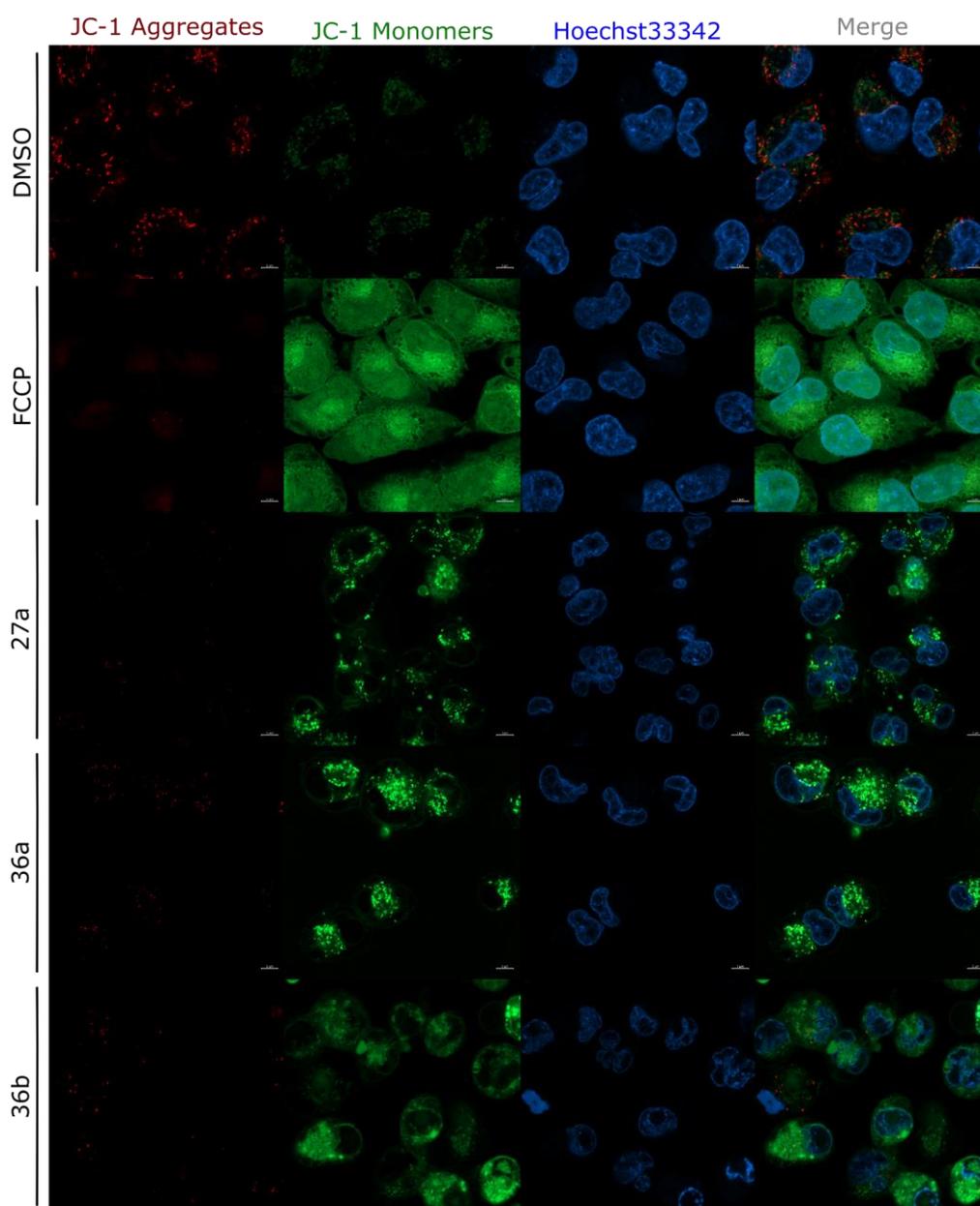
Figure 36 Assessment of alterations in mitochondrial potential MOMP was performed using JC-1 staining. Confocal live-cell imaging of A549 cells was captured following a 24 h treatment with **27a**, **36a**, and **36b**. DMSO and FCCP were used as references. The scale bar is set at 5μm.
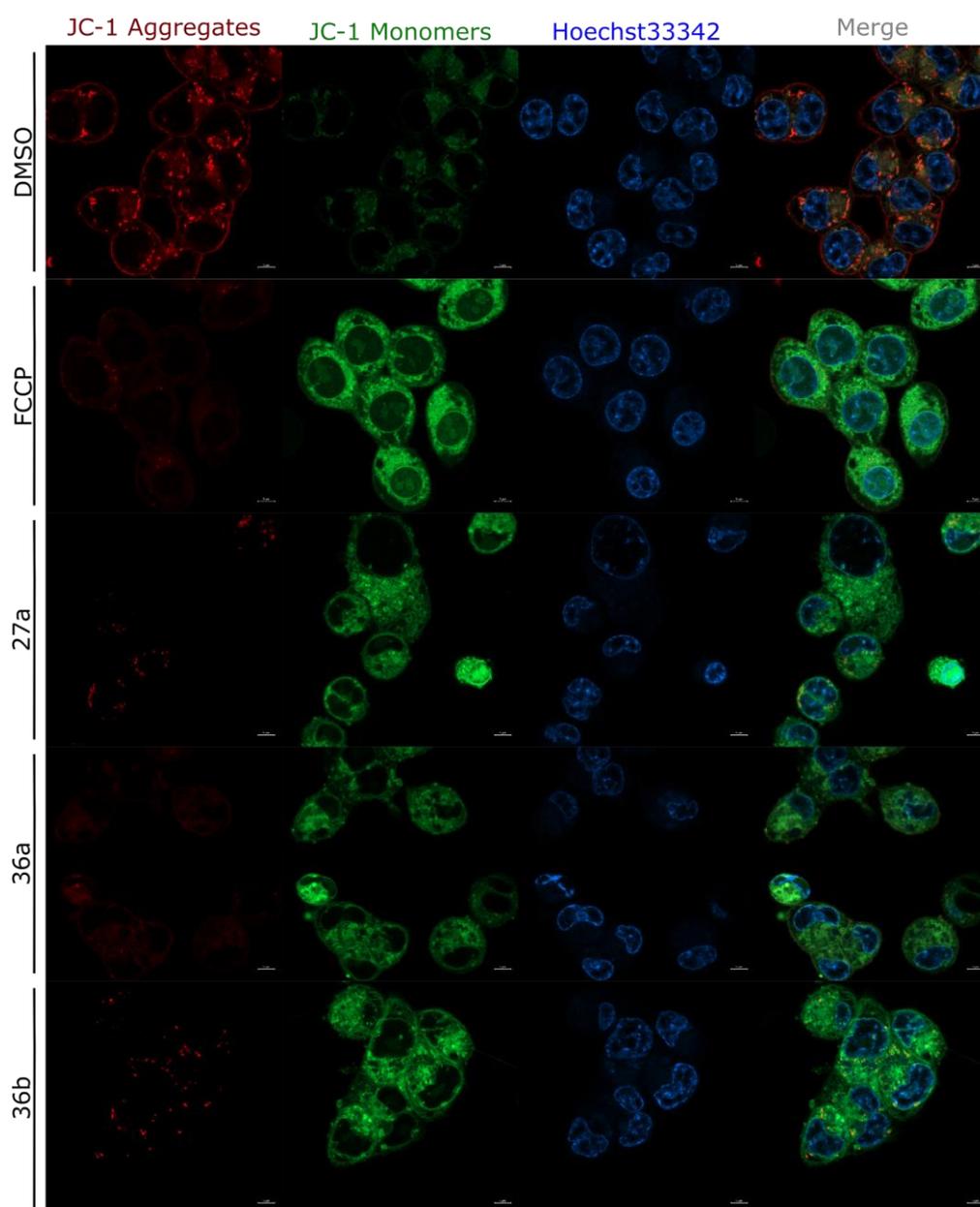
HCT-116

Figure 37 Assessment of alterations in mitochondrial potential was performed using JC-1 staining. Confocal live-cell imaging of HCT-116 cells was captured following a 24 h treatment with **27a**, **36a**, and **36b**. DMSO and FCCP were used as references. The scale bar is set at 5µm.
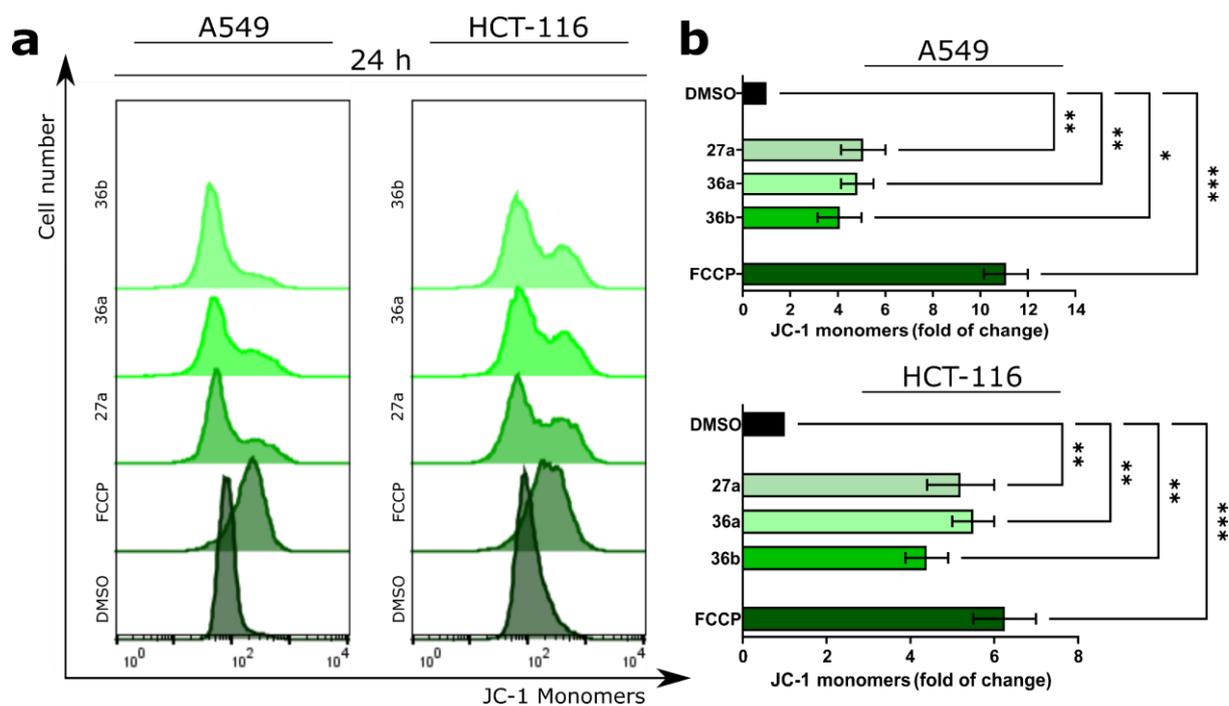
Figure 38 Assessment of alterations in mitochondrial potential MOMP in both A549 and HCT-116 cells was carried out via JC-1 staining. This analysis includes representative histograms (a), and bar charts (b) with accompanying statistical quantification after 24 h of **27a**, **36a**, and **36b** treatment. The data represent the mean ± SD of results obtained from three independent experiments. Statistical analysis was carried out using the one-way ANOVA test.

4.11 Carbazole derivatives disrupt calcium homeostasis

Calcium homeostasis is a pivotal factor in the process of apoptosis mediated by mitochondria and the endoplasmic reticulum (ER) [288]. The liberated calcium may amass within the mitochondria, resulting in the permeabilization of the outer mitochondrial membrane, probably facilitated by the mitochondrial permeability transition pore (mPTP) [289]. The mPTP's opening leads to the release of pro-apoptotic factors, thereby initiating the cellular apoptosis process [160]. To investigate this, A549 and HCT-116 cells were subjected to a 24 h and 48 h treatment with carbazole derivatives. The intracellular levels of calcium were monitored using the Ca^{2+} sensitive fluorescent dye Fluo-4 AM and analysed through flow cytometry (**Figures 39** and **40**). In the case of A549 cells, after 48 h of treatment, all tested compounds caused a remarkable increase in intracellular calcium levels, with over 80% of treated cells exhibiting this effect compared to the control sample treated with DMSO (****$p < 0.00001$). On the other hand, after 48 h of treatment of HCT-116 cells resulted in a significant efflux of calcium into the cytosol, with a striking 13.3-fold, 12.8-fold, and 16.6-fold increase observed for compounds **27a**, **36a**, and **36b**, respectively, in comparison to the vehicle control. ETP used as a reference, only elicited a calcium efflux in A549 cells and had no effect on the HCT-116 cell line. These findings suggest that carbazole derivatives induce alterations in calcium signalling in both A549 and HCT-116 cells.
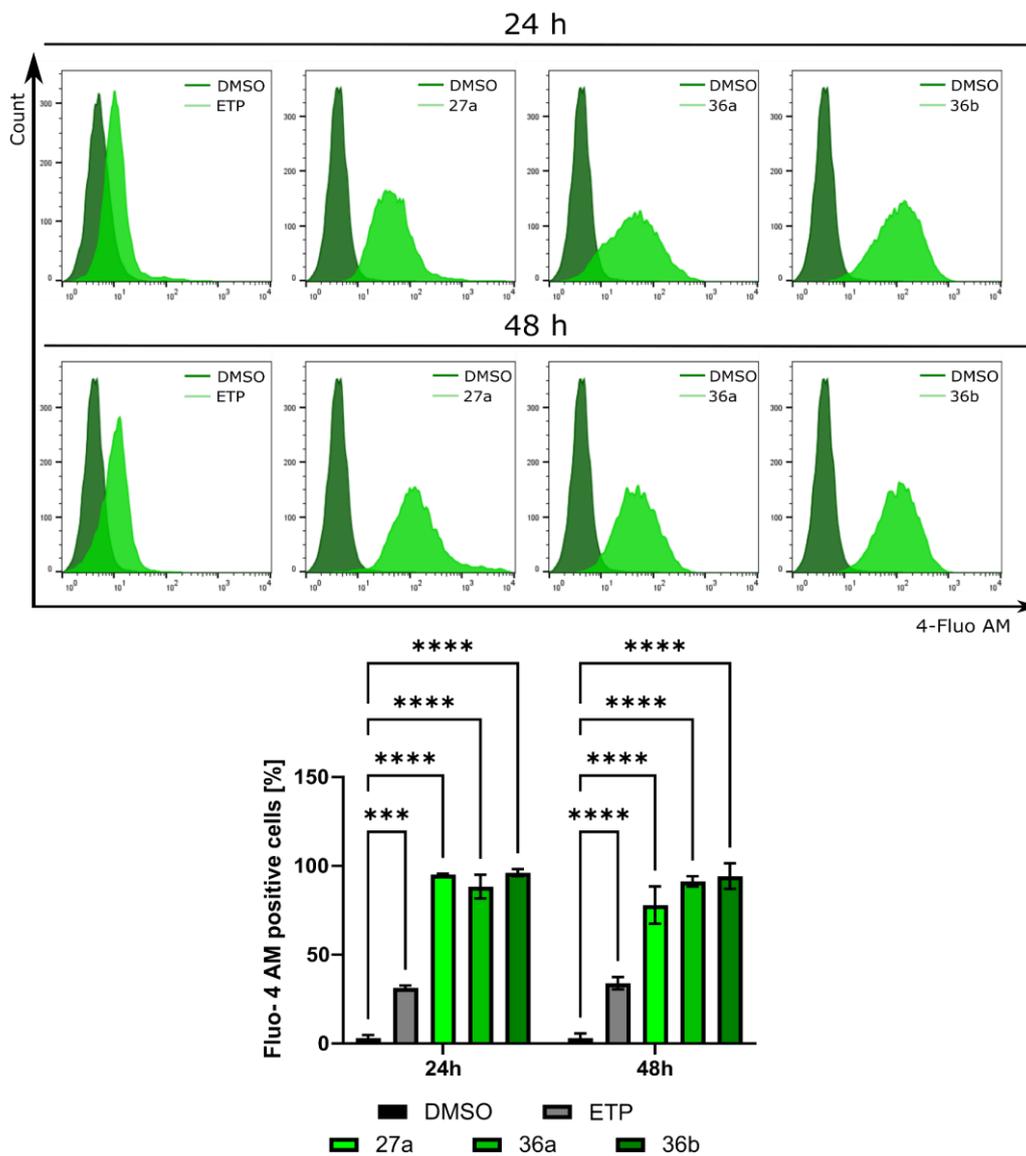
Figure 39 Flow cytometric examination of intracellular Ca^{2+} level in A549 cells after 24 and 48 h of treatment with **27a**, **36a**, **36b**. DMSO and ETP were used as reference compounds. Representative histograms are shown on top, and quantification is in the bottom panel. The data represent the mean ± SD of results obtained from three independent experiments. Statistical analysis was carried out using the two-way ANOVA test.

Figure 40 Flow cytometric examination of intracellular Ca^{2+} level in HCT-116 cells after 24 and 48 h of treatment with **27a**, **36a**, **36b**. DMSO and ETP were used as reference compounds. Representative histograms are shown on top, and quantification is in the bottom panel. The data represent the mean ± SD of results obtained from three independent experiments. Statistical analysis was carried out using the two-way ANOVA test.

4.12 Carbazole derivatives induce oxidative stress

Maintaining cellular redox balance is crucial for regulating numerous signalling pathways. Many anticancer therapies disrupt cellular redox states by increasing intracellular levels of reactive oxygen species (ROS) or inhibiting antioxidant processes. This elevation in ROS levels accelerates cumulative damage to cellular components, including lipids, proteins, and DNA, ultimately leading to the death of cancer cells. Consequently, a time-dependent kinetic analysis was conducted at 6 and 24 h of incubation to evaluate intracellular ROS levels in A549 and HCT-116 cells following treatment with **27a**, **36a**, and **36b**, both individually and in combination with N-acetylcysteine (NAC), serving as an antioxidant. H_2O_2 was used as a reference.

For the A549 cell line, the compounds exhibited the highest activity in inducing reactive oxygen species after 6 h of treatment. The most pro-oxidative activity was observed with **27a** and **36b**, which resulted in 51.75±4.75% and 57.25±4.25% of cells showing elevated ROS levels compared to the control (****$p < 0.00001$), respectively (**Figure 41**). When combined with NAC, none of the compounds caused a notable rise in ROS levels in A549 cells at both the 6 and 24 h ($p > 0.01$) (**Figure 41**). In the same manner, all the tested carbazole derivatives induced a significant increase in ROS levels, reaching approximately 30%, in HCT-116 cells after 6 h of treatment (**Figure 42**). After 24 h of treating HCT-116 cells with carbazole derivatives in combination with NAC, compounds **27a** and **36b** induced a lower but still significantly elevated level of ROS (****$p < 0.0001$; and *$p < 0.01$) in comparison to DMSO (**Figure 42**). The combination of **36a** with NAC did not lead to an increase in ROS levels in either of the tested cell lines (**Figures 41** and **42**). H_2O_2, used as a reference, had the most significant impact on A549 cells after 24 h (44.75±2.75%) and on HCT 116 cells after 6 h (72.95±2.95%).
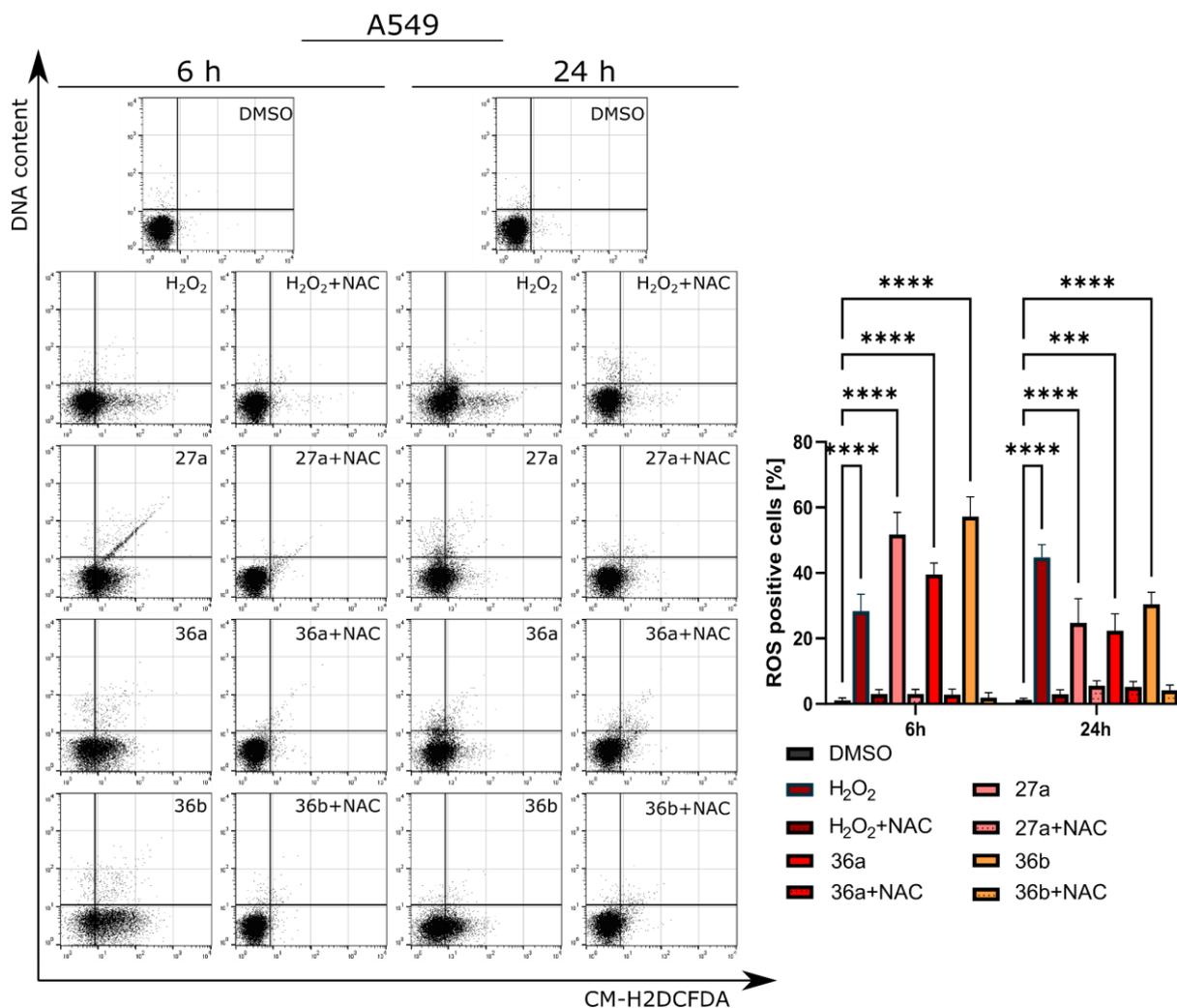
Figure 41 Flow cytometric examination of ROS induction in A549 cell line after 6 and 24 h of treatment with **27a**, **36a**, and **36b**.The left panel displays representative histograms while the right panel shows the quantification of these results. The data represent the mean ± SD of results obtained from three independent experiments. Statistical analysis was carried out using the two-way ANOVA test.

Figure 42 Flow cytometric examination of ROS induction in HCT-116 cell line after 6 and 24 h of treatment with **27a**, **36a**, and **36b**.The left panel displays representative histograms while the right panel shows the quantification of these results. The data represent the mean ± SD of results obtained from three independent experiments. Statistical analysis was carried out using the two-way ANOVA test.

4.13 Carbazole derivatives induce the release of cytochrome c

During the process of cell death, several proteins typically confined within the intermembrane space of mitochondria are released into the cytosol. These proteins include cytochrome c, apoptosis-inducing factor (AIF), and specific procaspase proteins [291]. The outcome of this release depends on the stimulus and can result in necrosis due to irreversible mitochondrial damage and energy depletion or in apoptosis through the activation of caspases, a family of proapoptotic proteases, by cytochrome c. In the cytosol, cytochrome c forms a complex with apoptotic-protease-activating factor-1 (Apaf-1), procaspase-9, and ATP or dATP, which activates the caspases. The release of cytochrome c from mitochondria during apoptosis is regulated by Bcl-2 family proteins: those that inhibit cell death (e.g., Bcl-2 and Bcl-xL) prevent cytochrome c release, while those that promote cell death (e.g., Bax and Bak) induce its release [292–294].

To determine whether the tested carbazole derivatives induce the release of cytochrome c from mitochondria in A549 and HCT-116 cell lines, confocal microscopy imaging was performed (**Figures 43** and **44**). In the case of the untreated sample (DMSO), the fluorescence signals from mitochondria (Mitotracker green) and cytochrome c (red) overlap. However, for the samples treated with the tested compounds in the A549 cell line (**Figure 43**), upon image overlay, it was clearly observed that the red fluorescence from cytochrome c does not overlap with the mitochondrial fluorescence signal. This indicates that under the influence of carbazole derivatives, cytochrome c is released from the mitochondrial membranes.
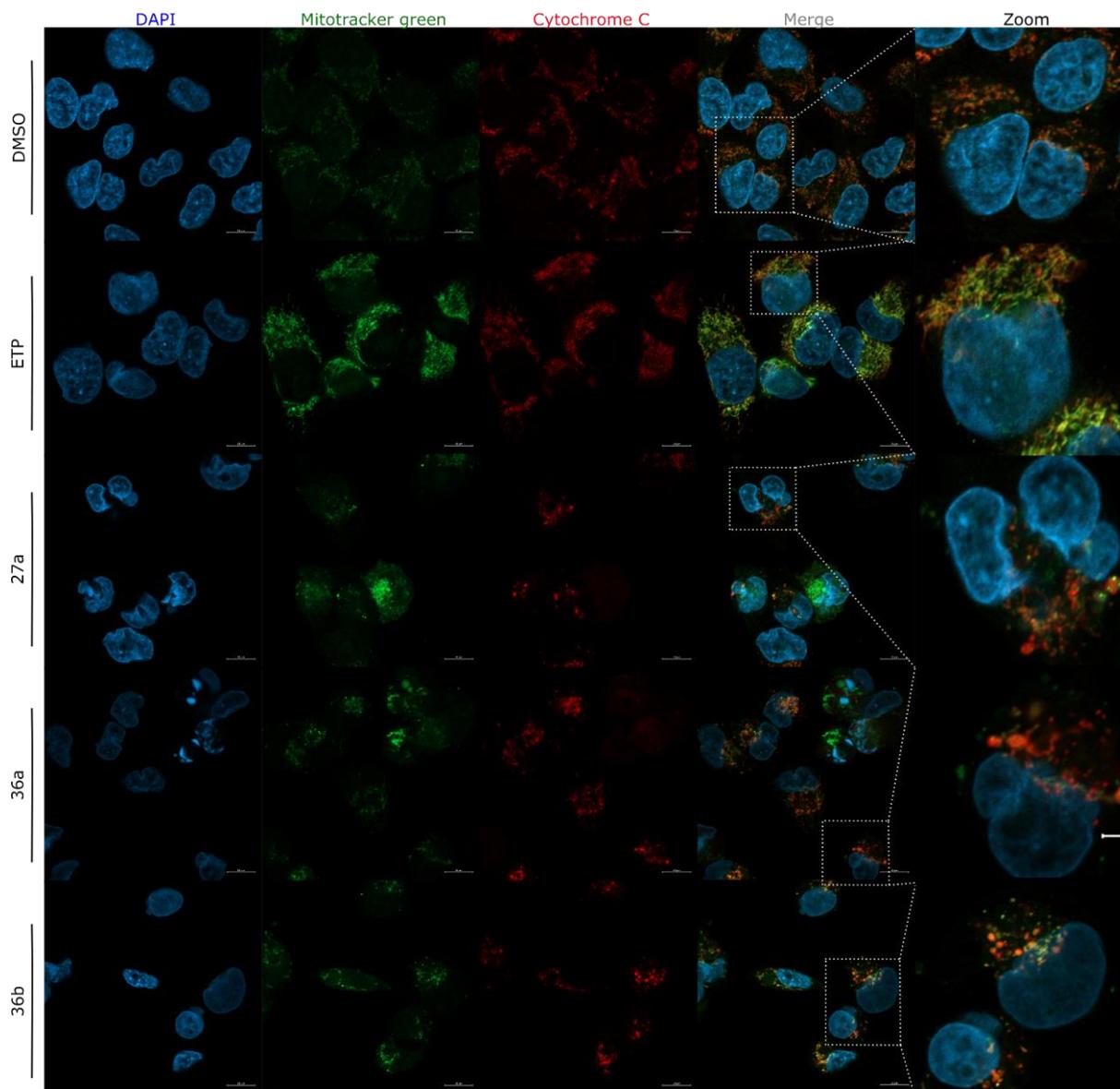
Figure 43 The provided images display immunofluorescence in A549 cells, highlighting the formation of cytochrome c foci, and alterations in mitochondrial structure following a 24 h treatment with carbazole derivatives. ETP and DMSO were employed as reference compounds for comparison. In the images, the Mitotracker is represented in green, cytochrome c in red, and the nucleus in blue (DAPI).

HCT-116
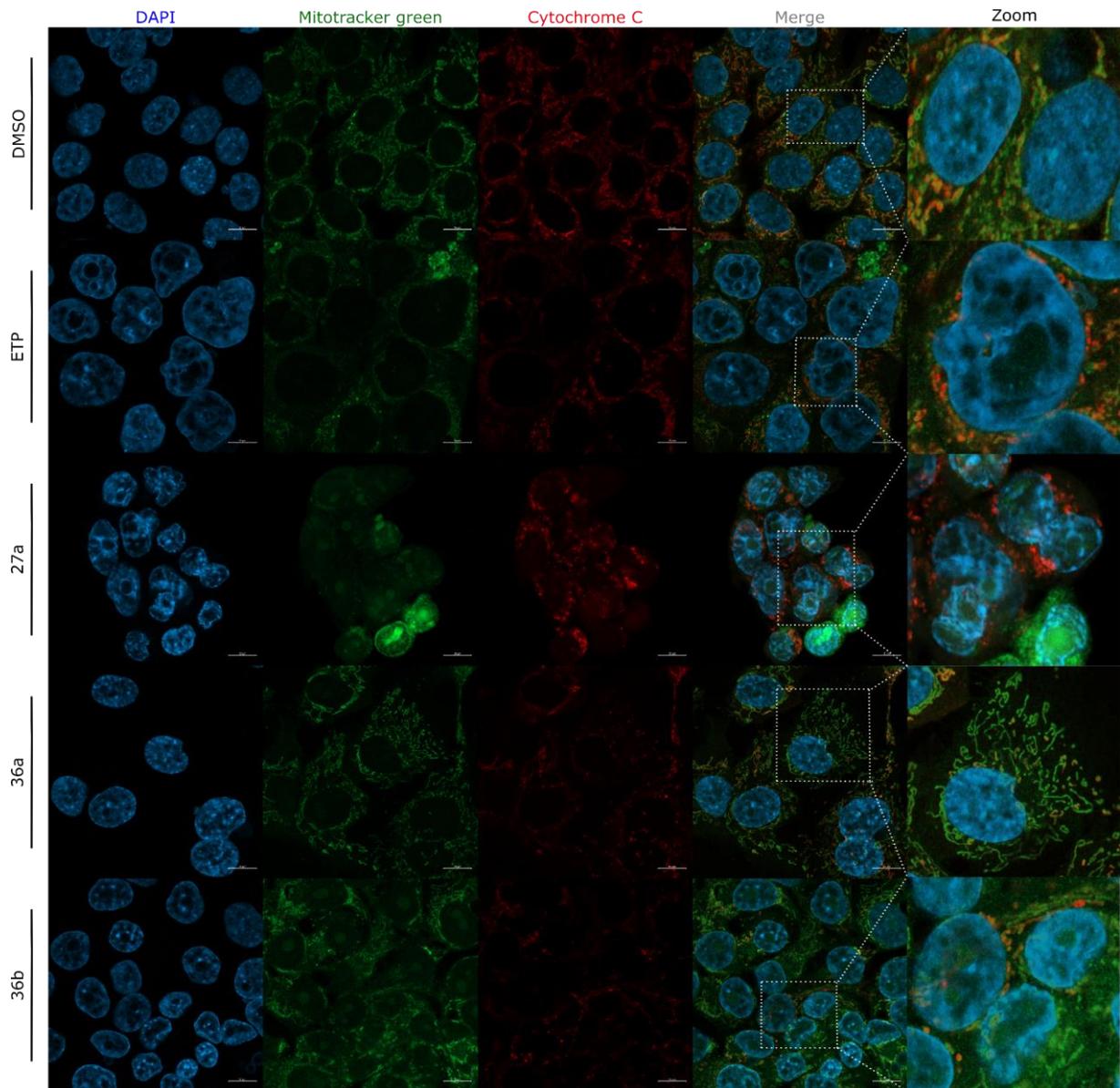
Figure 44 The provided images display immunofluorescence in HCT-116 cells, highlighting the formation of cytochrome c foci, and alterations in mitochondrial structure following a 24-h treatment with carbazole derivatives. ETP and DMSO were employed as reference compounds for comparison. In the images, the Mitotracker is represented in green, cytochrome c in red, and the nucleus in blue (DAPI).

4.14 Carbazole derivatives trigger the activation of caspases 3 and 7

One hallmark of cells undergoing apoptosis is the activation of cysteine proteases known as caspases, with executioner caspases 3 and 7 being key players in apoptotic cell death [280]. Caspases constitute a family of cysteine proteases that play a pivotal role in all phases of apoptosis. Based on their function in apoptosis, they are categorized as either upstream initiators (such as caspase-8 and caspase-9) or downstream executioners (like caspase-3, caspase-6, and caspase-7) [295]. Executioner caspases are considered a crucial point of no return in the process of apoptotic cell death [296]. Specifically, among them, caspase-3 governs DNA fragmentation, while caspase-7 regulates the production of reactive oxygen species (ROS) and is essential for the detachment of apoptotic cells [258,297]. To determine whether carbazoles induced caspase-dependent cell death, equitoxic concentrations of these compounds were administered to A549 and HCT-116 cells and analysed using flow cytometry. As depicted in **Figure 45**, after a 24 h treatment of A549 cells, carbazoles activated caspase-3/7, leading to a 3.4-fold, 5.7-fold, and 2.5-fold increase in apoptosis for **27a**, **36a**, and **36b**, respectively, compared to the control. Subsequent treatment of A549 cells for 48 h resulted in a modest increase in apoptotic cells. In comparison, exposure of HCT-116 cells to carbazole derivatives produced a similar increase in the subpopulation of cells with activated caspase 3/7, with approximately five times higher activity than in the control (DMSO), as shown in **Figure 46**. After 48 h of treatment with the compounds, caspase-3/7 activity in HCT-116 cells was enhanced by 1.5 to 2-fold compared to the vehicle (**Figure 46**). Additionally, ETP also significantly elevated caspase-3/7 activity in both cell lines; however, this effect was more pronounced than that of the carbazoles (**Figures 45** and **46**).
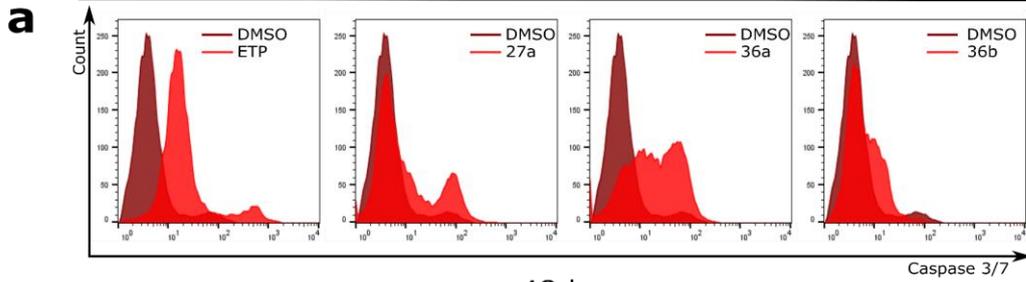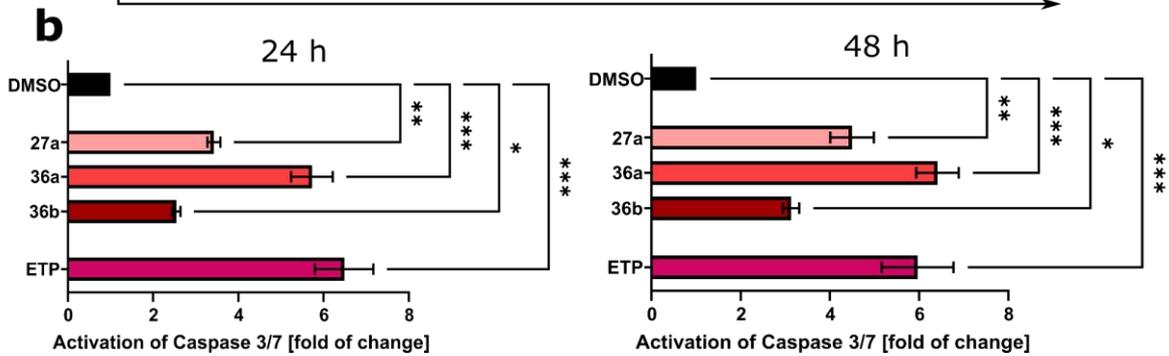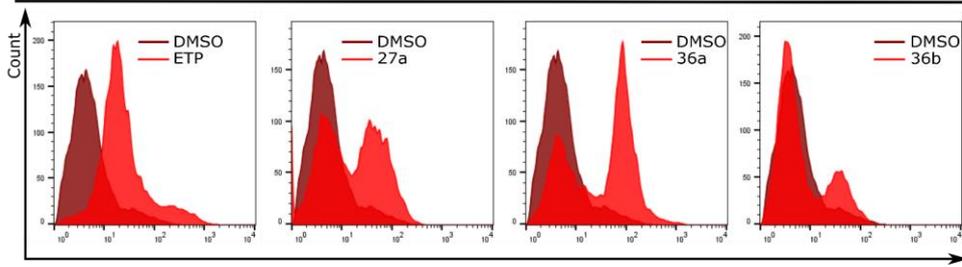
Figure 45 Modulation of caspase 3/7 in A549. Representative histograms (a) and quantification (b) of HCT-116 cells after 24 and 48 h of treatment with **27a**, **36a**, and **36b**. The data represent the mean ± SD of results obtained from three independent experiments. Statistical analysis was carried out using the one-way ANOVA test.
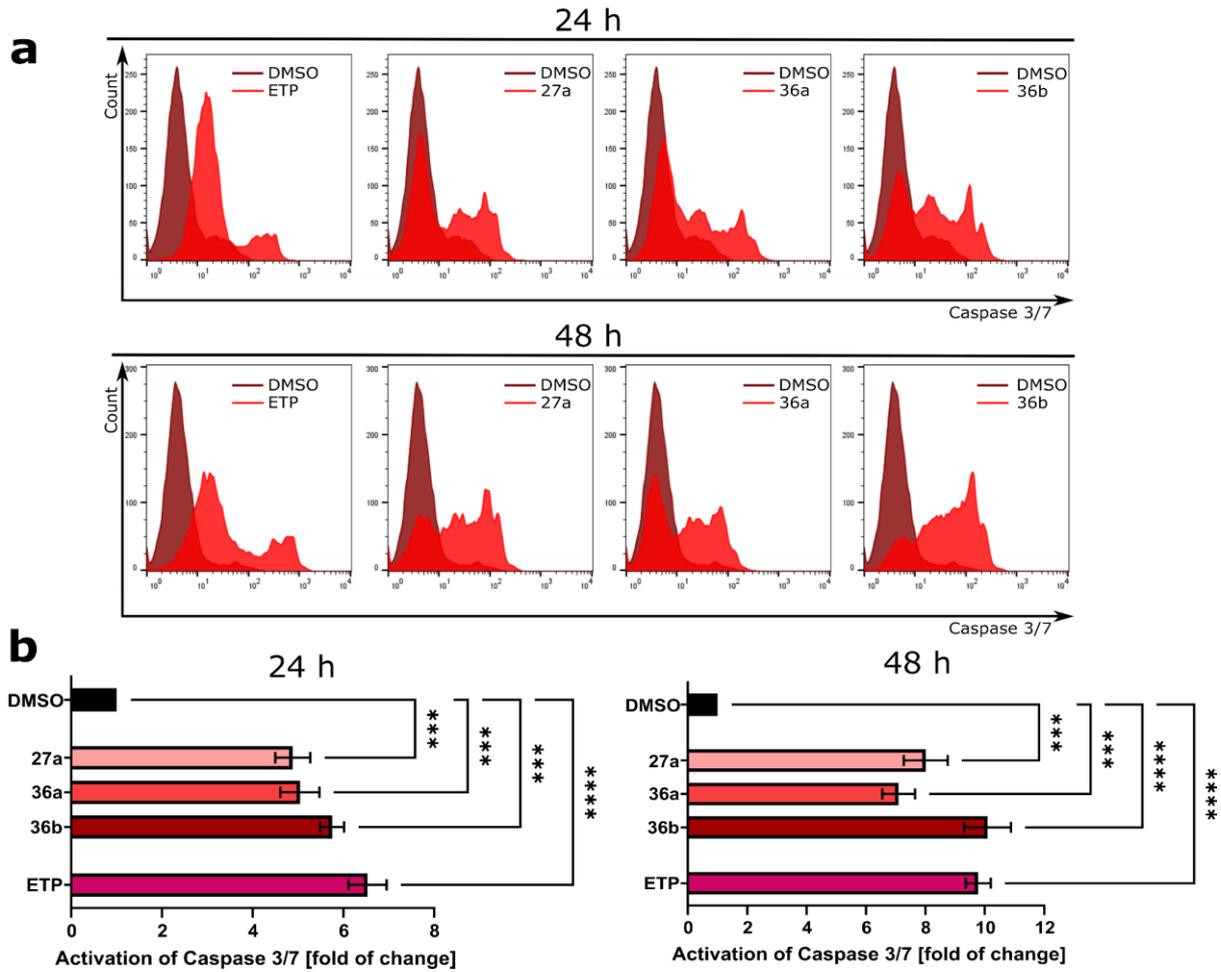
Figure 46 Modulation of caspase 3/7 in HCT-116. Representative histograms (a) and quantification (b) of HCT-116 cells after 24 and 48 h of treatment with **27a**, **36a**, and **36b**. The data represent the mean ± SD of results obtained from three independent experiments. Statistical analysis was carried out using the one-way ANOVA test.

4.15 Investigation of DNA damage induction and β-tubulin staining

Carbazole derivatives have demonstrated their ability to cause DNA damage by inducing DNA (DSB). To assess the potential of these compounds to elicit DNA damage, the level of phosphorylated histone H2AX at Ser 139 (γ-H2AX) was examined. In this research, A549 and HCT-116 cells, known for their increased sensitivity to carbazole derivatives, were chosen. These cells underwent treatment with equitoxic compound concentrations for both confocal imaging (**Figures 47** and **48**) over a 48 h period and flow cytometry analysis (**Figures 49** and **50**) at 24 and 48 h. **Figures 49** and **50** reveal that both cell lines exhibited a time-dependent increase in the accumulation of γ-H2AX-positive cells following treatment with carbazoles, indicating that these compounds induced DNA damage. The extent of DNA damage induction varied among the tested compounds and was influenced by the cell line. After 24 h of treatment, **27a**, **36a**, and **36b** led to a less than 20% rise in the number of γ-H2AX-positive cells in both A549 and HCT-116 cells. This increase was 2.7- and 3.2-fold lower, respectively, compared to ETP. However, after 48 h of treatment with these compounds, A549 cells exhibited a substantial 4.9-fold (**$p < 0.001$), 5.2-fold (**$p < 0.001$), and 8.1-fold (****$p < 0.00001$) increase in DNA damage, respectively. Exposure of HCT-116 cells to these compounds resulted in a notable 6.5-fold (***$p < 0.0001$), 6.2-fold (***$p < 0.0001$), and 5.1-fold (**$p < 0.001$) increase in γ-H2AX compared to the vehicle control-treated cells. ETP, a Topo II poison, rapidly elevated the number of γ-H2AX foci in comparison to DMSO in both tested cell lines. These findings indicate that all the tested carbazole derivatives strongly induce DNA damage, but only after 48 h of treatment, and their effectiveness in inducing DNA damage varies between the two tested cell lines, suggesting a different mode of action compared to ETP. As illustrated in **Figures 47** and **48**, the utilization of confocal imaging facilitated the visualization of induced DNA damage in the cells through immunofluorescence techniques. The presence of white arrows signifies the distinct accumulation of H2AX within the cell nuclei, which can be associated with the ongoing process of apoptosis in these cells. Moreover, B-tubulin was stained to assess whether the studied carbazole derivatives interfere with its polymerization. Microscopic imaging indicates that **27a**, **36a**, and **36b** did not exhibit an impact on its functions.
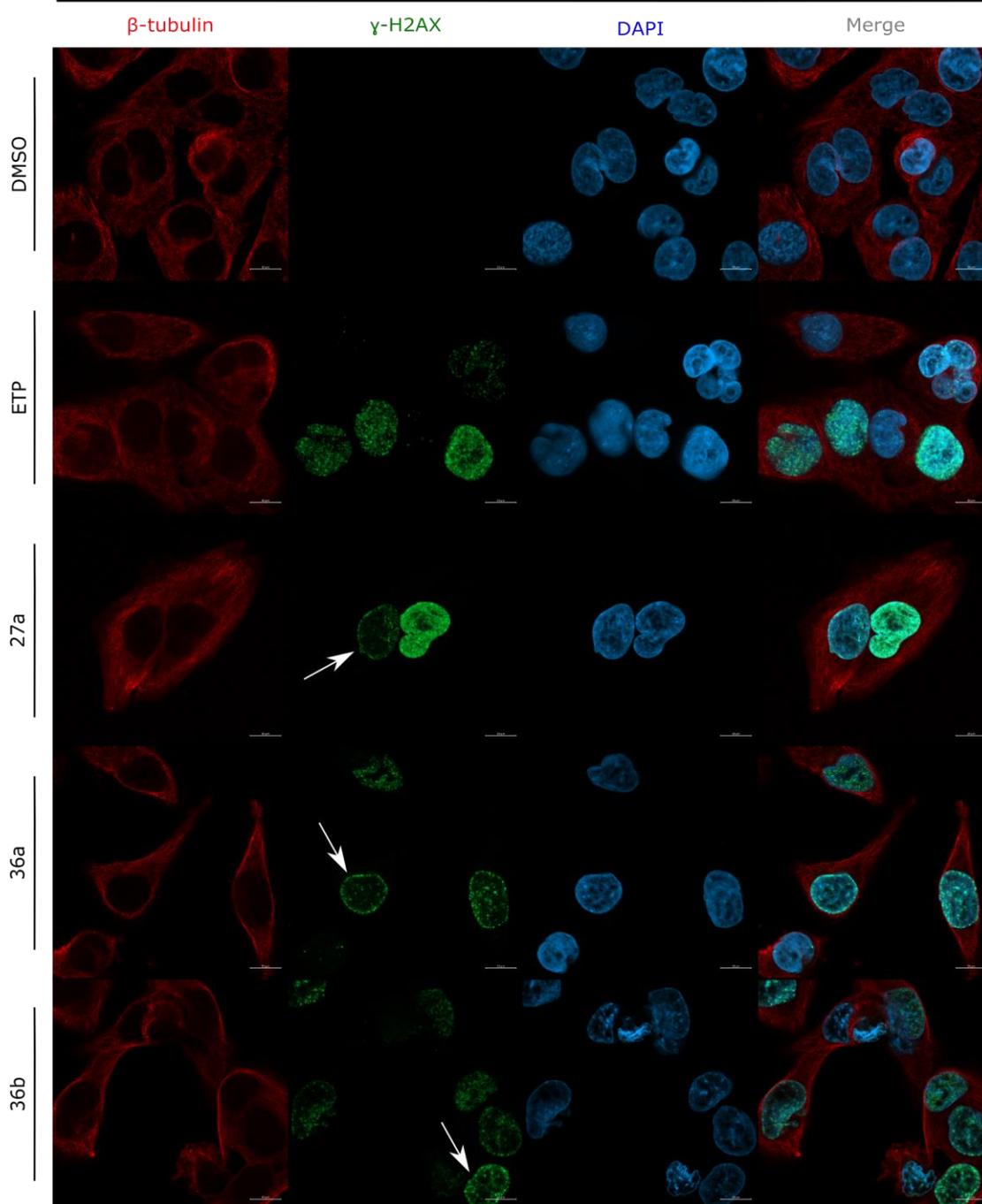
Figure 47 These microscopy images depict immunofluorescence in A549 cells, highlighting the formation of γ-H2AX foci and alterations in microtubule structure following a 48 h treatment with carbazole derivatives. The arrows indicate the cells with an accumulation of γ-H2AX foci forming apoptotic rings. ETP and DMSO were employed as reference compounds. The microtubules are represented in red, γ-H2AX in green, and the nucleus in blue (DAPI) in the images.
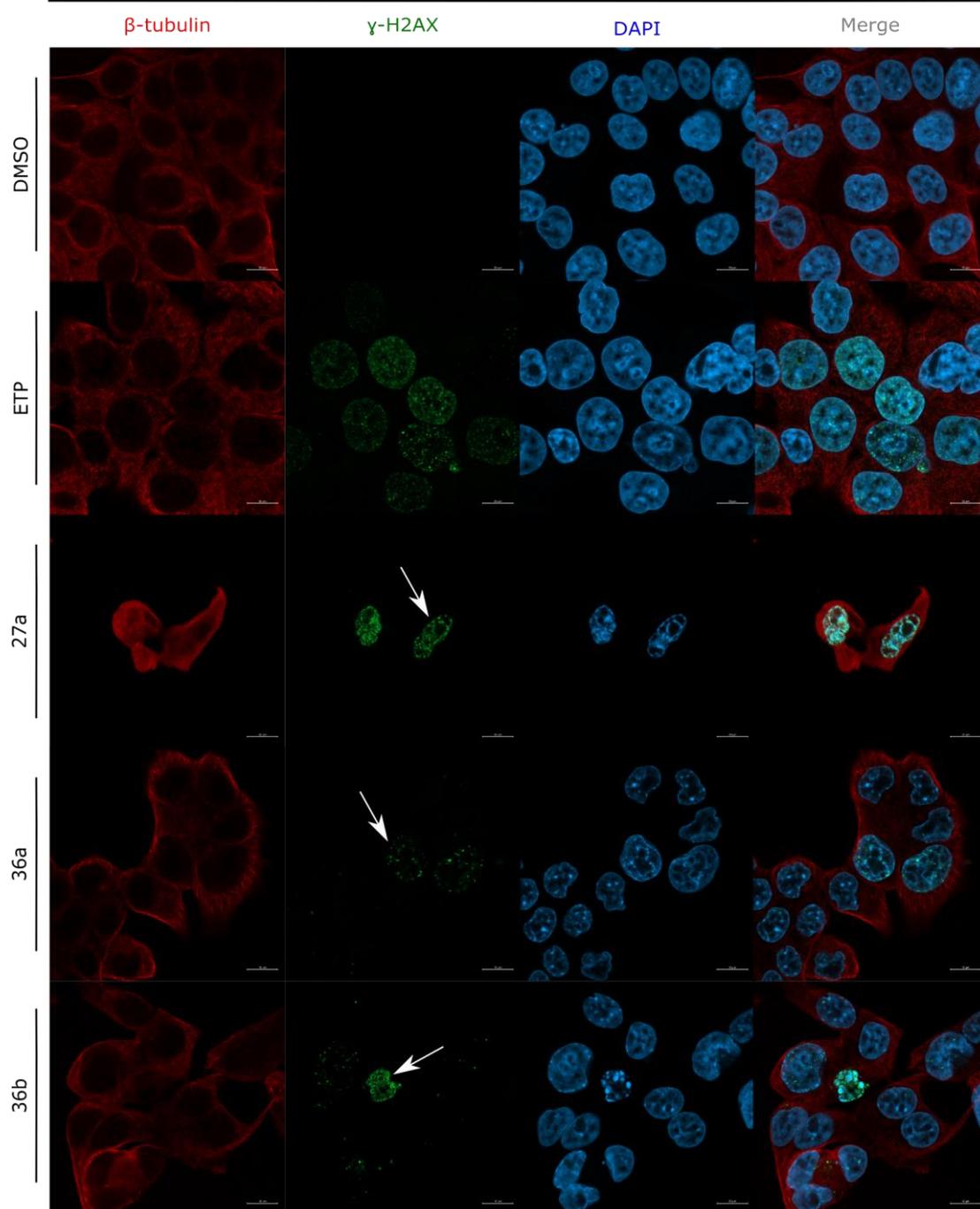
Figure 48 Microscopy images depict immunofluorescence in HCT-116 cells, highlighting the formation of γ-H2AX foci and alterations in microtubule structure following a 48 h treatment with carbazole derivatives. The arrows indicate the cells with an accumulation of γ-H2AX foci forming apoptotic rings. ETP and DMSO were employed as reference compounds. The microtubules are represented in red, γ-H2AX in green, and the nucleus in blue (DAPI) in the images.
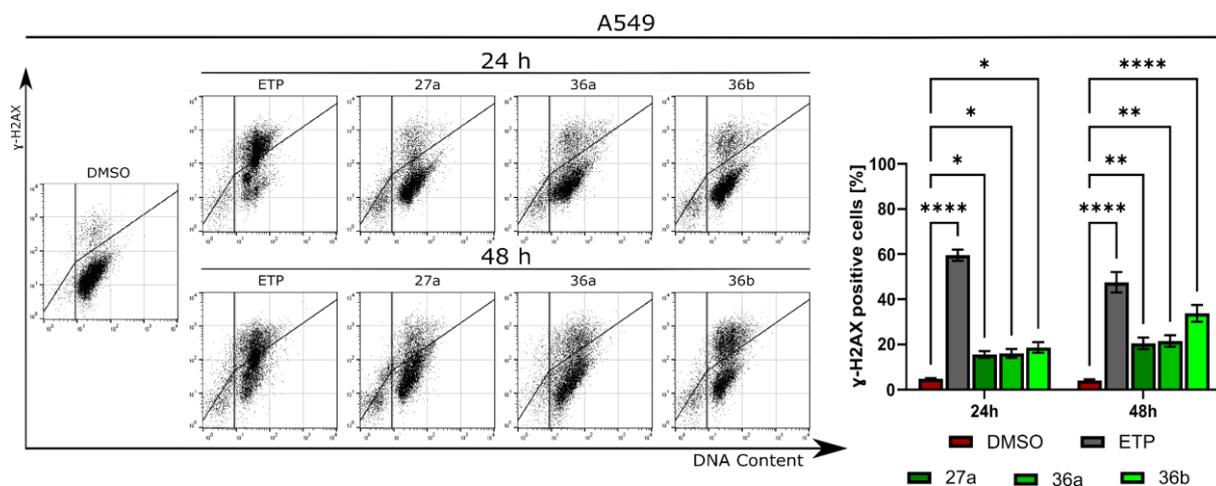
Figure 49 Flow cytometric analyses of induction γ-H2AX in A549 cells. Dot-plot diagrams illustrate γ-H2AX staining, along with a bar graph displaying the percentage of γ-H2AX-positive cells. The data represent the mean ± SD of results obtained from three independent experiments. Statistical analysis was carried out using the two-way ANOVA test.
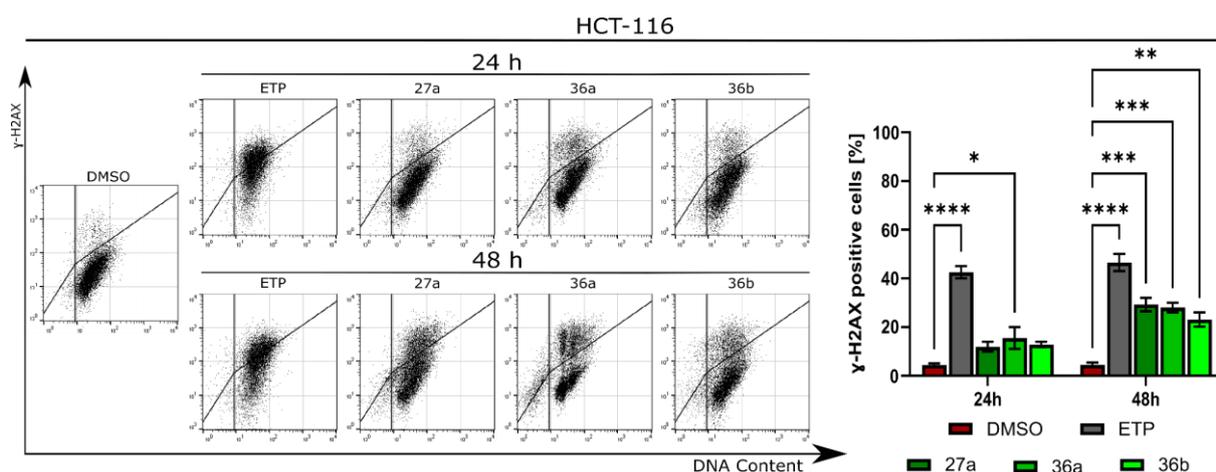
Figure 50 Flow cytometric analyses of induction γ-H2AX in HCT-116 cells. Dot-plot diagrams illustrate γ-H2AX staining, along with a bar graph displaying the percentage of γ-H2AX-positive cells. The data represent the mean ± SD of results obtained from three independent experiments. Statistical analysis was carried out using the two-way ANOVA test.

4.16 Assessment of the expression of proteins associated with apoptosis

AIF is an oxidoreductase containing flavin adenine dinucleotide, reliant on NADH, and located within the mitochondrial intermembrane space [298]. Its precise enzymatic function is yet to be determined. Following an apoptotic stimulus, AIF experiences proteolysis and migrates to the nucleus. There, it initiates chromatin condensation and substantial DNA degradation through a caspase-independent process [299]. Apart from its pivotal role in facilitating caspase-independent cell death, AIF has also been recognized as a crucial protein for cell survival [300,301]. BID is a proapoptotic BCL-2 protein characterized by the exclusive presence of the BH3 domain. Upon receipt of apoptotic signals, BID interacts with another BCL-2 family member, Bax, which initiates the integration of Bax into organelle membranes, primarily the outer mitochondrial membrane [302]. This interaction is believed to stimulate the opening of the mitochondrial voltage-dependent anion channel, leading to the release of cytochrome c and the activation of procaspase 9 [303].

Confocal imaging was employed to assess the effect of **27a**, **36a**, and **36b** on AIF activation. As shown in **Figures 51** and **52**, following a 24 h treatment of A549 and HCT-116 cells, these compounds did not elicit any observable alterations when compared to the DMSO control. Moreover, Western blotting was conducted to assess the expression of several apoptosis-related proteins. As depicted in **Figure 53**, the treatment of A549 cells with **36a** and **36b** resulted in a time-dependent modulation of the expression of all the investigated proteins. Notably, the expression of BID protein significantly decreased, while BAX expression showed a strong increase compared to the control sample (**Figure 53**). Treatment with carbazole derivatives also led to the disappearance of the band corresponding to intact PARP1, indicating its proteolytic cleavage and the formation of an 89-kDa fragment. Additionally, caspase-9 was cleaved into their respective catalytically active form. The expression of AIF remained unchanged when compared to the DMSO-treated control, which corroborates the observations from the confocal imaging (**Figures 51** and **52**) indicating that the treatment with **36a** and **36b** induces caspase-dependent cell death. These results present compelling evidence that the tested carbazole derivatives activate the intrinsic apoptosis pathway.
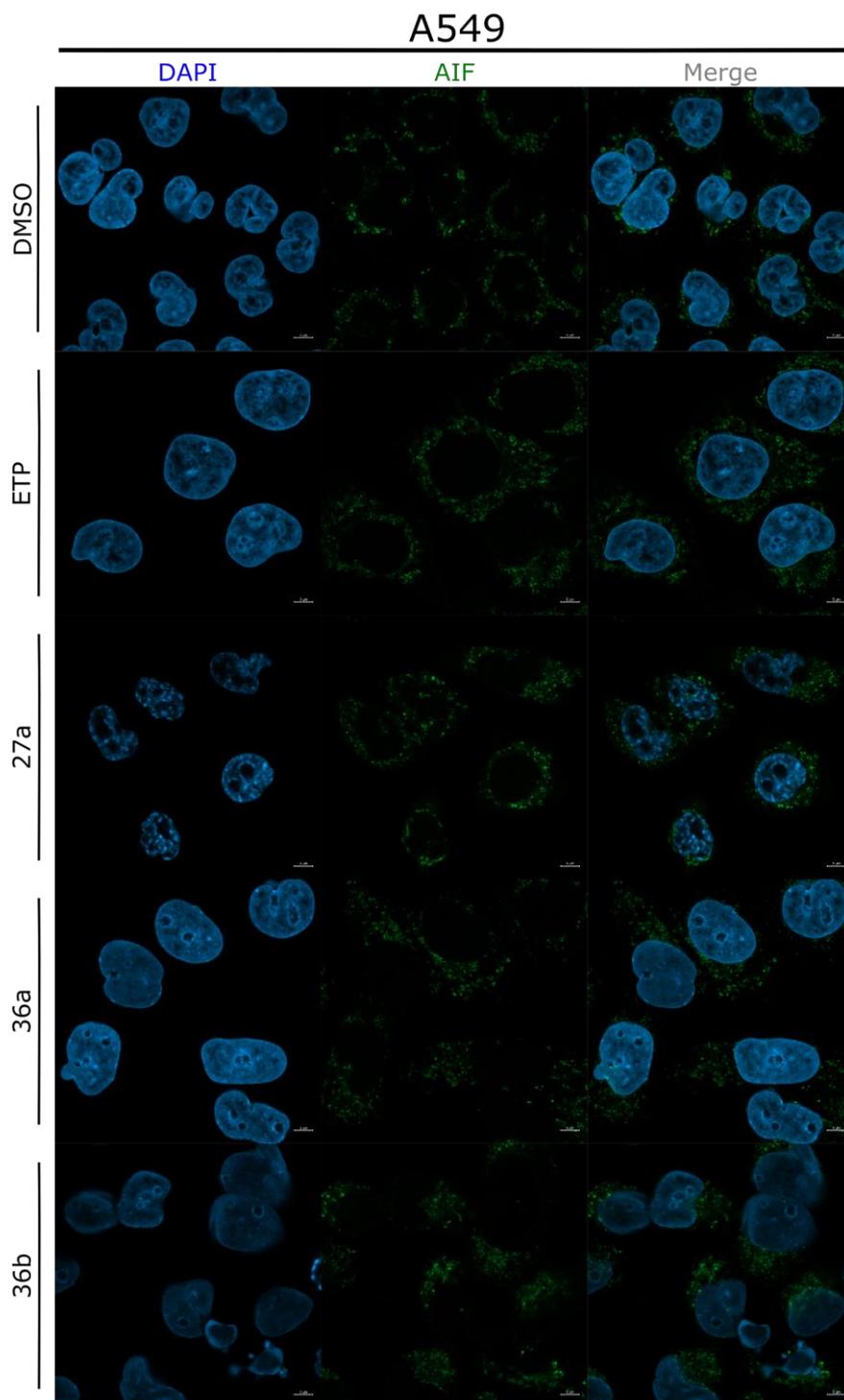
Figure 51 Microscopy images depict immunofluorescence in A549 cells, highlighting the formation of AIF foci following a 24 h treatment with carbazole derivatives. ETP and DMSO were employed as reference compounds. The AIF is represented in green, and the nucleus in blue (DAPI) in the images.
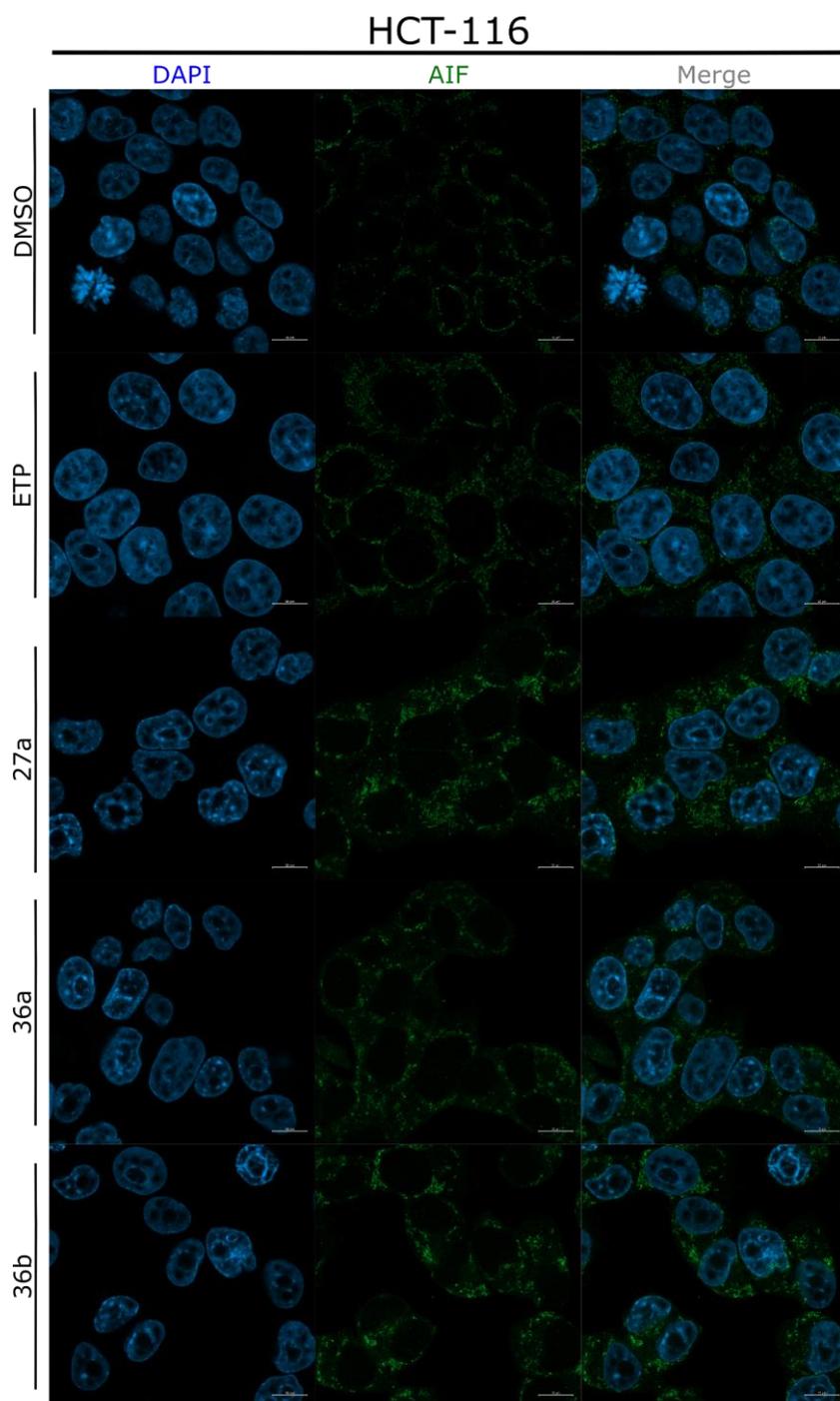
Figure 52 Microscopy images depict immunofluorescence in HCT-116 cells, highlighting the formation of AIF foci following a 24 h treatment with carbazole derivatives. ETP and DMSO were employed as reference compounds. The AIF is represented in green, and the nucleus in blue (DAPI) in the images.
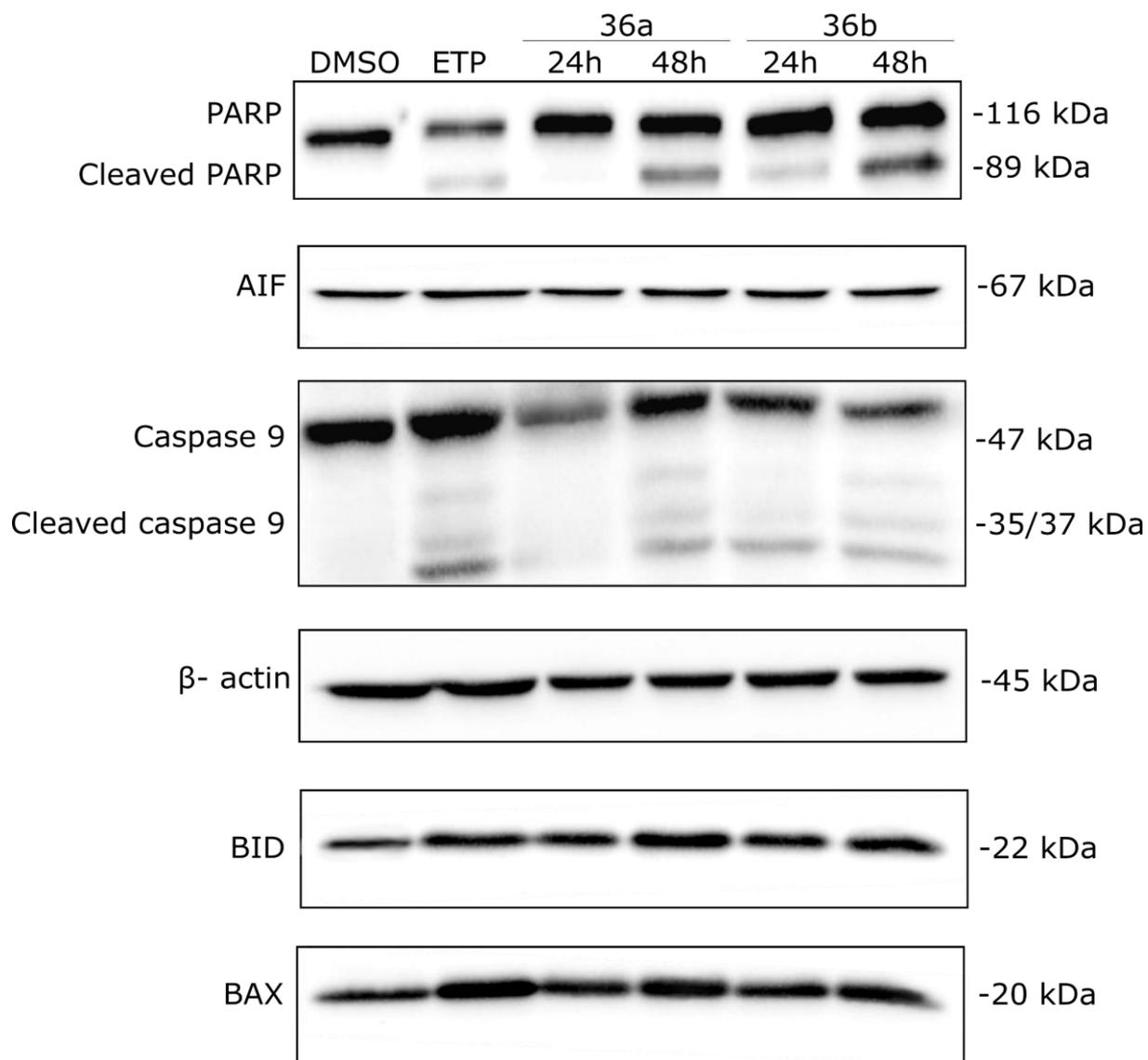
Figure 53 Western blot analysis demonstrates the impact of **36a** and **36b** on the expression of apoptosis-related proteins in the A549 cell line.

4.17 Carbazole derivatives induce DNA fragmentation

DNA fragmentation represents the conclusive stage of apoptosis, achieved through the activation of endonucleases, which cleave genomic DNA in dying cells into internucleosomal DNA fragments [304]. To validate the proapoptotic properties of the tested carbazoles, a TUNEL assay was conducted after subjecting A549 and HCT-116 cells to a 24 and 48 h treatment. As illustrated in **Figures 54** and **55**, all the compounds led to a time-dependent and significant increase in the proportion of TUNEL-positive cells in both cancer cell lines. Notably, the observed DNA fragmentation was more pronounced in HCT-116 cells than in A549 cells, with compound **27a** exhibiting the most substantial effect, consistent with the results obtained from the Annexin V-FITC/7-AAD assay (**Figures 32** and **33**).
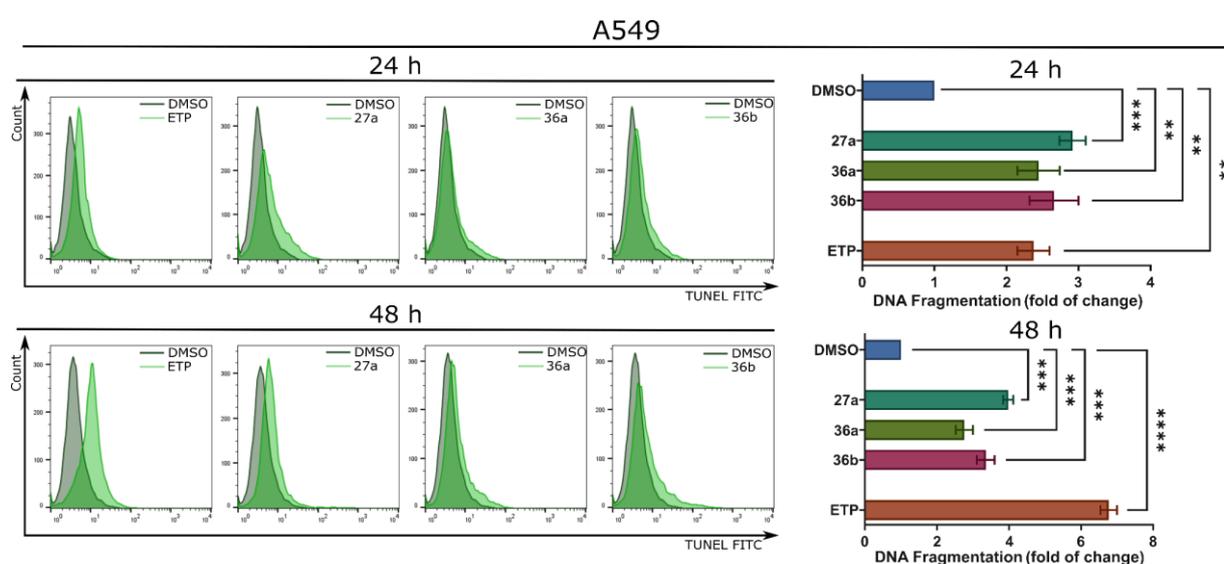
Figure 54 Flow cytometric analysis of DNA fragmentation after treatment with **27a**, **36a**, and **36b** in A549 cells. Representative histograms are presented on the left panel, and their quantification is depicted on the right panel. The data represent the mean ± SD of results obtained from three independent experiments. Statistical analysis was carried out using the one-way ANOVA test.
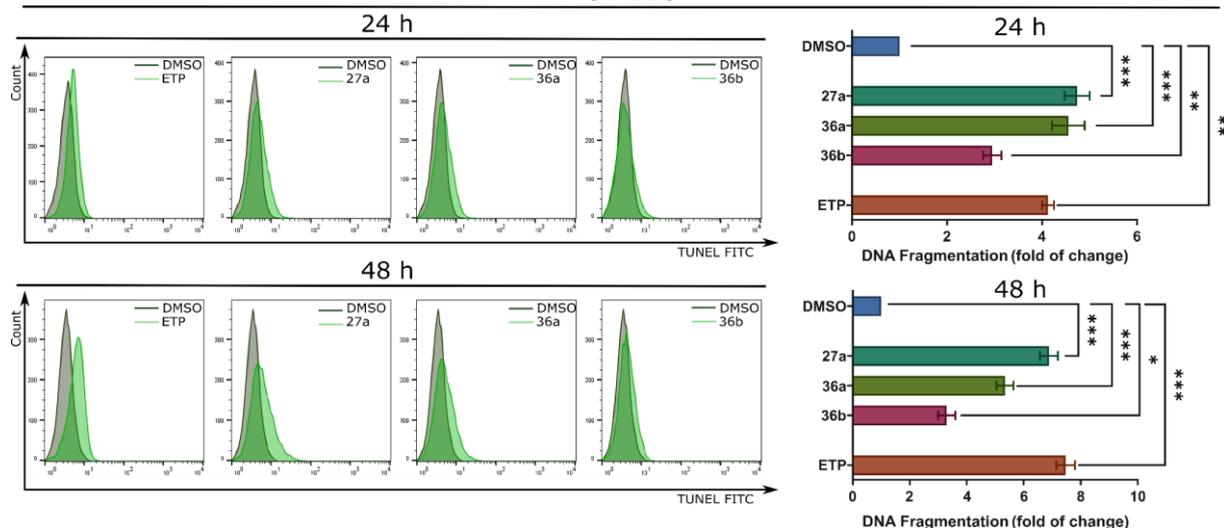
Figure 55 Flow cytometric analysis of DNA fragmentation after treatment with **27a**, **36a**, and **36b** in HCT-116 cells. Representative histograms are presented on the left panel, and their quantification is depicted on the right panel. The data represent the mean ± SD of results obtained from three independent experiments. Statistical analysis was carried out using the one-way ANOVA test.

4.18 Carbazole derivatives did not prompt senescence

Cell senescence is a broad concept encompassing the natural process of irreversible growth arrest, which can be initiated by telomere modifications or various types of stress [305]. Neoplastic transformation entails mechanisms that thwart the senescence program, and, until recently, it was believed that tumour cells had lost their ability to undergo senescence. However, it has now become evident that tumour cells can be induced to enter a state of senescence through genetic modifications or exposure to chemotherapy, radiation, or differentiation-inducing agents. Induced senescence, while sharing similarities with the replicative senescence of normal cells, has been identified as a crucial factor in the response of tumours to therapy, both *in vitro* and *in vivo* [306]. Even though senescent cells cease to proliferate, they remain metabolically active and secrete proteins with both tumour-suppressing and tumour-promoting properties [307].

A prior investigation validated the induction of apoptotic cell death by carbazole derivatives. In light of earlier research indicating that certain catalytic Topo II inhibitors can trigger cellular senescence [308], the tested compounds were evaluated using the Beta-Galactosidase (β-Gal) assay. β-gal activity is attributed to the gene responsible for lysosomal β-galactosidase (GLB1) and is a commonly employed indicator of cellular senescence. The increased GLB1 activity is a consequence of lysosomal compartment enlargement, which occurs due to the build-up of damaged macromolecules in senescent cells [309].

Compounds **27a**, **36a**, and **36b**, as depicted in **Figure 56**, did not induce distinctive changes suggestive of the senescent process in A549 and HCT-116 cell lines. After a 72 h treatment, the cells appeared smaller and more contracted compared to the DMSO sample. In contrast, the reference DOXO caused a distinct blue coloration indicative of cell aging. The results of microscopy studies confirm that the investigated carbazole derivatives do not induce cellular senescence, and consequently, further quantitative analysis was not conducted.
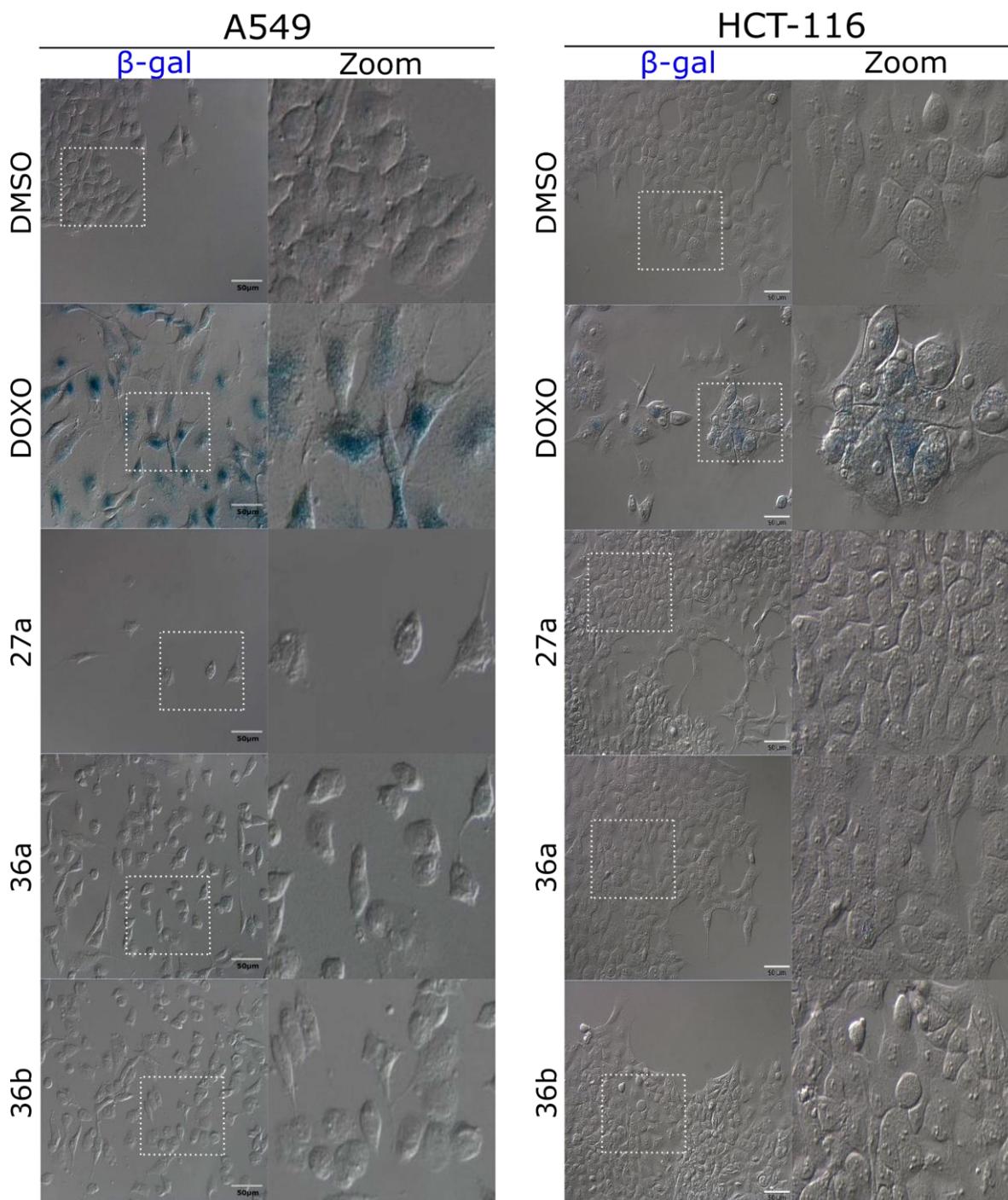
Figure 56 Representative microscopic images depicting A549, and HCT-116 cells following staining to visualize senescence-associated β-galactosidase activity. In this experiment, DMSO served as the negative control, while DOXO was used as the positive control. The scale bars indicate a length of 50 μm.

4.19 Carbazole derivatives inhibit activity of protein tyrosine kinases

Prior research indicates that the compounds under examination may also exhibit unintended effects, such as inducing cell death. Carbazole-scaffold-based compounds have the potential to exert anticancer effects through various pathways, including interactions with topoisomerases, kinases, and DNA intercalation. Numerous literature sources suggest that carbazole derivatives effectively suppress the activity of PTKs [310–312].

Protein kinases constitute a substantial group of enzymes that play a vital role in the process of protein phosphorylation, thereby overseeing numerous signalling pathways. The human protein kinase superfamily encompasses 518 members, forming a complex system characterized by intricate internal and external interactions [313]. This diverse group of protein kinases can be divided into two primary families, depending on their ability to phosphorylate either tyrosine or serine and threonine residues. Within the category of tyrosine kinases, there are 90 genes, with 58 being of the receptor type, further classified into 20 distinct groups, while the remaining 32 are nonreceptor kinases, distributed across 10 groups [314]. Tyrosine kinases hold a central role in the regulation of a wide range of cellular responses, including but not limited to cell division, metabolic processes, cell migration, cell-cell and cell-matrix adhesion, as well as the delicate balance between cell survival and apoptosis [315–317].

Considering the significance of PTK and the structural characteristics of carbazoles, the compounds were investigated using an enzyme-linked immunosorbent assay (ELISA) to assess their potential inhibitory effects on PTK. Imatinib, a selective PTKI used in medical treatments, served as a reference. As illustrated in **Figure 57**, two tested compounds, **36a** and **36b** exhibited a concentration-dependent reduction in PTK activity. **36a** and **36b** demonstrated the most potent inhibitory activity against PTK and were more effective at a concentration of 1 μM (***$p < 0.0001$) than imatinib ($p > 0.01$). To further assess the compounds' ability to suppress PTK phosphorylation, high serum-supported A549 cells were treated with increasing concentrations of the compounds and analysed using flow cytometry. Representative histograms and their quantification are presented in **Figures 58a** and **58b**. All the compounds, including **27a** displayed a concentration-dependent decrease in p-Tyr phosphorylation. Differential activity of compound **27a** in ELISA and flow cytometry assays may indicate that the inhibition of tyrosine kinase phosphorylation is an indirect effect. Compound **36a** exhibited the strongest inhibitory activity at every tested concentration, leading to a significant reduction in protein tyrosine phosphorylation (10 μM: ****$p < 0.00001$; 5 μM: **$p < 0.001$; 1 μM:*$p < 0.01$). This resulted in a substantial decrease in p-Tyr expression when compared to the DMSO control. Moreover, all the compounds demonstrated greater activity in comparison to imatinib.

Due to the lack of selectivity of the investigated carbazole derivatives against kinases and the high cost associated with conducting further research related to the identification of inhibited tyrosine kinases, this research direction was not pursued further.
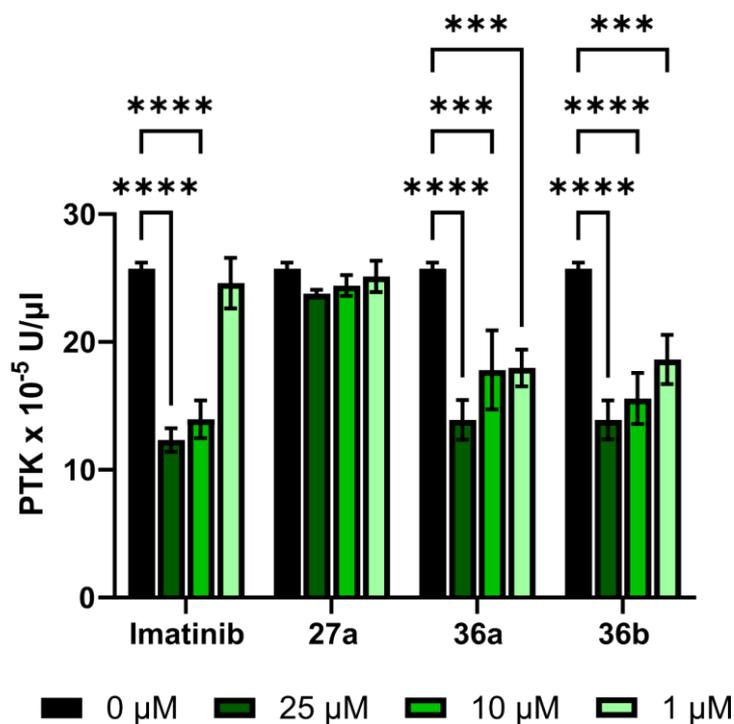
Figure 57 Analysis of tyrosine kinase phosphorylation changes following treatment with **27a**, **36a**, and **36b** was conducted, employing DMSO and imatinib as negative and positive controls, respectively. *In vitro* determination of PTK activity using A549 extracts determined by ELISA. The data presented here represent the mean ± SD of results obtained from three independent experiments. Statistical analysis was carried out using the two-way ANOVA test.
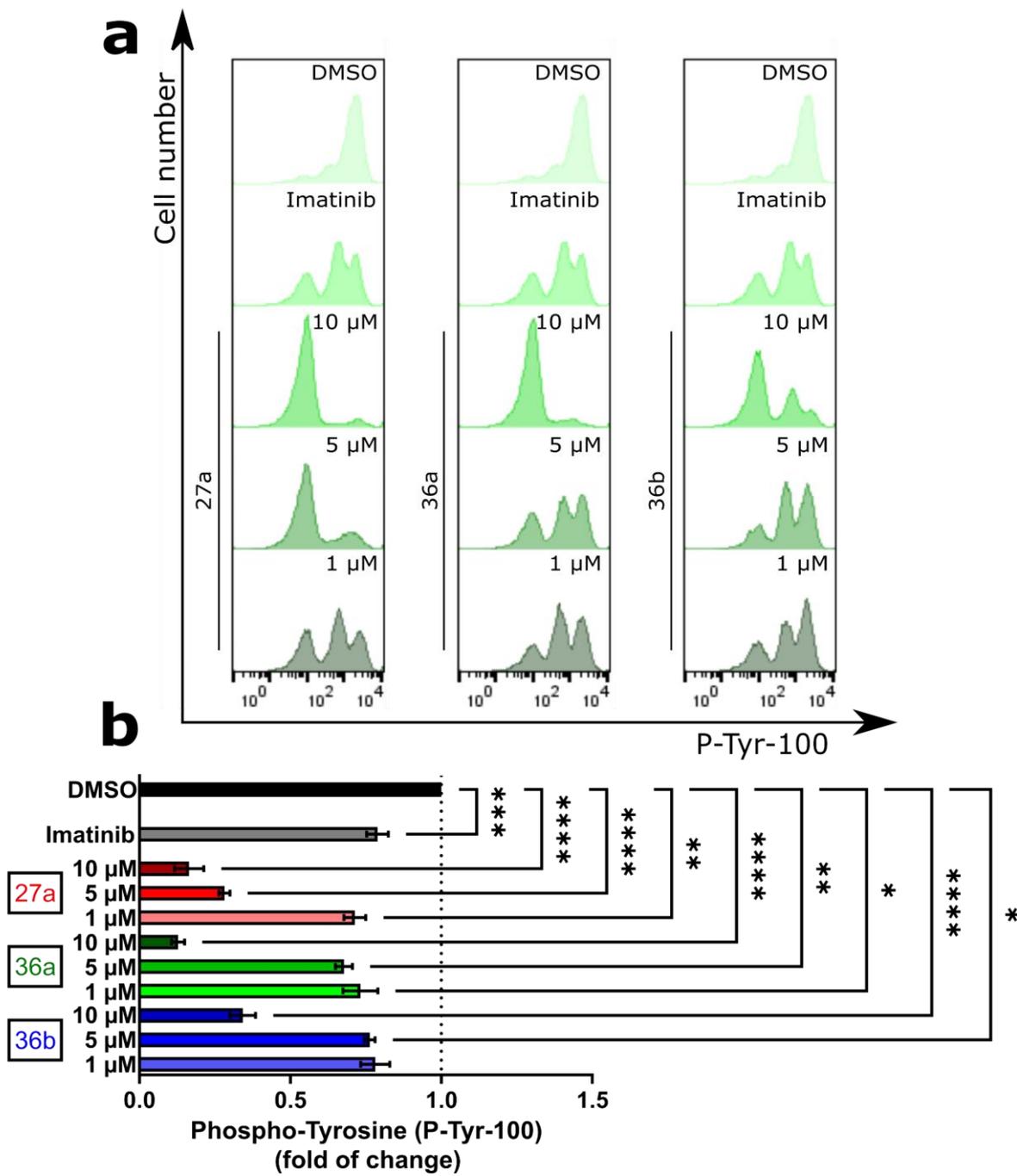
Figure 58 Analysis of tyrosine kinase phosphorylation changes following treatment with **27a**, **36a**, and **36b** was conducted, employing DMSO and imatinib as negative and positive controls, respectively. Presentation of representative histograms depicting the impact of compound treatment on A549 cells, as evaluated through intracellular phospho-flow cytometry (a). Quantification of the intracellular phospho-flow cytometry results, with error bars illustrating the standard error of the mean for data collected from n=3 independent experiments (b). Statistical analysis was carried out using the one-way ANOVA test.

5. DISCUSSION

The global cancer burden has been steadily increasing, leading to rising incidence and mortality rates. According to the 2020 Globocan report, there were 19.3 million newly diagnosed cancer cases and 10 million deaths worldwide. Notably, lung cancer represented 18% of these cases, making it one of the deadliest forms of the disease. Similarly, colon cancer accounted for 9.4% of cases, posing a significant health threat. Among men, lung and colon cancers were particularly prominent, while among women, breast, colon, and lung cancers were the leading types [7]. The future is expected to see a significant increase in the incidence of lung and colorectal cancer, driven by factors such as genetic mutations, an aging population, and growing resistance to conventional pharmacological treatments. Given this alarming trend, it is imperative to prioritize the development of novel and effective treatments, especially for lung, colon, and breast cancers [318,319].

Carbazole-based compounds play a significant role in the search for anticancer drugs.Three compounds, **27a**, **36a**, and **36b**, symmetrically substituted furan or thiophene derivatives of carbazole, were the subjects of my doctoral dissertation research. These compounds were rational designed as potential telomerase inhibitors. However, due to their lack of activity against telomerase and their interesting cytotoxic properties, I initiated an investigation leading to elucidating their molecular mode of action, which was the primary objective of my research.

Targeting Topo II with anticancer drugs is a systematic strategy in clinical oncology. Conventional chemotherapy medications like DOXO and ETP were initially chosen for their strong capacity to trigger cell death but have since been discovered to specifically interact with Topo II. These agents, known as Topo II poisons, possess the capability to stabilize the cleavable complex between Topo II and DNA, leading to the buildup of DNA double-strand breaks in the cell [320]. In contrast, catalytic inhibitors inhibit Topo II's activity without directly causing DNA damage. Numerous drugs have been identified to inhibit the catalytic activity of Topo II, and recent research suggests that these inhibitors operate through diverse mechanisms [172]. The specific cellular effects of these drugs can vary significantly depending on the step or steps of the Topo II catalytic cycle they target [321]. In this study, I found that the tested carbazole compounds did not stabilize the DNA/Topo II complex involved in the cleavage process. Compound **36a** exhibited promising inhibitory properties against the catalytic activity of Topo IIα and demonstrated high selectivity for the Topo IIα isoform, in contrast to most human Topo II inhibitors that affect both α and β isoforms [322]. This isoform selectivity is particularly noteworthy given recent research emphasizing the need for isoform-selective agents to reduce side effects associated with Topo II poisons [179]. Furthermore,

106

targeting Topo IIβ with chemotherapeutics has been linked to adverse effects, highlighting the growing interest in compounds that selectively inhibit one isoform [323–325].

I also found that **36a** might exert its mechanism of action by inhibiting a specific step in the catalytic cycle of the enzyme before the formation of the cleavable complex between Topo II and DNA, akin to the action of merbarone. Prior research has indicated that the carbazole group may possess the capability to intercalate with DNA [326–328]. I explored the possibility that the tested carbazole derivatives could disrupt the interaction between Topo II and DNA by distorting the DNA's helical structure. However, these findings suggest that their inhibitory effect on Topo II was direct and not mediated through DNA binding, as none of the compounds investigated in this study bound to DNA.

Topo I, unlike Topo II, is responsible for alleviating both positive and negative supercoiling in DNA by creating single-stranded breaks in the DNA molecule. Notably, Topo I does not rely on ATP for its enzymatic activity. Both Topo I and Topo II are established targets for cancer therapy. These two targets exhibit overlapping functions in DNA metabolism and play crucial roles in the regular cell cycle progression [140]. Thus, the simultaneous targeting of Topo I and Topo II may potentially result in synergistic anti-cancer effects [329]. In this study, the relaxation test results clearly indicate that **27a**, **36a**, and **36b** exhibited inhibitory effects on human Topo I. In particular, **36a** significantly inhibited Topo I at a concentration of 4 μM, suggesting a similar high activity as against Topo IIα. Furthermore, the DNA cleavage assay conducted in the presence of Topo I revealed that the observed reduction in nicked monomers from the relaxed and supercoiled monomers was lower for the tested carbazoles in comparison to CPT, employed as a reference Topo I poison. This outcome suggests that **36a** inhibits Topo I without inducing the formation of Topo cleavage complexes. Dual inhibitors targeting both Topo I and Topo II have emerged as an alternative to combination therapy strategies. Numerous studies in tumour models have demonstrated that compounds capable of inhibiting both targets exhibit enhanced *in vitro* efficacy when compared to single-target drugs. Additionally, these dual inhibitors hold the potential for reduced toxicity compared to combination therapies. To date, several dual inhibitors of Topo I and Topo II have been identified and characterized [330]. According to Denny et al. [329], these dual inhibitors can be categorized into three primary groups based on their structural features: intercalators, conjugates (hybrid inhibitors), and non-intercalative molecules [329]. According to this study, **36a** can be characterized as an innovative instance of non-intercalative dual inhibitors affecting both Topo I and Topo II within the carbazole derivatives group. Similarly, tafluposide, a derivative of ETP, displays dual catalytic inhibition against both Topo I and Topo II, and it exhibits enhanced activity against Topo I when compared to the original compound. The

remarkable cytotoxic effects of tafluposide are attributed to its capacity to induce mitochondrion-mediated apoptosis [331]. Furthermore, tafluposide demonstrates substantial *in vivo* efficacy in various tumour models [332]. Another example of Topo I/Topo II inhibitors is elomotecan, which was derived from the Topo I inhibitor CPT. It retains the activity of the parent molecule against Topo I and also possesses catalytic inhibitory activity against Topo II [144].

To assess their antiproliferative activity, I evaluated carbazole derivatives in various cancer cell lines, including bone, breast, colon, and lung. Among the tested cancer cell lines, **36a**, **36b**, and **27a** showed significant nanomolar IC_{50} values, effectively suppressing cancer cell proliferation and inhibiting colony formation. Interestingly, when considering cytotoxicity, **36a** showed a relatively weaker impact on the HEK293 cell line compared to the other cancer cell lines investigated in this study. However, its effectiveness was on par with that of the reference compound, ETP. The MTT results for NHBE and HMEC cell lines reveal that carbazoles did not exhibit selectivity towards normal cells. The results of cytotoxic activity on a panel of non-tumour and normal cell lines suggest that **36a** cannot be developed as a drug candidate. However, due to its interesting anticancer properties, it would be worthwhile to consider modifying its chemical structure to reduce its toxicity.The investigations conducted by Ortega's team demonstrated that after 72 h merbarone, functioning as a catalytic inhibitor, displayed notably diminished cytotoxic effects on A549 and MCF-7 cell lines [333]. The calculated IC_{50} values were 40±2.7 µM for A549 and 83.9±3.0 µM for MCF-7, when compared to **36a** [333].These findings underscore the potent inhibitory effect of **36a** on Topo II catalytic activity and its ability to suppress the proliferation of lung and colon cancer cells at nanomolar levels.

Regulation of the cell cycle plays a pivotal role in the development of malignancies and resistance to chemotherapy [334]. Notably, various catalytic inhibitors of Topo IIα have been found to operate via distinct mechanisms to suppress the cell cycle when compared to Topo II poisons [198]. Among all the compounds, **36a** displayed a substantial reduction in cell proliferation and induced G1-phase cell cycle arrest in most assessed cancer cell lines. However, in the case of U-2-OS cells, I observed a time-dependent G2/M phase blockade. These observations align with the research conducted by Perdih's group, who uncovered a novel chemical class of Topo IIα catalytic inhibitors that induced G1-phase cell cycle arrest in MCF-7 and Hep-G2 cells [336]. Similarly, Kang et al. reported a distinct effect of a catalytic inhibitor of Topo IIα, causing cell cycle arrest in the S phase and inhibiting the viability of ovarian cancer cells [337]. In contrast, Chen et al. described a G2/M phase delay in fibrosarcoma cells treated with ICRF-193 [338]. These studies provide further evidence that the cellular response to catalytic inhibitors of Topo II differs from that induced by Topo II poisons, particularly with regard to their impact on cell cycle progression[268]. The action of multiple Topo

I inhibitors disrupts the cell cycle. A new compound discovered by the Zhao team, DIA-001, induces cell arrest in the G2/M phase of the cell cycle by forming a stable Topo I/DNA complex [339].

In a study conducted by Ferrara and colleagues [340], it was shown that CPT, the most well-known TOPO I inhibitor, caused a significant shift in the cell population of colorectal cancer cells (DLD-1) when they were treated with CPT, pushing them predominantly into the late S/early G2 phase. These findings align with expectations since CPT induces DSBs during the S phase, which require repair before cells can progress through the cell cycle. **36a**, despite its high activity against Topo I, typically induced cell cycle arrest in the G1 phase, indicating that its action triggered a different cellular response than CPT.

ROS disrupt the delicate cellular redox balance, resulting in substantial and irreversible damage that ultimately leads to cell death. ROS encompasses both free radicals, such as hydroxyl and superoxide radicals, and nonradicals, including hydrogen peroxide and singlet oxygen. Many cytotoxic anticancer agents disturb the cellular redox state [341]. Therefore, I conducted a time-dependent kinetic assessment of intracellular ROS levels in both lung and colon cancer cell lines following treatment with **27a**, **36a**, and **36b**. The findings indicate that carbazole derivatives function as inducers of elevated ROS levels in both examined cell lines. Furthermore, when combined with compounds containing NAC, an antioxidant, the production of ROS was suppressed and did not differ from the control sample. Topo inhibitors that generate high levels of ROS include DOXO, ETP, and CPT [341,342]. In the context of apoptosis induced by chemotherapeutic agents, which involves the release of cytochrome c from the mitochondria, NADH dehydrogenase and reduced coenzyme Q10 reroute electrons from the electron transport system to oxygen, resulting in the formation of superoxide radicals [342,343]. In conclusion, it appears that cellular stress plays a substantial role in the anticancer effectiveness of these carbazole analogs with symmetric substitutions.

Conventional cancer pharmacological treatments often result in a reduction of mitochondrial membrane potential ($\Delta\Psi m$) and permeabilization of the mitochondrial membrane. This leads to the release of apoptotic factors and the activation of caspases, initiating cellular degradation through the targeted proteolysis of various cellular proteins [255]. In this research, I explored the impact of carbazole derivatives on the activities of Topoisomerase I (Topo I) and Topoisomerase II (Topo II) and their implications for apoptosis. The results revealed that these derivatives effectively inhibited the functions of Topo I and Topo II, thereby initiating apoptosis through mitochondrial mechanisms. Notably, compounds **27a**, **36a**, and **36b** induced apoptotic cell death in A549 and HCT-116 cell lines in a time-dependent manner. In the intrinsic-mediated pathway, a pivotal event known as MOMP, which

signifies a point of no return, directly triggers the release of pro-apoptotic proteins. This process involves a brief exposure of the Bak or Bax BH3 domain, allowing the efflux of cytochrome c into the cytoplasm. Cytochrome c, in conjunction with apoptotic protease activating factor 1, activates the initiator caspase 9. Activated caspase-9 subsequently cleaves and activates downstream effector caspases, caspase-3 and caspase-7, leading to the cleavage and activation of PARP1 protein. The extrusion of the mitochondrial inner membrane into the cytosol, along with its permeabilization, widens the Bax/Bak pores, triggering the release of mitochondrial DNA. Apoptosis can be initiated either through the direct activation of caspase-3 or by cleavage of Bid. This, in turn, results in mitochondrial dysfunction and subsequent activation of caspase-9 and caspase-3 [279,344]. Numerous established Topo II poisons, such as ETP, DOXO, and mitoxantrone, are known to induce apoptosis [345,346]. Similarly, prior studies have shown that Topo II catalytic inhibitors, like ICRF-187 and ICRF-193, induce apoptosis by activating caspases and causing internucleosomal DNA fragmentation [347,348]. As reported in the study by Alaaeldin et al [349]., novel ciprofloxacin derivatives have demonstrated dual inhibition of both human Topo I and Topo II. These derivatives not only exhibit antiproliferative effects but also effectively hinder cell migration and colony formation abilities in A549 and HepG2 cancer cell lines. Moreover, they initiate the apoptotic pathway by activating the caspase 3 signaling cascade [349], similar to the carbazole derivatives investigated in this research.

As previously mentioned, Topo II catalytic inhibitors were initially considered a promising alternative to Topo II poisons, as they were not expected to elevate the levels of Topo II-DNA complexes responsible for DNA damage. In fact, early reports appeared to support the idea that Topo II catalytic inhibitors, such as merbarone and bisdioxopiperazines, did not stabilize cleavable DNA-Topo II complexes and were ineffective as agents causing DNA damage. However, more recent investigations have revealed that merbarone and structurally related bisdioxopiperazines (ICRF-193 and ICRF-187) induced potent, dose-dependent genotoxic effects in mammalian cells, resembling those observed with the Topo II poison ETP [321,350]. Studies of carbazole derivatives for A549 and HCT-116 cell lines showed that carbazole derivatives caused the most significant increase in the level of γ-H2AX-positive cells after the longest treatment time point, correlated with the occurrence of massive apoptosis in the cells at the same time. This discovery could be associated with the occurrence of secondary DNA damage, the accumulation of γ-H2AX on the outer periphery of the nucleus, and the development of a distinctive apoptotic ring during the process of cell death. These phenomena may result from DNA damage triggered by the activation of caspase 3 [351,352].

Kinase signaling pathways play crucial roles in maintaining normal cellular functions, and aberrant kinase activities are frequently associated with various diseases, including cancer. Among the most successful anticancer drugs available today are kinase inhibitors [353]. Notably, certain carbazole derivatives, particularly **36a** and **36b**, exhibited potent inhibitory effects against protein tyrosine kinases in both ELISA and phospho flow cytometry assays. Cardenas et al. have reported that the activity of Topo II can be modulated through kinase phosphorylation [354]. Leveraging the structural elements of sunitinib, a tyrosine kinase inhibitor, and ciprofloxacin, a bacterial Topo II inhibitor, researchers designed and synthesized HMNE3. HMNE3 distinguishes itself as a ciprofloxacin dimer, incorporating the chalcone-like structural motif of sunitinib. Notably, HMNE3 exhibited inhibitory activity against both tyrosine kinases and Topo II, and it displayed cytotoxic effects in six chosen cell lines, including Panc-1, T24, BGC-823, PU145, HCG-27, and Capan-1 cells, with IC_{50} values within the low micromolar range. [355].

6. CONCLUSIONS

This study offers compelling *in vitro* evidence regarding the anticancer effectiveness of symmetric carbazole derivatives. All three investigated compounds **27a**, **36a**, and **36b** exhibited high cytotoxic activity and strong antiproliferative properties against various cancer cell lines. Moreover, the compounds were tested for their activity in inhibiting human topoisomerases as their potential molecular anticancer target. Additionally, **27a**, **36a**, and **36b** demonstrated prooxidative characteristics, disrupted calcium homeostasis, and induced robust mitochondria-dependent apoptosis in A549 and HCT-116 cells. Furthermore, the results indicate that these compounds inhibit the activity of protein tyrosine kinases in A549 cells. In particular, compound **36a**, which incorporates a furyl group, effectively inhibits cell proliferation and predominantly induces G1-phase arrest in cancer cells. **36a** represents a novel and promising class of dual non-intercalating catalytic inhibitors targeting Topo I and Topo II. It exhibits substantial selectivity in inhibiting the relaxation and decatenation activities of the Topo IIα isoform, and its mechanism involves the induction of apoptosis via the intrinsic pathway, accompanied by DNA fragmentation.

Moreover, structural adjustments, such as the flattening of the structure (**27a**) or the substitution of the *O*-heteroatom in the pyrrole ring (**36a**) with an *S*-heteroatom in the thiophene substituent (**36b**), distinctly modify the properties of the compounds. These alterations are prominently reflected in the outcomes of biological tests performed on Topo II. This information could have a significant impact on the design of novel carbazole derivative structures. Compound **36a** is particularly intriguing because it features two highly electronegative oxygen atoms that are configurationally compatible with the active site of the enzyme under investigation. In contrast, **36b**, which contains sulphur atoms (larger and less electronegative than oxygen in **36a**), cannot establish such robust interactions with the isoforms of Topo II. As for **27a**, its linear structure may account for its incompatibility with the size of the active centre pocket of the Topo II isoforms considered in this study.

36a serves as a promising exemplar or model molecule of symmetrically substituted carbazoles with potent anticancer properties. However, to gain a comprehensive understanding of how compound **36a** inhibits the catalytic activity of Topo IIα, further extensive studies are required. Such future investigations will unveil the intricate molecular interactions and signalling pathways contributing to the anticancer effects of this compound.

7. REFERENCES

1.   Prager, G. W., Braga, S., Bystricky, B., Qvortrup, C., Criscitiello, C., Esin, E., Sonke, G. S., Martínez, G. A., Frenel, J. S., Karamouzis, M., Strijbos, M., Yazici, O., Bossi, P., Banerjee, S., Troiani, T., Eniu, A., Ciardiello, F., Tabernero, J., Zielinski, C. C., Casali, P. G., Cardoso, F., Douillard, J. Y., Jezdic, S., McGregor, K., Bricalli, G., Vyas, M. & Ilbawi, A. Global cancer control: responding to the growing burden, rising costs and inequalities in access. *ESMO Open* **3,** 285 (2018).

2.   Upadhyay, A. Cancer: An unknown territory; rethinking before going ahead. *Genes & Diseases* **8,** 655 (2021).

3.   Feitelson, M. A., Arzumanyan, A., Kulathinal, R. J., Blain, S. W., Holcombe, R. F., Mahajna, J., Marino, M., Martinez-Chantar, M. L., Nawroth, R., Sanchez-Garcia, I., Sharma, D., Saxena, N. K., Singh, N., Vlachostergios, P. J., Guo, S., Honoki, K., Fujii, H., Georgakilas, A. G., Bilsland, A., Amedei, A., Niccolai, E., Amin, A., Ashraf, S. S., Boosani, C. S., Guha, G., Ciriolo, M. R., Aquilano, K., Chen, S., Mohammed, S. I., Azmi, A. S., Bhakta, D., Halicka, D., Keith, W. N. & Nowsheen, S. Sustained proliferation in cancer: Mechanisms and novel therapeutic targets. *Seminars in Cancer Biology* **35,** 25–54 (2015).

4.   Cooper, G. M. The cell: A molecular approach, 2nd edition: The development and causes of cancer. *Sinauer Associates* (2000).

5.   Hanahan, D. & Weinberg, R. A. Hallmarks of cancer: The next generation. *Cell* **144,** 646–674 (2011).

6.   Stark, L. L., Tofthagen, C., Visovsky, C. & McMillan, S. C. The symptom experience of patients with cancer. *Journal of Hospice and Palliative Nursing* **14,** 61 (2012).

7.   Deo, S. V. S., Sharma, J. & Kumar, S. GLOBOCAN 2020 Report on global cancer burden: challenges and opportunities for surgical oncologists. *Annals of Surgical Oncology* **29,** 6497–6500 (2022).

8.   Bray, F., Ferlay, J., Soerjomataram, I., Siegel, R. L., Torre, L. A. & Jemal, A. Global cancer statistics 2018: GLOBOCAN estimates of incidence and mortality worldwide for 36 cancers in 185 countries. *Cancer Journal for Clinicians* **68,** 394–424 (2018).

9.   Siegel, R. L., Miller, K. D., & Jemal, A. Cancer statistics. *Cancer Journal for Clinicians* **68,** 7–30 (2018).

10.   Haier, J. & Schaefers, J. Economic perspective of cancer care and its consequences for vulnerable groups. *Cancers* **14,** 3158 (2022).

11.   Debela, D. T., Muzazu, S. G., Heraro, K. D., Ndalama, M. T., Mesele, B. W., Haile, D. C., Kitui, S. K. & Manyazewal, T. New approaches and procedures for cancer treatment: Current perspectives. *SAGE Open Medicine* **9,** 205031212110343 (2021).

12.   Anand, P., Kunnumakara, A. B., Sundaram, C., Harikumar, K. B., Tharakan, S. T., Lai, O. S., Sung, B. & Aggarwal, B. B. Cancer is a preventable disease that requires major lifestyle changes. *Pharmaceutical Research* **25,** 2097–2116 (2008).

13.   Loomans-Kropp, H. A. & Umar, A. Cancer prevention and screening: the next step in the era of precision medicine. *NPJ Precision Oncology* **3,** 3 (2019).

14.   Dunn, B. K. & Kramer, B. S. Cancer prevention: Lessons learned and future directions. *Trends in Cancer* **2,** 713–722 (2016).

15.   Anand, U., Dey, A., Chandel, A. K. S., Sanyal, R., Mishra, A., Pandey, D. K., De Falco, V., Upadhyay, A., Kandimalla, R., Chaudhary, A., Dhanjal, J. K., Dewanjee, S., Vallamkondu, J. & Pérez de la Lastra, J. M. Cancer chemotherapy and beyond: Current status, drug candidates, associated risks and progress in targeted therapeutics. *Genes & Diseases* **10,** 1367–1401 (2023).

16.   Khalil, A. S., Jaenisch, R. & Mooney, D. J. Engineered tissues and strategies to overcome challenges in drug development. *Advanced Drug Delivery Reviews* **158,** 116–139 (2020).

17.   Kaitin, K. I. Deconstructing the drug development process: The new face of innovation. *Clinical Pharmacology & Therapeutics* **87,** 356–361 (2010).

18.   Zhong, L., Li, Y., Xiong, L., Wang, W., Wu, M., Yuan, T., Yang, W., Tian, C., Miao, Z., Wang, T. & Yang, S. Small molecules in targeted cancer therapy: advances, challenges, and future perspectives. *Signal Transduction and Targeted Therapy* **6,** 1–48 (2021).

19.   Kandi, V. & Vadakedath, S. Clinical trials and clinical research: a comprehensive review. *The Cureus Journal of Medical Science* **15,** e35077 (2023).

20.   Minami, H., Kiyota, N., Kimbara, S., Ando, Y., Shimokata, T., Ohtsu, A., Fuse, N., Kuboki, Y., Shimizu, T., Yamamoto, N., Nishio, K., Kawakami, Y., Nihira, S. ichi, Sase, K., Nonaka, T., Takahashi, H., Komori, Y. & Kiyohara, K. Guidelines for clinical evaluation of anti-cancer drugs. *Cancer Science* **112,** 2563–2577 (2021).

21.   Spreafico, A., Hansen, A. R., Abdul Razak, A. R., Bedard, P. L. & Siu, L. L. The future of clinical trials design in oncology. *Cancer Discovery* **11,** 822–837 (2021).

22.   Sahu, R. K., Yadav, R., Prasad, P., Roy, A. & Chandrakar, S. Adverse drug reactions monitoring: prospects and impending challenges for pharmacovigilance. *Springer Plus* **3,** 695 (2014).

23.   Hughes, J., Rees, S., Kalindjian, S. & Philpott, K. Principles of early drug discovery. *British Journal of Pharmacology* **162,** 1239–1249 (2011).

24.   Spedding, M. New directions for drug discovery. *Dialogues in Clinical Neuroscience* **8,** 295 (2006).

25.   Osterloh, I. H. The discovery and development of Viagra. Sildenafil. *Milestones in Drug Therapy* **21,** 1–13 (2004).

26. Smith, A. Screening for drug discovery: The leading question. *Nature* **418,** 453–455 (2002).

27. Szymański, P., Markowicz, M. & Mikiciuk-Olasik, E. Adaptation of high-throuput screening in drug discovery - toxicological screening tests. *International Journal of Molecular Sciences* **13,** 427–452 (2011).

28. Carnero, A. High throughput screening in drug discovery. *Clinical and Translational Oncology* **8,** 482–490 (2006).

29. Vincent, F., Nueda, A., Lee, J., Schenone, M., Prunotto, M. & Mercola, M. Phenotypic drug discovery: recent successes, lessons learned and new directions. *Nature Reviews Drug Discovery* **21,** 899–914 (2022).

30. Moffat, J. G., Rudolph, J. & Bailey, D. Phenotypic screening in cancer drug discovery - past, present and future. *Nature Reviews Drug Discovery* **13,** 588–602 (2014).

31. Kore, P. P., Mutha, M. M., Antre, R. V., Oswal, R. J. & Kshirsagar, S. S. Computer-aided drug design: an innovative tool for modeling. *Open Journal of Medicinal Chemistry* **2,** 139-148 (2012).

32. Jayakanthan, M., Wadhwa, G., Mohan, T. M., Arul, L., Balasubramanian, P. & Sundar, D. Computer-aided drug design for cancer-causing H-Ras p21 mutant protein. *Letters in Drug Design & Discovery* **6,** 14–20 (2009).

33. Sabe, V. T., Ntombela, T., Jhamba, L. A., Maguire, G. E. M., Govender, T., Naicker, T. & Kruger, H. G. Current trends in computer aided drug design and a highlight of drugs discovered via computational techniques: A review. *European Journal of Medicinal Chemistry* **224,** 113705 (2021).

34. Kapetanovic, I. M. Computer-aided drug discovery and development (CADDD): in silico-chemico-biological approach. *Chemico-biological interactions* **171,** 165 (2008).

35. Batool, M., Ahmad, B. & Choi, S. A structure-based drug discovery paradigm. *International Journal of Molecular Sciences* **20,** 2783 (2019).

36. Kirsch, P., Hartman, A. M., Hirsch, A. K. H. & Empting, M. Concepts and core principles of fragment-based drug design. *Molecules* **24,** 4309 (2019).

37. Anderson, A. C. The process of structure-based drug design. *Chemistry & Biology* **10,** 787–797 (2003).

38. Lee, C.-H., Huang, H.-C. & Juan, H.-F. Reviewing ligand-based rational drug design: The search for an ATP synthase inhibitor. *International Journal of Molecular Sciences* **12,** 5304–5318 (2011).

39. Acharya, C., Coop, A., Polli, J. E. & MacKerell, A. D. Recent advances in ligand-based drug design: Relevance and utility of the conformationally sampled pharmacophore approach. *Current Computer-Aided Drug Design* **7,** 10–22 (2011).

40.   Anderson, A. C. Structure-based functional design of drugs: from target to lead compound. *Methods in Molecular Biology* **823,** 359–366 (2012).

41.   Wilson, G. & Lill, M. Integrating structure-based and ligand-based approaches for computational drug design. *Future Medicinal Chemistry* **3,** 735–50 (2011).

42.   Bembenek, S. D., Tounge, B. A. & Reynolds, C. H. Ligand efficiency and fragment-based drug discovery. *Drug Discovery Today* **14,** 278–283 (2009).

43.   Sun, H., Tawa, G. & Wallqvist, A. Classification of scaffold hopping approaches. *Drug Discovery Today* **17,** 310–324 (2012).

44.   Dimova, D., Stumpfe, D. & Bajorath, J. Computational design of new molecular scaffolds for medicinal chemistry, part II: generalization of analog series-based scaffolds. *Future Science OA* **4,** FSO267 (2017).

45.   Schuffenhauer, A., Ertl, P., Roggo, S., Wetzel, S., Koch, M. A. & Waldmann, H. The scaffold tree--visualization of the scaffold universe by hierarchical scaffold classification. *Journal of Chemical Information and Modeling* **47,** 47–58 (2007).

46.   Hu, Y., Stumpfe, D. & Bajorath, J. Computational exploration of molecular scaffolds in medicinal chemistry. *Journal of Medicinal Chemistry* **59,** 4062–76 (2016).

47.   Bemis, G. W. & Murcko, M. A. The properties of known drugs. 1. Molecular frameworks. *Journal of Medicinal Chemistry* **39,** 2887–2893 (1996).

48.   Schuffenhauer, A. Computational methods for scaffold hopping. *Wiley Interdisciplinary Reviews: Computational Molecular Science* **2,** 842-867 (2012).

49.   Zheng, S., Lei, Z., Ai, H., Chen, H., Deng, D. & Yang, Y. Deep scaffold hopping with multimodal transformer neural networks. *Journal of Cheminformatics* **13,** 87 (2021).

50.   Hu, Y., Stumpfe, D. & Bajorath, J. Recent advances in scaffold hopping. *Journal of Medicinal Chemistry* **60,** 1238–1246 (2017).

51.   Welsch, M. E., Snyder, S. A. & Stockwell, B. R. Privileged scaffolds for library design and drug discovery. *Current Opinion in Chemical Biology* **14,** 347–361 (2010).

52.   Petrou, A., Fesatidou, M. & Geronikaki, A. Thiazole ring-a biologically active scaffold. *Molecules* **26,** 3166 (2021).

53.   Sharma, A. & Piplani, P. Acridine: A scaffold for the development of drugs for Alzheimer's disease. *Current Topics in Medicinal Chemistry* **23,** 1260–1276 (2023).

54.   Çapan, İ., Hawash, M., Jaradat, N., Sert, Y., Servi, R. & Koca, İ. Design, synthesis, molecular docking and biological evaluation of new carbazole derivatives as anticancer, and antioxidant agents. *BMC Chemistry* **17,** 60 (2023).

55.   S. Tsutsumi, L., Gündisch, D. & Sun, D. Carbazole scaffold in medicinal chemistry and natural products: A review from 2010-2015. *Current Topics in Medicinal Chemistry* **16,** 1290–1313 (2016).

56.   Issa, S., Prandina, A., Bedel, N., Rongved, P., Yous, S., Le Borgne, M. & Bouaziz, Z. Carbazole scaffolds in cancer therapy: a review from 2012 to 2018. *Journal of Enzyme Inhibition and Medicinal Chemistry* **34,** 1321 (2019).

57.   Ito, C., Itoigawa, M., Nakao, K., Murata, T., Tsuboi, M., Kaneda, N. & Furukawa, H. Induction of apoptosis by carbazole alkaloids isolated from Murraya koenigii. *International Journal of Phytotherapy and Phytopharmacology* **13,** 359–365 (2006).

58.   Witkowska, M., Maciejewska, N., Ryczkowska, M., Olszewski, M., Bagiński, M. & Makowiec, S. From tryptophan to novel mitochondria-disruptive agent, synthesis and biological evaluation of 1,2,3,6-tetrasubstituted carbazoles. *European Journal of Medicinal Chemistry* **238,** 114453 (2022).

59.   Mongre, R. K., Mishra, C. B., Prakash, A., Jung, S., Lee, B. S., Kumari, S., Hong, J. T. & Lee, M. S. Novel carbazole-piperazine hybrid small molecule induces apoptosis by targeting BCL-2 and inhibits tumor progression in lung adenocarcinoma in vitro and xenograft mice model. *Cancers* **11,** 1245 (2019).

60.   Lin, W., Wang, Y., Lin, S., Li, C., Zhou, C., Wang, S., Huang, H., Liu, P., Ye, G. & Shen, X. Induction of cell cycle arrest by the carbazole alkaloid Clauszoline-I from Clausena vestita D. D. Tao via inhibition of the PKCδ phosphorylation. *European Journal of Medicinal Chemistry* **47,** 214–220 (2012).

61.   Arbiser, J. L., Govindarajan, B., Battle, T. E., Lynch, R., Frank, D. A., Ushio-Fukai, M., Perry, B. N., Stern, D. F., Bowden, G. T., Liu, A., Klein, E., Kolodziejski, P. J., Eissa, N. T., Hossain, C. F. & Nagle, D. G. Carbazole is a naturally occurring inhibitor of angiogenesis and inflammation isolated from antipsoriatic coal tar. *The Journal of Investigative Dermatology* **126,** 1396–1402 (2006).

62.   Wei, R., Ma, Q., Li, T., Liu, W., Sang, Z., Li, M. & Liu, S. Carbazole alkaloids with antiangiogenic activities from Clausena sanki. *Bioorganic chemistry* **77,** 387–392 (2018).

63.   Nakamura, K., Sugumi, H., Yamaguchi, A., Uenaka, T., Kotake, Y., Okada, T., Kamata, J., Niijima, J., Nagasu, T., Koyanagi, N., Yoshino, H., Kitoh, K. & Yoshimatsu, K. Antitumor activity of ER-37328, a novel carbazole topoisomerase II inhibitor. *Molecular Cancer Therapeutics* **1,** 169-175 (2002).

64.   Ceramella, J., Iacopetta, D., Barbarossa, A., Caruso, A., Grande, F., Bonomo, M. G., Mariconda, A., Longo, P., Carmela, S. & Sinicropi, M. S. Carbazole derivatives as kinase-targeting inhibitors for cancer treatment. *Mini Reviews in Medicinal Chemistry* **20,** 444–465 (2020).

65.   Sun, L., Han, L., Zhang, L., Chen, C. & Zheng, C. Design, synthesis, and antitumor activity evaluation of carbazole derivatives with potent HDAC inhibitory activity. *Medicinal Chemistry Research* **32,** 1677–1689 (2023).

66.   Ropero, S. & Esteller, M. The role of histone deacetylases (HDACs) in human cancer. *Molecular Oncology* **1,** 19–25 (2007).

67. Gluszynska, A. Biological potential of carbazole derivatives. *European Journal of Medicinal Chemistry* **94,** 405–426 (2015).

68. Stafylas, P. C. & Sarafidis, P. A. Carvedilol in hypertension treatment. *Vascular Health and Risk Management* **4,** 23–30 (2008).

69. Ruffolo, R. R. & Feuerstein, G. Z. Pharmacology of carvedilol: Rationale for use in hypertension, coronary artery disease, and congestive heart failure. *Cardiovascular Drugs and Therapy* **11,** 247–256 (1997).

70. Zhao, Y., Xu, Y., Zhang, J. & Ji, T. Cardioprotective effect of carvedilol: inhibition of apoptosis in H9c2 cardiomyocytes via the TLR4/NF-κB pathway following ischemia/reperfusion injury. *Experimental and Therapeutic Medicine* **8,** 1092 (2014).

71. Liu, Q., Zhang, J., Xu, Y., Huang, Y. & Wu, C. Effect of carvedilol on cardiomyocyte apoptosis in a rat model of myocardial infarction: A role for toll-like receptor 4. *Indian Journal of Pharmacology* **45,** 458 (2013).

72. Ortiz, V. D., Türck, P., Teixeira, R., Lima-Seolin, B. G., Lacerda, D., Fraga, S. F., Hickmann, A., Gatelli Fernandes, T. R., Belló-Klein, A., Luz de Castro, A. & da Rosa Araujo, A. S. Carvedilol and thyroid hormones co-administration mitigates oxidative stress and improves cardiac function after acute myocardial infarction. *European Journal of Pharmacology* **854,** 159–166 (2019).

73. Zawadzka, K., Bernat, P., Felczak, A., Różalska, S. & Lisowska, K. Antibacterial activity of high concentrations of carvedilol against Gram-positive and Gram-negative bacteria. *International Journal of Antimicrobial Agents* **51,** 458–467 (2018).

74. Eid, A. H., Gad, A. M., Fikry, E. M. & Arab, H. H. Venlafaxine and carvedilol ameliorate testicular impairment and disrupted spermatogenesis in rheumatoid arthritis by targeting AMPK/ERK and PI3K/AKT/mTOR pathways. *Toxicology and Applied Pharmacology* **364,** 83–96 (2019).

75. Ruffolo, R. R., Gellai, M., Hieble, J. P., Willette, R. N. & Nichols, A. J. The pharmacology of carvedilol. *European Journal of Clinical Pharmacology* **38,** 82–88 (1990).

76. Chang, C. C., Kuo, I. C., Lin, J. J., Lu, Y. C., Chenc, C. T., Back, H. T., Lou, P. J. & Chang, T. C. A novel carbazole derivative, BMVC: a potential antitumor agent and fluorescence marker of cancer cells. *Chemistry & Biodiversity* **1,** 1377–1384 (2004).

77. Chen, L., Dickerhoff, J., Sakai, S. & Yang, D. DNA G-quadruplex in human telomeres and oncogene promoters: structures, functions, and small molecule targeting. *Accounts of Chemical Research* **55,** 2628–2646 (2022).

78. Huang, F.-C., Chang, C.-C., Lou, P.-J., Kuo, I.-C., Chien, C.-W., Chen, C.-T., Shieh, F.-Y., Chang, T.-C. & Lin, J.-J. G-quadruplex stabilizer 3,6-bis(1-methyl-4-vinylpyridinium)carbazole diiodide induces accelerated senescence and inhibits tumorigenic properties in cancer cells. *Molecular Cancer Research* **6,** 955–964 (2008).

79.   Tse, T.-Y., Chang, C.-C., Lin, J.-J. & Chang, T.-C. A fluorescent anti-cancer agent, 3,6-bis(1-methyl-4-vinylpyridinium) carbazole diiodide, stains g-quadruplexes in cells and inhibits tumor growth. *Current Topics in Medicinal Chemistry* **15,** 1964–1970 (2015).

80.   Chang, C.-C., Kuo, I.-C., Lin, J.-J., Lu, Y.-C., Chen, C.-T., Back, H.-T., Lou, P.-J. & Chang, T.-C. A novel carbazole derivative, BMVC: a potential antitumor agent and fluorescence marker of cancer cells. *Chemistry & Biodiversity* **1,** 1377–1384 (2004).

81.   Fox, S. M. & Johnston, S. A. Use of carprofen for the treatment of pain and inflammation in dogs. *Journal of the American Veterinary Medical Association* **210,** 1493–1498 (1997).

82.   Buseman, M., Blong, A. E. & Walton, R. A. L. Successful management of severe carprofen toxicity with manual therapeutic plasma exchange in a dog. *Journal of Veterinary Emergency and Critical Care* **32,** 675–679 (2022).

83.   Delgado, C., Bentley, E., Hetzel, S. & Smith, L. J. Carprofen provides better post-operative analgesia than tramadol in dogs after enucleation: A randomized, masked clinical trial. *Journal of the American Veterinary Medical Association* **245,** 1375–1381 (2014).

84.   Dumitrascu, F., Udrea, A.-M., Caira, M. R., Nuta, D. C., Limban, C., Chifiriuc, M. C., Popa, M., Bleotu, C., Hanganu, A., Dumitrescu, D. & Avram, S. In silico and experimental investigation of the biological potential of some recently developed carprofen derivatives. *Molecules* **27,** 2722 (2022).

85.   Nakano, H. & Omura, S. Chemical biology of natural indolocarbazole products: 30 years since the discovery of staurosporine. *Journal of Antibiotics* **62,** 17–26 (2009).

86.   Ōmura, S., Asami, Y. & Crump, A. Staurosporine: new lease of life for parent compound of today's novel and highly successful anti-cancer drugs. *Journal of Antibiotics* **71,** 688–701 (2018).

87.   Salas, A. P., Zhu, L., Sánchez, C., Braña, A. F., Rohr, J., Méndez, C. & Salas, J. A. Deciphering the late steps in the biosynthesis of the anti-tumour indolocarbazole staurosporine: sugar donor substrate flexibility of the StaG glycosyltransferase. *Molecular Microbiology* **58,** 17–27 (2005).

88.   Tanramluk, D., Schreyer, A., Pitt, W. R. & Blundell, T. L. On the origins of enzyme inhibitor selectivity and promiscuity: A case study of protein kinase binding to staurosporine. *Chemical Biology & Drug Design* **74,** 16–24 (2009).

89.   Park, B. S., Abdel-Azeem, A. Z., Al-Sanea, M. M., Yoo, K. H., Tae, J. S. & Lee, S. H. Staurosporine analogues from microbial and synthetic sources and their biological activities. *Current Medicinal Chemistry* **20,** 3872–3902 (2013).

90.   Goodwin, S., Smith, A. F. & Horning, E. C. Alkaloids of Ochrosia elliptica Labill. *Journal of the American Chemical Society* **81,** 1903–1908 (1959).

91.   Miller, C. M., O'Sullivan, E. C. & McCarthy, F. O. Novel 11-substituted ellipticines as potent anticancer agents with divergent activity against cancer cells. *Pharmaceuticals* **12,** 90 (2019).

92. Multon, E., Riou, J. F., LeFevre, D., Ahomadegbe, J. C. & Riou, G. Topoisomerase II-mediated DNA cleavage activity induced by ellipticines on the human tumor cell line N417. *Biochemical Pharmacology* **38,** 2077–2086 (1989).

93. Weber, G. F. DNA damaging drugs. *Molecular Therapies of Cancer* **9**, 112 (2014).

94. Rouëssé, J., Spielmann, M., Turpin, F., Le Chevalier, T., Azab, M. & Mondésir, J. M. Phase II study of elliptinium acetate salvage treatment of advanced breast cancer. *European Journal of Cancer* **29,** 856–859 (1993).

95. Sinicropi, M., Lacopetta, D., Rosano, C., Randino, R., Caruso, A., Saturnino, C., Muià, N., Ceramella, J., Puoci, F., Rodriquez, M., Longo, P. & Plutino, M. N-thioalkylcarbazoles derivatives as new anti-proliferative agents: synthesis, characterisation and molecular mechanism evaluation. *Journal of Enzyme Inhibition and Medicinal Chemistry* **33,** 434–444 (2018).

96. Larkins, E., Blumenthal, G. M., Chen, H., He, K., Agarwal, R., Gieser, G., Stephens, O., Zahalka, E., Ringgold, K., Helms, W., Shord, S., Yu, J., Zhao, H., Davis, G., McKee, A. E., Keegan, P. & Pazdur, R. FDA approval: Alectinib for the treatment of metastatic, ALK-positive non-small cell lung cancer following crizotinib. *Clinical Cancer Research* **22,** 5171–5176 (2016).

97. Paik, J. & Dhillon, S. Alectinib: A review in advanced, ALK-positive NSCLC. *Drugs* **78,** 1247–1257 (2018).

98. Attwa, M. W., AlRabiah, H., Mostafa, G. A. E. & Kadi, A. A. Evaluation of alectinib metabolic stability in HLMs using fast LC-MS/MS method: In silico ADME profile, P450 metabolic lability, and toxic alerts screening. *Pharmaceutics* **15,** 2449 (2023).

99. Gallogly, M. M., Lazarus, H. M. & Cooper, B. W. Midostaurin: a novel therapeutic agent for patients with FLT3-mutated acute myeloid leukemia and systemic mastocytosis. *Therapeutic Advances in Hematology* **8,** 245–261 (2017).

100. Kayser, S., Levis, M. J. & Schlenk, R. F. Midostaurin treatment in FLT3-mutated acute myeloid leukemia and systemic mastocytosis. *Expert Review of Clinical Pharmacology* **10,** 1177–1189 (2017).

101. Tzogani, K., Yu, Y., Meulendijks, D., Herberts, C., Hennik, P., Verheijen, R., Wangen, T., Håkonsen, G., Kaasboll, T., Dalhus M., Bolstad, B., Salmonson, T., Gisselbrecht Ch. & Pignatti F. European Medicines Agency review of midostaurin (Rydapt) for the treatment of adult patients with acute myeloid leukaemia and systemic mastocytosis. *ESMO Open* **4,** e000606 (2019).

102. Sly, N. & Gaspar, K. Midostaurin for the management of FLT3-mutated acute myeloid leukemia and advanced systemic mastocytosis. *American Journal of Health-System Pharmacy* **76,** 268–274 (2019).

103. Deweese, J. E., Osheroff, M. A. & Osheroff, N. DNA topology and topoisomerases. *Biochemistry and Molecular Biology Education* **37,** 2–10 (2009).

104.   Kuzminov, A. When DNA topology turns deadly. *Trend in Genetics* **34,** 111–120 (2018).

105.   Duprey, A. & Groisman, E. A. The regulation of DNA supercoiling across evolution. *Protein Science* **30,** 2042–2056 (2021).

106.   Gómez-González, B. & Aguilera, A. Transcription-mediated replication hindrance: A major driver of genome instability. *Genes & Development* **33,** 1008–1026 (2019).

107.   Bettotti, P., Visone, V., Lunelli, L., Perugino, G., Ciaramella, M. & Valenti, A. Structure and properties of DNA molecules over the full range of biologically relevant supercoiling states. *Scientific Reports* **8,** 6163 (2018).

108.   Liu, L. F. & Wang, J. C. Supercoiling of the DNA template during transcription. *Proceedings of the National Academy of Sciences of the USA* **84,** 7024–7027 (1987).

109.   McKie, S. J., Neuman, K. C. & Maxwell, A. DNA topoisomerases: Advances in understanding of cellular roles and multi-protein complexes via structure-function analysis. *Bioessays* **43,** e2000286 (2021).

110.   Moulton, D. E., Grandgeorge, P. & Neukirch, S. Stable elastic knots with no self-contact. *Journal of the Mechanics and Physics of Solids* **116,** 33–53 (2018).

111.   Espeli, O. & Marians, K. J. Untangling intracellular DNA topology. *Molecular Microbiology* **52,** 925–931 (2004).

112.   Falaschi, A., Abdurashidova, G., Sandoval, O., Radulescu, S., Biamonti, G. & Riva, S. Molecular and structural transactions at human DNA replication origins. *Cell Cycle* **6,** 1705–1712 (2007).

113.   Wang, J. C. Cellular roles of DNA topoisomerases: a molecular perspective. *Nature Reviews Molecular Cell Biology* **3,** 430–440 (2002).

114.   Nitiss, J. L. Investigating the biological functions of DNA topoisomerases in eukaryotic cells. *Biochimica et Biophysica Acta* **1400,** 63–81 (1998).

115.   Pommier, Y., Nussenzweig, A., Takeda, S. & Austin, C. Human topoisomerases and their roles in genome stability and organization. *Nature Reviews Molecular Cell Biology* **23,** 407 (2022).

116.   Wang, J. C. DNA Topoisomerases. *Annual Review of Biochemistry* **65,** 635–692 (1996).

117.   Bizard, A. H. & Hickson, I. D. The many lives of type IA topoisomerases. *Journal of Biological Chemistry* **295,** 7138–7153 (2020).

118.   Viard, T. & de la Tour, C. B. Type IA topoisomerases: A simple puzzle? *Biochimie* **89,** 456–467 (2007).

119.   Pommier, Y., Sun, Y., Huang, S.-Y. N. & Nitiss, J. L. Roles of eukaryotic topoisomerases in transcription, replication and genomic stability. *Nature Reviews Molecular Cell Biology* **17,** 703–721 (2016).

120.   Roca, J. Transcriptional inhibition by DNA torsional stress. *Transcription* **2,** 82–85 (2011).

121.   Lee, S. K. & Wang, W. Roles of topoisomerases in heterochromatin, aging, and diseases. *Genes* **10,** 884 (2019).

122.   Nitiss, J. L. DNA topoisomerase II and its growing repertoire of biological functions. *Nature reviews Cancer* **9,** 327 (2009).

123.   Baker, N. M., Rajan, R. & Mondragón, A. Structural studies of type I topoisomerases. *Nucleic Acids Research* **37,** 693–701 (2009).

124.   Morimoto, S., Tsuda, M., Bunch, H., Sasanuma, H., Austin, C. & Takeda, S. Type II DNA topoisomerases cause spontaneous double-strand breaks in genomic DNA. *Genes* **10,** 868 (2019).

125.   Wang, J. C. Interaction between DNA and an Escherichia coli protein omega. *Journal of Molecular Biology* **55,** 523–533 (1971).

126.   Turley, H., Comley, M., Houlbrook, S., Nozaki, N., Kikuchi, A., Hickson, I. D., Gatter, K. & Harris, A. L. The distribution and expression of the two isoforms of DNA topoisomerase II in normal and neoplastic human tissues. *British Journal of Cancer* **75,** 1340–1346 (1997).

127.   Kondapi, A. K., Satyanarayana, N. & Saikrishna, A. D. A study of the topoisomerase II activity in HIV-1 replication using the ferrocene derivatives as probes. *Archives of Biochemistry and Biophysics* **450,** 123–132 (2006).

128.   Sun, Y., Saha, S., Wang, W., Saha, L. K., Huang, S.-Y. N. & Pommier, Y. Excision repair of topoisomerase DNA-protein crosslinks (TOP-DPC). *DNA Repair* **89,** 102837 (2020).

129.   Deweese, J. E. & Osheroff, N. The DNA cleavage reaction of topoisomerase II: wolf in sheep's clothing. *Nucleic Acids Research* **37,** 738–748 (2009).

130.   Hevener, K. E., Verstak, T. A., Lutat, K. E., Riggsbee, D. L. & Mooney, J. W. Recent developments in topoisomerase-targeted cancer chemotherapy. *Acta Pharmaceutica Sinica B* **8,** 844–861 (2018).

131.   Venditto, V. J. & Simanek, E. E. Cancer therapies utilizing the camptothecins: A review of in vivo literature. *Molecular Pharmaceutics* **7,** 307–349 (2010).

132.   Khaiwa, N., Maarouf, N. R., Darwish, M. H., Alhamad, D. W. M., Sebastian, A., Hamad, M., Omar, H. A., Orive, G. & Al-Tel, T. H. Camptothecin's journey from discovery to WHO essential medicine: fifty years of promise. *European Journal of Medicinal Chemistry* **223,** 113639 (2021).

133.   Tesauro, C., Simonsen, A. K., Andersen, M. B., Petersen, K. W., Kristoffersen, E. L., Algreen, L., Hansen, N. Y., Andersen, A. B., Jakobsen, A. K., Stougaard, M., Gromov, P., Knudsen, B. R. & Gromova, I. Topoisomerase I activity and sensitivity to camptothecin in breast cancer-derived cells: a comparative study. *BMC Cancer* **19,** 1158 (2019).

134.   Sakasai, R. & Iwabuchi, K. The distinctive cellular responses to DNA strand breaks caused by a DNA topoisomerase I poison in conjunction with DNA replication and RNA transcription. *Genes & Genetic Systems* **90,** 187–194 (2016).

135.   Del Poeta, M., Chen, S.-F., Von Hoff, D., Dykstra, C. C., Wani, M. C., Manikumar, G., Heitman, J., Wall, M. E. & Perfect, J. R. Comparison of in vitro activities of camptothecin and nitidine derivatives against fungal and cancer cells. *Antimicrobial Agents and Chemotherapy* **43,** 2862–2868 (1999).

136.   Hertzberg, R. P., Busby, R. W., Caranfa, M. J., Holden, K. G., Johnson, R. K., Hecht, S. M. & Kingsbury, W. D. Irreversible trapping of the DNA-topoisomerase I covalent complex. Affinity labeling of the camptothecin binding site. *Journal of Biological Chemistry* **265,** 19287–19295 (1990).

137.   Pommier, Y. Topoisomerase I inhibitors: camptothecins and beyond. *Nature Reviews Cancer* **6,** 789–802 (2006).

138.   Pommier, Y., Barcelo, J., Rao, V. A., Sordet, O., Jobson, A. G., Thibaut, L., Miao, Z., Seiler, J., Zhang, H., Marchand, C., Agama, K. & Redon, C. Repair of topoisomerase I-mediated DNA damage. *Progress in Nucleic Acid Research and Molecular Biology* **81,** 179–229 (2006).

139.   Czuwara-Ladykowska, J., Makiela, B., Smith, E. A., Trojanowska, M. & Rudnicka, L. The inhibitory effects of camptothecin, a topoisomerase I inhibitor, on collagen synthesis in fibroblasts from patients with systemic sclerosis. *Arthritis Research & Therapy* **3,** 311–318 (2001).

140.   Pommier, Y. DNA topoisomerase I inhibitors: Chemistry, biology, and interfacial inhibition. *Chemical Reviews* **109,** 2894–2902 (2009).

141.   Gongora, C., Vezzio-Vie, N., Tuduri, S., Denis, V., Causse, A., Auzanneau, C., Collod-Beroud, G., Coquelle, A., Pasero, P., Pourquier, P., Martineau, P. & Del Rio, M. New topoisomerase I mutations are associated with resistance to camptothecin. *Molecular Cancer* **10,** 64 (2011).

142.   Kojiri, K., Kondo, H., Yoshinari, T., Arakawa, H., Nakajima, S., Satoh, F., Kawamura, K., Okura, A., Suda, H. & Okanishi, M. A new antitumor substance, BE-13793C, produced by a Streptomycete taxonomy, fermentation, isolation, structure determination and biological activity. *Journal of Antibiotics* **44,** 723–728 (1991).

143.   Kathiravan, M. K., Khilare, M. M., Nikoomanesh, K., Chothe, A. S. & Jain, K. S. Topoisomerase as target for antibacterial and anticancer drug discovery. *Journal of Enzyme Inhibition and Medicinal Chemistry* **28,** 419–435 (2013).

144.   Li, F., Jiang, T., Li, Q. & Ling, X. Camptothecin (CPT) and its derivatives are known to target topoisomerase I (Top1) as their mechanism of action: did we miss something in CPT analogue molecular targets for treating human disease such as cancer? *American Journal of Cancer Research* **7,** 2350–2394 (2017).

145.   Bansal, S., Bajaj, P., Pandey, S. & Tandon, V. Topoisomerases: Resistance versus sensitivity, how far we can go? *Medicinal Research Reviews* **37,** 404–438 (2017).

146.   Li, T.-K., Houghton, P. J., Desai, S. D., Daroui, P., Liu, A. A., Hars, E. S., Ruchelman, A. L., LaVoie, E. J. & Liu, L. F. Characterization of ARC-111 as a novel topoisomerase I-targeting anticancer drug. *Cancer Research* **63,** 8400–8407 (2003).

147.   Marzi, L., Agama, K., Murai, J., Difilippantonio, S., James, A., Peer, C. J., Figg, W. D., Beck, D., Elsayed, Mohamed. S. A., Cushman, M. & Pommier, Y. Novel fluoroindenoisoquinoline non-camptothecin topoisomerase I inhibitors. *Molecular Cancer Therapeutics* **17,** 1694–1704 (2018).

148.   Gokduman, K. Strategies targeting DNA topoisomerase I in cancer chemotherapy: camptothecins, nanocarriers for camptothecins, organic non-camptothecin compounds and metal complexes. *Current drug targets* **17,** 1928-1939 (2016).

149.   Lee, J. H. & Berger, J. M. Cell cycle-dependent control and roles of DNA topoisomerase II. *Genes* **10,** 859 (2019).

150.   McClendon, A. K. & Osheroff, N. DNA Topoisomerase II, genotoxicity, and cancer. *Mutation research* **623,** 83 (2007).

151.   Fortune, J. M. & Osheroff, N. Topoisomerase II as a target for anticancer drugs: when enzymes stop being nice. *Progress in Nucleic Acid Research and Molecular Biology* **64,** 221–253 (2000).

152.   Cuvier, O. & Hirano, T. A role of topoisomerase II in linking DNA replication to chromosome condensation. *Journal of Cell Biology* **160,** 645–655 (2003).

153.   Mengoli, V., Jonak, K., Lyzak, O., Lamb, M., Lister, L. M., Lodge, C., Rojas, J., Zagoriy, I., Herbert, M. & Zachariae, W. Deprotection of centromeric cohesin at meiosis II requires APC/C activity but not kinetochore tension. *EMBO Journal* **40,** e106812 (2021).

154.   Clarke, D. J. & Azuma, Y. Non-catalytic roles of the topoisomerase IIα C-terminal domain. *International Journal of Molecular Sciences* **18,** 2438 (2017).

155.   Antoniou-Kourounioti, M., Mimmack, M. L., Porter, A. C. G. & Farr, C. J. The impact of the C-Terminal region on the interaction of topoisomerase II alpha with mitotic chromatin. *International Journal of Molecular Sciences* **20,** 1238 (2019).

156.   Kozuki, T., Chikamori, K., Surleac, M. D., Micluta, M. A., Petrescu, A. J., Norris, E. J., Elson, P., Hoeltge, G. A., Grabowski, D. R., Porter, A. C. G., Ganapathi, R. N. & Ganapathi, M. K. Roles of the C-terminal domains of topoisomerase IIα and topoisomerase IIβ in regulation of the decatenation checkpoint. *Nucleic Acids Research* **45,** 5995–6010 (2017).

157.   Crewe, M. & Madabhushi, R. Topoisomerase-mediated DNA damage in neurological disorders. *Frontiers in Aging Neuroscience* **13,** 751742 (2021).

158.   Madabhushi, R. The roles of DNA topoisomerase IIβ in transcription. *International Journal of Molecular Sciences* **19,** 1917 (2018).

159. Calderwood, S. K. A critical role for topoisomerase IIβ and DNA double-strand breaks in transcription. *Transcription* **7,** 75–83 (2016).

160. Zaim, M. & Isik, S. DNA topoisomerase IIβ stimulates neurite outgrowth in neural differentiated human mesenchymal stem cells through regulation of Rho-GTPases (RhoA/Rock2 pathway) and Nurr1 expression. *Stem Cell Research & Therapy* **9,** 114 (2018).

161. Mandraju, R. K. & Kondapi, A. K. Regulation of topoisomerase II α and β in HIV-1 infected and uninfected neuroblastoma and astrocytoma cells: Involvement of distinct nordihydroguaretic acid sensitive inflammatory pathways. *Archives of Biochemistry and Biophysics* **461,** 40–49 (2007).

162. McNamara, S., Wang, H., Hanna, N. & Miller Jr., W. H. Topoisomerase IIβ negatively modulates retinoic acid receptor α function: a novel mechanism of retinoic acid resistance. *Molecular and Cellular Biology* **28,** 2066–2077 (2008).

163. Bollimpelli, V. S., Dholaniya, P. S. & Kondapi, A. K. Topoisomerase IIβ and its role in different biological contexts. *Archives of Biochemistry and Biophysics* **633,** 78–84 (2017).

164. Dougherty, A. C., Hawaz, M. G., Hoang, K. G., Trac, J., Keck, J. M., Ayes, C. & Deweese, J. E. Exploration of the role of the C-terminal domain of human DNA topoisomerase IIα in catalytic activity. *ACS Omega* **6,** 25892–25903 (2021).

165. Nitiss, J. L. Targeting DNA topoisomerase II in cancer chemotherapy. *Nature Reviews Cancer* **9,** 338–350 (2009).

166. Vann, K. R., Oviatt, A. A. & Osheroff, N. Topoisomerase II poisons: converting essential enzymes into molecular scissors. *Biochemistry* **60,** 1630–1641 (2021).

167. Chène, P., Rudloff, J., Schoepfer, J., Furet, P., Meier, P., Qian, Z., Schlaeppi, J.-M., Schmitz, R. & Radimerski, T. Catalytic inhibition of topoisomerase II by a novel rationally designed ATP-competitive purine analogue. *BMC Chemical Biology* **9,** 1 (2009).

168. Skok, Ž., Zidar, N., Kikelj, D. & Ilaš, J. Dual inhibitors of human DNA topoisomerase ii and other cancer-related targets. *Journal of Medicinal Chemistry* **63,** 884–904 (2020).

169. Okoro, C. O. & Fatoki, T. H. A mini review of novel topoisomerase II inhibitors as future anticancer agents. *International Journal of Molecular Sciences* **24,** 2532 (2023).

170. Gellert, M., O'Dea, M. H., Itoh, T. & Tomizawa, J. Novobiocin and coumermycin inhibit DNA supercoiling catalyzed by DNA gyrase. *Proceedings of the National Academy of Sciences of the USA* **73,** 4474–4478 (1976).

171. Nitiss, J. L., Pourquier, P. & Pommier, Y. Aclacinomycin A stabilizes topoisomerase I covalent complexes. *Cancer Research* **57,** 4564–4569 (1997).

172. Larsen, A. K., Escargueil, A. E. & Skladanowski, A. Catalytic topoisomerase II inhibitors in cancer therapy. *Pharmacology and Therapeutics* **99,** 167–181 (2003).

173.   Hande, K. R. Topoisomerase II inhibitors. *Update on Cancer Therapeutics* **3,** 13–26 (2008).

174.   Classen, S., Olland, S. & Berger, J. Structure of the topoisomerase II ATPase region and its mechanism of inhibition by the chemotherapeutic agent ICRF-187. *Proceedings of the National Academy of Sciences of the USA* **100,** 10629–10634 (2003).

175.   Hasinoff, B. B., Abram, M. E., Barnabé, N., Khélifa, T., Allan, W. P. & Yalowich, J. C. The catalytic DNA topoisomerase II inhibitor dexrazoxane (ICRF-187) induces differentiation and apoptosis in human leukemia K562 cells. *Molecular Pharmacology* **59,** 453–461 (2001).

176.   Deng, S., Yan, T., Nikolova, T., Fuhrmann, D., Nemecek, A., Gödtel-Armbrust, U., Kaina, B. & Wojnowski, L. The catalytic topoisomerase II inhibitor dexrazoxane induces DNA breaks, ATF3 and the DNA damage response in cancer cells. *British Journal of Pharmacology* **172,** 2246–2257 (2015).

177.   Zidar, N., Secci, D., Tomašič, T., Mašič, L. P., Kikelj, D., Passarella, D., Argaez, A. N. G., Hyeraci, M. & Via, L. D. Synthesis, antiproliferative effect, and topoisomerase II inhibitory activity of 3-methyl-2-phenyl-1H-indoles. *ACS Medicinal Chemistry Letters* **11,** 691 (2020).

178.   Baldwin, E. L. & Osheroff, N. Etoposide, topoisomerase II and cancer. *Current Medicinal Chemistry - Anti-Cancer Agents* **5,** 363–372 (2005).

179.   Azarova, A. M., Lyu, Y. L., Lin, C. P., Tsai, Y. C., Lau, J. Y. N., Wang, J. C. & Liu, L. F. Roles of DNA topoisomerase II isozymes in chemotherapy and secondary malignancies. *Proceedings of the National Academy of Sciences of the USA* **104,** 11014–11019 (2007).

180.   Imbert, T. F. Discovery of podophyllotoxins. *Biochimie* **80,** 207–222 (1998).

181.   Zhang, W., Gou, P., Dupret, J.-M., Chomienne, C. & Rodrigues-Lima, F. Etoposide, an anticancer drug involved in therapy-related secondary leukemia: Enzymes at play. *Translational Oncology* **14,** 101169 (2021).

182.   Buttmann, M., Seuffert, L., Mäder, U. & Toyka, K. V. Malignancies after mitoxantrone for multiple sclerosis. *Neurology* **86,** 2203–2207 (2016).

183.   Bethesda, M. D. In LiverTox*:* Clinical and research information on drug-induced liver injury - mitoxantrone. *National Institute of Diabetes and Digestive and Kidney Diseases* (2012)

184.   Larripa, I. B., Carballo, M. A., Mudry, M. M. & Labal de Vinuesa, M. L. Etoposide and teniposide: in vivo and in vitro genotoxic studies. *Clinical Drug Investigation* **4,** 365–375 (1992).

185.   Tanabe, K., Ikegami, Y., Ishida, R. & Andoh, T. Inhibition of topoisomerase II by antitumor agents bis(2,6-dioxopiperazine) derivatives. *Cancer Research* **51,** 4903–4908 (1991).

186.   Skok, Ž., Durcik, M., Gramec Skledar, D., Barančoková, M., Peterlin Mašič, L., Tomašič, T., Zega, A., Kikelj, D., Zidar, N. & Ilaš, J. Discovery of new ATP-competitive inhibitors of human DNA topoisomerase IIα through screening of bacterial topoisomerase inhibitors. *Bioorganic Chemistry* **102,** 104049 (2020).

187.   Fortune, J. M. & Osheroff, N. Merbarone inhibits the catalytic activity of human topoisomerase IIα by blocking DNA cleavage. *Journal of Biological Chemistry* **273,** 17643–17650 (1998).

188.   Kim, H. S., Kim, Y. H., Yoo, O. J. & Lee, J. J. Aclacinomycin X, a novel anthracycline antibiotic produced by Streptomyces galilaeus ATCC 31133. *Bioscience, Biotechnology, and Biochemistry* **60,** 906–908 (1996).

189.   Cresteil, T. Reference module in biomedical sciences*:* Aclarubicin. *Elsevier* (2017).

190.   Röthig, H. J., Kraemer, H. P. & Sedlacek, H. H. Aclarubicin: experimental and clinical experience. *Drugs under experimental and clinical research* **11,** 123–125 (1985).

191.   Brouwer, T. P., van der Zanden, S. Y., van der Ploeg, M., van Eendenburg, J. D. H., Bonsing, B. A., de Miranda, N. F. C. C., Neefjes, J. J. & Vahrmeijer, A. L. The identification of the anthracycline aclarubicin as an effective cytotoxic agent for pancreatic cancer. *Anticancer Drugs* **33,** 614–621 (2022).

192.   Rogalska, A., Szwed, M. & Jóźwiak, Z. Aclarubicin-induced apoptosis and necrosis in cells derived from human solid tumours. *Mutatation Research* **700,** 1–10 (2010).

193.   Sehested, M. & Jensen, P. B. Mapping of DNA topoisomerase II poisons (etoposide, clerocidin) and catalytic inhibitors (aclarubicin, ICRF-187) to four distinct steps in the topoisomerase II catalytic cycle. *Biochemical Pharmacolology* **51,** 879–886 (1996).

194.   Cresteil, T. Reference module in biomedical sciences: Aclarubicin. Elsevier (2017).

195.   Lu, D.-Y. & Lu, T.-R. Anticancer activities and mechanisms of bisdioxopiperazine compounds probimane and MST-16. *Anti-Cancer Agents in Medicinal Chemistry* **10,** 78–91 (2010).

196.   Bavlovič Piskáčková, H., Jansová, H., Kubeš, J., Karabanovich, G., Váňová, N., Kollárová-Brázdová, P., Melnikova, I., Jirkovská, A., Lenčová-Popelová, O., Chládek, J., Roh, J., Šimůnek, T., Štěrba, M. & Štěrbová-Kovaříková, P. Development of water-soluble prodrugs of the bisdioxopiperazine topoisomerase IIβ inhibitor ICRF-193 as potential cardioprotective agents against anthracycline cardiotoxicity. *Scientific Reports* **11,** 4456 (2021).

197.   Sato, M., Ishida, R., Narita, T., Kato, J., Ikeda, H., Fukazawa, H. & Andoh, T. Interaction of the DNA topoisomerase II catalytic inhibitor meso-2,3-bis(3,5-dioxopiperazine-1-yl)butane (ICRF-193), a bisdioxopiperazine derivative, with the conserved region(s) of eukaryotic but not prokaryotic enzyme. *Biochemical Pharmacology* **54,** 545–550 (1997).

198.   Perrin, D., van Hille, B. & Hill, B. T. Differential sensitivities of recombinant human topoisomerase II alpha and beta to various classes of topoisomerase II-interacting agents. *Biochemical Pharmacolology* **56,** 503–507 (1998).

199.   Nakazawa, N., Mehrotra, R., Arakawa, O. & Yanagida, M. ICRF-193, an anticancer topoisomerase II inhibitor, induces arched telophase spindles that snap, leading to a ploidy increase in fission yeast. *Genes Cells* **21,** 978–993 (2016).

200.   Germe, T. & Hyrien, O. Topoisomerase II–DNA complexes trapped by ICRF-193 perturb chromatin structure. *EMBO reports* **6,** 729–735 (2005).

201.   Arencibia, J. M., Brindani, N., Franco-Ulloa, S., Nigro, M., Kuriappan, J. A., Ottonello, G., Bertozzi, S. M., Summa, M., Girotto, S., Bertorelli, R., Armirotti, A. & De Vivo, M. Design, synthesis, dynamic docking, biochemical characterization, and in vivo pharmacokinetics studies of novel topoisomerase ii poisons with promising antiproliferative activity. *Journal of Medicinal Chemistry* **63,** 3508–3521 (2020).

202.   Murphy, M. B., Mercer, S. L. & Deweese, J. E. Advances in Molecular Toxicology. **11,** 203–240 (2017).

203.   Fortune, J. M. & Osheroff, N. Merbarone inhibits the catalytic activity of human topoisomerase IIα by blocking DNA cleavage. *Journal of Biological Chemistry* **273,** 17643–17650 (1998).

204.   Pastor, N., Domínguez, I., Orta, M. L., Campanella, C., Mateos, S. & Cortés, F. The DNA topoisomerase II catalytic inhibitor merbarone is genotoxic and induces endoreduplication. *Mutation Research* **738–739,** 45–51 (2012).

205.   Spallarossa, A., Lusardi, M., Caneva, C., Profumo, A., Rosano, C. & Ponassi, M. Bicyclic basic merbarone analogues as antiproliferative agents. *Molecules* **26,** 557 (2021).

206.   Glover, A., Chun, H. G., Kleinman, L. M., Cooney, D. A., Plowman, J., Grieshaber, C. K., Malspeis, L. & Leyland-Jones, B. Merbarone: an antitumor agent entering clinical trials. *Investigational New Drugs* **5,** 137–143 (1987).

207.   Gedik, C. M. & Collins, A. R. Comparison of effects of fostriecin, novobiocin, and camptothecin, inhibitors of DNA topoisomerases, on DNA replication and repair in human cells. *Nucleic Acids Research* **18,** 1007–1013 (1990).

208.   Maxwell, A. The interaction between coumarin drugs and DNA gyrase. *Molecular Microbiology* **9,** 681–686 (1993).

209.   Sekiguchi, J., Stivers, J. T., Mildvan, A. S. & Shuman, S. Mechanism of inhibition of vaccinia DNA topoisomerase by novobiocin and coumermycin. *Journal of Biological Chemistry* **271,** 2313–2322 (1996).

210.   Schwartz, G. N., Teicher, B. A., Eder, J. P., Korbut, T., Holden, S. A., Ara, G. & Herman, T. S. Modulation of antitumor alkylating agents by novobiocin, topotecan, and lonidamine. *Cancer Chemotherapy and Pharmacology* **32,** 455–462 (1993).

211.   Singh, G., Jayanarayan, K. G. & Dey, C. S. Novobiocin induces apoptosis-like cell death in topoisomerase II over-expressing arsenite resistant Leishmania donovani. *Molecular and Biochemical Parasitology* **141,** 57–69 (2005).

212. Vermeulen, K., Van Bockstaele, D. R. & Berneman, Z. N. The cell cycle: a review of regulation, deregulation and therapeutic targets in cancer. *Cell Proliferation* **36,** 131–149 (2003).

213. Cooper, G. M. in The Cell: A Molecular Approach. Cell Proliferation in Development and Differentiation. 2nd edition, *Sinauer Associates* (2000).

214. Tyson, J. J., Csikasz-Nagy, A. & Novak, B. The dynamics of cell cycle regulation. *Bioessays* **24,** 1095–1109 (2002).

215. Heuvel, S. van den. Cell cycle regulation. *Pasadena* (2018).

216. Hunt, T., Nasmyth, K. & Novák, B. The cell cycle. *Philosophical Transactions of the Royal Society B* **366,** 3494–3497 (2011).

217. Zou, T. & Lin, Z. The involvement of ubiquitination machinery in cell cycle regulation and cancer progression. *International Journal of Molecular Sciences* **22,** 5754 (2021).

218. Al Bitar, S. & Gali-Muhtasib, H. The role of the cyclin dependent kinase inhibitor p21cip1/waf1 in targeting cancer: molecular mechanisms and novel therapeutics. *Cancers* **11,** 1475 (2019).

219. Malumbres, M. & Barbacid, M. Mammalian cyclin-dependent kinases. *Trends in Biochemical Sciences* **30,** 630–641 (2005).

220. Malumbres, M. Cyclin-dependent kinases. *Genome Biology* **15,** 122 (2014).

221. Topacio, B. R., Zatulovskiy, E., Cristea, S., Xie, S., Tambo, C. S., Rubin, S. M., Sage, J., Kõivomägi, M. & Skotheim, J. M. Cyclin D-Cdk4,6 drives cell-cycle progression via the retinoblastoma protein's C-terminal helix. *Molecular Cell* **74,** 758-770.e4 (2019).

222. Mazumder, S., DuPree, E. L. & Almasan, A. a dual role of cyclin E in cell proliferation and apotosis may provide a target for cancer therapy. *Current Cancer Drug Targets* **4,** 65–75 (2004).

223. Fagundes, R. & Teixeira, L. K. Cyclin E/CDK2: DNA replication, replication stress and genomic instability. *Frontiers in Cell and Developmental Biology* **9,** 774845 (2021).

224. Chibazakura, T., Kamachi, K., Ohara, M., Tane, S., Yoshikawa, H. & Roberts, J. M. Cyclin A promotes S-phase entry via interaction with the replication licensing factor Mcm7. *Molecular and Cellular Biology* **31,** 248–255 (2011).

225. Otto, T. & Sicinski, P. Cell cycle proteins as promising targets in cancer therapy. *Nature Reviews Cancer* **17,** 93–115 (2017).

226. Williams, G. H. & Stoeber, K. The cell cycle and cancer. *The Journal of Pathology* **226,** 352–364 (2012).

227. Peyressatre, M., Prével, C., Pellerano, M. & Morris, M. C. Targeting cyclin-dependent kinases in human cancers: from small molecules to peptide inhibitors. *Cancers* **7,** 179–237 (2015).

228. Suski, J. M., Braun, M., Strmiska, V. & Sicinski, P. Targeting cell-cycle machinery in cancer. *Cancer Cell* **39,** 759–778 (2021).

229. Cannan, W. J. & Pederson, D. S. Mechanisms and consequences of double-strand DNA break formation in chromatin. *Journal of Cellular Physiology* **231,** 3–14 (2016).

230. Terasawa, M., Shinohara, A. & Shinohara, M. Double-strand break repair-adox: Restoration of suppressed double-strand break repair during mitosis induces genomic instability. *Cancer Science* **105,** 1519–1525 (2014).

231. Chatterjee, N. & Walker, G. C. Mechanisms of DNA damage, repair and mutagenesis. *Environmental and Molecular Mutagenesis* **58,** 235–263 (2017).

232. Bonner, W. M., Redon, C. E., Dickey, J. S., Nakamura, A. J., Sedelnikova, O. A., Solier, S. & Pommier, Y. γH2AX and cancer. *Nature Reviews Cancer* **8,** 957 (2008).

233. Nikolova, T., Dvorak, M., Jung, F., Adam, I., Krämer, E., Gerhold-Ay, A. & Kaina, B. The γH2AX assay for genotoxic and nongenotoxic agents: comparison of H2AX phosphorylation with cell death response. Toxicological Sciences **140,** 103–117 (2014).

234. Podhorecka, M., Skladanowski, A. & Bozko, P. H2AX phosphorylation: Its role in DNA damage response and cancer therapy. *Journal of Nucleic Acids* **2010,** 920161 (2010).

235. Kuo, L. J. & Yang, L.-X. Gamma-H2AX - a novel biomarker for DNA double-strand breaks. *In vivo* **22,** 305–309 (2008).

236. Nakamura, H. & Takada, K. Reactive oxygen species in cancer: Current findings and future directions. *Cancer Science* **112,** 3945–3952 (2021).

237. Afzal, S., Abdul Manap, A. S., Attiq, A., Albokhadaim, I., Kandeel, M. & Alhojaily, S. M. From imbalance to impairment: the central role of reactive oxygen species in oxidative stress-induced disorders and therapeutic exploration. *Frontiers in Pharmacology* **14,** 1269581 (2023).

238. Bardaweel, S. K., Gul, M., Alzweiri, M., Ishaqat, A., ALSalamat, H. A. & Bashatwah, R. M. Reactive oxygen species: the dual role in physiological and pathological conditions of the human body. *The Eurasian Journal of Medicine* **50,** 193–201 (2018).

239. M, R.-D. & DA, A.-B. Activation of apoptosis signalling pathways by reactive oxygen species. *Biochimica et biophysica acta* **1863,** 2977–2992 (2016).

240. Jiang, H., Zuo, J., Li, B., Chen, R., Luo, K., Xiang, X., Lu, S., Huang, C., Liu, L., Tang, J. & Gao, F. Drug-induced oxidative stress in cancer treatments: Angel or devil? *Redox Biology* **63,** 102754 (2023).

241. Carreras-Sureda, A., Pihán, P. & Hetz, C. Calcium signaling at the endoplasmic reticulum: Fine-tuning stress responses. *Cell Calcium* **70,** 24–31 (2018).

242. Giorgi, C., Baldassari, F., Bononi, A., Bonora, M., De Marchi, E., Marchi, S., Missiroli, S., Patergnani, S., Rimessi, A., Suski, J. M., Wieckowski, M. R. & Pinton, P. Mitochondrial Ca^{2+} and apoptosis. *Cell Calcium* **52,** 36–43 (2012).

243. Pinton, P., Giorgi, C., Siviero, R., Zecchini, E. & Rizzuto, R. Calcium and apoptosis: ER-mitochondria Ca2+ transfer in the control of apoptosis. *Oncogene* **27,** 6407–6418 (2008).

244. Kim, M., Baek, M. & Joon Kim, D. Protein Tyrosine signaling and its potential therapeutic implications in carcinogenesis. *Current Pharmaceutical Design* **23,** 4226–4246 (2017).

245. Paul, M. K. & Mukhopadhyay, A. K. Tyrosine kinase – role and significance in cancer. *International Journal of Medical Sciences* **1,** 101–115 (2004).

246. Du, Z. & Lovly, C. M. Mechanisms of receptor tyrosine kinase activation in cancer. *Molecular Cancer* **17,** 58 (2018).

247. Iqbal, N. & Iqbal, N. Imatinib: A breakthrough of targeted therapy in cancer. *Chemotherapy Research and Practice* **2014,** 357027 (2014).

248. Rossari, F., Minutolo, F. & Orciuolo, E. Past, present, and future of Bcr-Abl inhibitors: from chemical development to clinical efficacy. *Journal of Hematology & Oncology* **11,** 84 (2018).

249. Lindauer, M. & Hochhaus, A. Dasatinib. *Recent Results in Cancer Research* **184,** 83–102 (2010).

250. Cortes, J., Hochhaus, A., Hughes, T. & Kantarjian, H. Front-line and salvage therapies with tyrosine kinase inhibitors and other treatments in chronic myeloid leukemia. *Journal of Clinical Oncology* **29,** 524–531 (2011).

251. Cohen, P., Cross, D. & Jänne, P. A. Kinase drug discovery 20 years after imatinib: progress and future directions. *Nature Reviews Drug Discovery* **20,** 551–569 (2021).

252. Chen, Y. & Fu, L. Mechanisms of acquired resistance to tyrosine kinase inhibitors. *Acta Pharmaceutica Sinica B* **1,** 197–207 (2011).

253. Pfeffer, C. M. & Singh, A. T. K. Apoptosis: a target for anticancer therapy. *International Journal of Molecular Sciences* **19,** 448 (2018).

254. Jan, R. & Chaudhry, G.-S. Understanding apoptosis and apoptotic pathways targeted cancer therapeutics. *Advanced Pharmaceutical Bulletin* **9,** 205–218 (2019).

255. Wong, R. S. Y. Apoptosis in cancer: from pathogenesis to treatment. *Journal of Experimental & Clinical Cancer Research* **30,** 87 (2011).

256. Van Opdenbosch, N. & Lamkanfi, M. Caspases in cell death, inflammation and disease. *Immunity* **50,** 1352–1364 (2019).

257.   Shi, Y. Caspase activation, inhibition, and reactivation: A mechanistic view. *Protein Science* **13,** 1979–1987 (2004).

258.   Li, J. & Yuan, J. Caspases in apoptosis and beyond. *Oncogene 2008* **27,** 6194–6206 (2008).

259.   Olsson, M. & Zhivotovsky, B. Caspases and cancer. *Cell Death Differ* **18,** 1441–1449 (2011).

260.   Singh, R., Letai, A. & Sarosiek, K. Regulation of apoptosis in health and disease: the balancing act of BCL-2 family proteins. *Nature Reviews Molecular Cell Biology* **20,** 175–193 (2019).

261.   Kale, J., Osterlund, E. J. & Andrews, D. W. BCL-2 family proteins: changing partners in the dance towards death. *Cell Death & Differentiation* **25,** 65–80 (2017).

262.   Papaliagkas, V., Anogianaki, A., Anogianakis, G. & Ilonidis, G. The proteins and the mechanisms of apoptosis: A mini-review of the fundamentals. *Hippokratia* **11,** 108–113 (2007).

263.   Morales, J. C., Li, L., Fattah, F. J., Dong, Y., Bey, E. A., Patel, M., Gao, J. & Boothman, D. A. Review of Poly (ADP-ribose) Polymerase (PARP) mechanisms of action and rationale for targeting in cancer and other diseases. *Critical Reviews in Eukaryotic Gene Expression* **24,** 15–28 (2014).

264.   Luo, X. & Kraus, W. L. On PAR with PARP: cellular stress signaling through poly(ADP-ribose) and PARP-1. *Genes & Development* **26,** 417–432 (2012).

265.   Murata, M. M., Kong, X., Moncada, E., Chen, Y., Imamura, H., Wang, P., Berns, M. W., Yokomori, K. & Digman, M. A. NAD+ consumption by PARP1 in response to DNA damage triggers metabolic shift critical for damaged cell survival. *Molecular Biology of the Cell* **30,** 2584–2597 (2019).

266.   Smulson, M. E., Simbulan-Rosenthal, C. M., Boulares, A. H., Yakovlev, A., Stoica, B., Iyer, S., Luo, R., Haddad, B., Wang, Z. Q., Pang, T., Jung, M., Dritschilo, A. & Rosenthal, D. S. Roles of poly(ADP-ribosyl)ation and PARP in apoptosis, DNA repair, genomic stability and functions of p53 and E2F-1. *Advances in Enzyme Regulation* **40,** 183–215 (2000).

267.   Boulares, A. H., Yakovlev, A. G., Ivanova, V., Stoica, B. A., Wang, G., Iyer, S. & Smulson, M. Role of Poly(ADP-ribose) Polymerase (PARP) cleavage in apoptosis: caspase 3-resistant PARP mutant increases rates of apoptosis in transfected cells. *Journal of Biological Chemistry* **274,** 22932–22940 (1999).

268.   Makin, G. & Hickman, J. A. Apoptosis and cancer chemotherapy. *Cell and Tissue Research* **301,** 143–152 (2000).

269.   Melo, F. D. S. E., Vermeulen, L., Fessler, E. & Medema, J. P. Cancer heterogeneity - a multifaceted view. *EMBO Reports* **14,** 686–695 (2013).

270.   Bousbaa, H. Novel anticancer strategies. *Pharmaceutics* **13,** 275 (2021).

271.   Kalathiya, U., Padariya, M. & Baginski, M. Molecular modeling and evaluation of novel dibenzopyrrole derivatives as telomerase inhibitors and potential drug for cancer therapy. *Transactions on Computational Biology and Bioinformatics* **11,** 1198–1207 (2014).

272.   Dimri, G. P., Lee, X., Basile, G., Acosta, M., Scott, G., Roskelley, C., Medrano, E. E., Linskens, M., Rubelj, I. & Pereira-Smith, O. A biomarker that identifies senescent human cells in culture and in aging skin in vivo. *Proceedings of the National Academy of Sciences of the USA* **92,** 9363–9367 (1995).

273.   Liu, X., Shan, K., Shao, X., Shi, X., He, Y., Liu, Z., Jacob, J. A. & Deng, L. Nanotoxic effects of silver nanoparticles on normal HEK-293 cells in comparison to cancerous HeLa cell line. *International Journal of Nanomedicine* **16,** 753–761 (2021).

274.   Ridd, K., Dhir, S., Smith, A. G. & Gant, T. W. Defective TPA signalling compromises HaCat cells as a human in vitro skin carcinogenesis model. *Toxicology In Vitro* **24,** 910–915 (2010).

275.   Coelho, M., Moz, M., Correia, G., Teixeira, A., Medeiros, R. & Ribeiro, L. Antiproliferative effects of β-blockers on human colorectal cancer cells. *Oncology Reports* **33,** 2513–2520 (2015).

276.   Shen, Y., Vignali, P. & Wang, R. Rapid profiling cell cycle by flow cytometry using concurrent staining of DNA and mitotic markers. *Bio Protocol* **7,** e2517 (2017).

277.   Li, S., Cooper, V., Thonhauser, T., Lundqvist, B. & Langreth, D. Stacking interactions and DNA intercalation. *The Journal of Physical Chemistry B* **113,** 11166–72 (2009).

278.   McKnight, R. E., Gleason, A. B., Keyes, J. A. & Sahabi, S. Binding mode and affinity studies of DNA-binding agents using topoisomerase I DNA unwinding assay. *Bioorganic & Medicinal Chemistry Letters* **17,** 1013–1017 (2007).

279.   Fernald, K. & Kurokawa, M. Evading apoptosis in cancer. *Trends in cell biology* **23,** 620 (2013).

280.   Elmore, S. Apoptosis: A review of programmed cell death. *Toxicologic pathology* **35,** 495 (2007).

281.   Häcker, G. The morphology of apoptosis. *Cell and Tissue Research* **301,** 5–17 (2000).

282.   Doonan, F. & Cotter, T. G. Morphological assessment of apoptosis. *Methods* **44,** 200–204 (2008).

283.   Engeland, M., Nieland, L. J., Ramaekers, F. C., Schutte, B. & Reutelingsperger, C. P. Annexin V-affinity assay: a review on an apoptosis detection system based on phosphatidylserine exposure. *Cytometry* **31,** 1–9 (1998).

284.   Tait, S. W. G. & Green, D. R. Mitochondrial regulation of cell death. *Cold Spring Harbor Perspectives in Biology* **5,** a008706 (2013).

285.   Kari, S., Subramanian, K., Altomonte, I. A., Murugesan, A., Yli-Harja, O. & Kandhavelu, M. Programmed cell death detection methods: a systematic review and a categorical comparison. *Apoptosis* **27,** 482–508 (2022).

286.	Elefantova, K., Lakatos, B., Kubickova, J., Sulova, Z. & Breier, A. Detection of the mitochondrial membrane potential by the cationic dye JC-1 in L1210 cells with massive overexpression of the plasma membrane ABCB1 drug transporter. *International Journal of Molecular Sciences* **19,** 1985 (2018).

287.	Sivandzade, F., Bhalerao, A. & Cucullo, L. Analysis of the mitochondrial membrane potential using the cationic JC-1 dyeas a sensitive fluorescent probe. *Bio-protocol* **9,** e3128 (2019).

288.	Panda, S., Behera, S., Alam, M. F. & Syed, G. H. Endoplasmic reticulum & mitochondrial calcium homeostasis: The interplay with viruses. *Mitochondrion* **58,** 227–242 (2021).

289.	Bonora, M. & Pinton, P. The mitochondrial permeability transition pore and cancer: molecular mechanisms involved in cell death. *Frontiers in Oncology* **4,** 302 (2014).

290.	Wong, R., Steenbergen, C. & Murphy, E. Mitochondrial permeability transition pore and calcium handling. *Methods in Molecular Biology* **810,** 235–242 (2012).

291.	Garrido, C., Galluzzi, L., Brunet, M., Puig, P. E., Didelot, C. & Kroemer, G. Mechanisms of cytochrome c release from mitochondria. *Cell Death Differ* **13,** 1423–1433 (2006).

292.	Von Ahsen, O., Waterhouse, N. J., Kuwana, T., Newmeyer, D. D. & Green, D. R. The 'harmless' release of cytochrome c. *Cell Death Differ* **7,** 1192–1199 (2000).

293.	Kluck, R. M., Bossy-Wetzel, E., Green, D. R. & Newmeyer, D. D. The release of cytochrome c from mitochondria: A primary site for Bcl-2 regulation of apoptosis. *Science* **275,** 1132–1136 (1997).

294.	Lim, M. L. R., Lum, M.-G., Hansen, T. M., Roucou, X. & Nagley, P. On the release of cytochrome c from mitochondria during cell death signaling. *Journal of Biomedical Science* **9,** 488–506 (2002).

295.	McIlwain, D. R., Berger, T. & Mak, T. W. Caspase functions in cell death and disease. *Cold Spring Harbor Perspectives in Biology* **5,** 1–28 (2013).

296.	Sun, G. Death and survival from executioner caspase activation. *Seminars in Cell & Developmental Biology* **156,** 66–73 (2024).

297.	Brentnall, M., Rodriguez-Menocal, L., De Guevara, R. L., Cepero, E. & Boise, L. H. Caspase-9, caspase-3 and caspase-7 have distinct roles during intrinsic apoptosis. *BMC Cell Biology* **14,** 32 (2013).

298.	Sevrioukova, I. F. Apoptosis-inducing factor: structure, function, and redox regulation. *Antioxidants & Redox Signaling* **14,** 2545–2579 (2011).

299.	O'Brien, M. A. & Kirby, R. Apoptosis: A review of pro-apoptotic and anti-apoptotic pathways and dysregulation in disease. *Journal of Veterinary Emergency and Critical Care* **18,** 572–585 (2008).

300.	Daugas, E., Nochy, D., Ravagnan, L., Loeffler, M., Susin, S. A., Zamzami, N. & Kroemer, G. Apoptosis-inducing factor (AIF): a ubiquitous mitochondrial oxidoreductase involved in apoptosis. *FEBS Letters* **476,** 118–123 (2000).

301.   Bano, D. & Prehn, J. H. M. Apoptosis-inducing factor (AIF) in physiology and disease: The tale of a repented natural born killer. *EBioMedicine* **30,** 29–37 (2018).

302.   Eskes, R., Desagher, S., Antonsson, B. & Martinou, J.-C. Bid Induces the oligomerization and insertion of Bax into the outer mitochondrial membrane. *Molecular and Cellular Biology* **20,** 929–935 (2000).

303.   Billen, L. P., Shamas-Din, A. & Andrews, D. W. Bid: a Bax-like BH3 protein. *Oncogene* **27,** 93–104 (2008).

304.   LC, C., BJ, M. & NJ, W. Detection of DNA Fragmentation in Apoptotic Cells by TUNEL. *Cold Spring Harbor protocols* **2016,** 900–905 (2016).

305.   Jeyapalan, J. C. & Sedivy, J. M. Cellular senescence and organismal aging. *Mechanisms of Ageing and Development* **129,** 467–474 (2008).

306.   Ewald, J. A., Desotelle, J. A., Wilding, G. & Jarrard, D. F. Therapy-induced senescence in cancer. *Journal of the National Cancer Institute* **102,** 1536–1546 (2010).

307.   Roninson, I. B. Tumor cell senescence in cancer treatment. *Cancer Research* **63,** 2705–2715 (2003).

308.   Lee, S. F., Hirpara, J. L., Qu, J., Yadav, S. K., Sachaphibulkij, K. & Pervaiz, S. Identification of a novel catalytic inhibitor of topoisomerase II alpha that engages distinct mechanisms in p53wt or p53−/− cells to trigger G2/M arrest and senescence. *Cancer Letters* **526,** 284–303 (2022).

309.   Lee, B. Y., Han, J. A., Im, J. S., Morrone, A., Johung, K., Goodwin, E. C., Kleijer, W. J., DiMaio, D. & Hwang, E. S. Senescence-associated beta-galactosidase is lysosomal beta-galactosidase. *Aging Cell* **5,** 187–195 (2006).

310.   Dandu, R., Zulli, A. L., Bacon, E. R., Underiner, T., Robinson, C., Chang, H., Miknyoczki, S., Grobelny, J., Ruggeri, B. A., Yang, S., Albom, M. S., Angeles, T. S., Aimone, L. D. & Hudkins, R. L. Design and synthesis of dihydroindazolo[5,4-a]pyrrolo[3,4-c]carbazole oximes as potent dual inhibitors of TIE-2 and VEGF-R2 receptor tyrosine kinases. *Bioorganic & Medicinal Chemistry Letters* **18,** 1916–1921 (2008).

311.   Gingrich, D. E., Reddy, D. R., Iqbal, M. A., Singh, J., Aimone, L. D., Angeles, T. S., Albom, M., Yang, S., Ator, M. A., Meyer, S. L., Robinson, C., Ruggeri, B. A., Dionne, C. A., Vaught, J. L., Mallamo, J. P., & Hudkins, R. L. A new class of potent vascular endothelial growth factor receptor tyrosine kinase inhibitors: structure-activity relationships for a series of 9-alkoxymethyl-12-(3-hydroxypropyl)indeno[2,1-a]pyrrolo[3,4-c]carbazole-5-ones and the identification of CEP-5214 and its dimethylglycine ester prodrug clinical candidate CEP-7055. *Journal of Medicinal Chemistry* **46,** 5375–5388 (2003).

312.   Hou, S., Yi, Y. W., Kang, H., Zhang, L., Kim, H., Kong, Y., Liu, Y., Wang, K., Kong, H., Grindrod, S., Bae, I. & Brown, M. Novel carbazole inhibits phospho-STAT3 through Induction of protein-tyrosine phosphatase PTPN6. *Journal of Medicinal Chemistry* **57,** 6342-6353 (2014).

313. Shchemelinin, I., Sefc, L. & Necas, E. Protein kinases, their function and implication in cancer and other diseases. *Folia Biologica* **52,** 81–100 (2006).

314. Roskoski, R. A historical overview of protein kinases and their targeted small molecule inhibitors. *Pharmacological Research* **100,** 1–23 (2015).

315. Kim, H.-J., Lin, D., Lee, H.-J., Li, M. & Liebler, D. C. Quantitative profiling of protein tyrosine kinases in human cancer cell lines by multiplexed parallel reaction monitoring assays. *Molecular & Cellular Proteomics* **15,** 682–691 (2016).

316. Gocek, E., Moulas, A. N. & Studzinski, G. P. Non-receptor protein tyrosine kinases signaling pathways in normal and cancer cells. *Critical Reviews in Clinical Laboratory Sciences* **51,** 125–137 (2014).

317. K Bhanumathy, K., Balagopal, A., Vizeacoumar, F. S., Vizeacoumar, F. J., Freywald, A. & Giambra, V. Protein tyrosine kinases: Their roles and their targeting in leukemia. *Cancers* **13,** 184 (2021).

318. Zappa, C. & Mousa, S. A. Non-small cell lung cancer: current treatment and future advances. *Translational Lung Cancer Research* **5,** 288–300 (2016).

319. Van Der Jeught, K., Xu, H. C., Li, Y. J., Lu, X. B. & Ji, G. Drug resistance and new therapies in colorectal cancer. *World Journal of Gastroenterology* **24,** 3834–3848 (2018).

320. Arlt, A., Vorndamm, J., Breitenbroich, M., Fölsch, U. R., Kalthoff, H., Schmidt, W. E. & Schäfer, H. Inhibition of NF-κB sensitizes human pancreatic carcinoma cells to apoptosis induced by etoposide (VP16) or doxorubicin. *Oncogene* **20,** 859–868 (2001).

321. Pastor, N., Domínguez, I., Luís Orta, M., Campanella, C., Mateos, S. & Cortés, F. The DNA topoisomerase II catalytic inhibitor merbarone is genotoxic and induces endoreduplication. *Mutation Research* **738-739,** 45–51 (2012).

322. Bau, J. T., Kang, Z., Austin, C. A. & Kurz, E. U. Salicylate, a catalytic inhibitor of topoisomerase II, inhibits DNA cleavage and is selective for the α isoform. *Molecular Pharmacology* **85,** 198–207 (2014).

323. Toyoda, E., Kagaya, S., Cowell, I. G., Kurosawa, A., Kamoshita, K., Nishikawa, K., Iiizumi, S., Koyama, H., Austin, C. A. & Adachi, N. NK314, a topoisomerase II inhibitor that specifically targets the α isoform. *Journal of Biological Chemistry* **283,** 23711–23720 (2008).

324. Line Auzanneau, C., Le Montaudon, D., Mi Jacquet, R., Phane Puyo, S., Pouysé, L., Deffieux, D., Elkaoukabi-Chaibi, A., De Giorgi, F. & Pourquier, P. The polyphenolic ellagitannin vescalagin acts as a preferential catalytic inhibitor of the α isoform of human DNA topoisomerase II. *Molecular Pharmacology* **82,** 134-141 (2012).

325. Ortega, J. A., Arencibia, J. M., Minniti, E., Byl, J. A. W., Franco-Ulloa, S., Borgogno, M., Genna, V., Summa, M., Bertozzi, S. M., Bertorelli, R., Armirotti, A., Minarini, A., Sissi, C., Osheroff, N. & De

Vivo, M. Novel, potent, and druglike tetrahydroquinazoline inhibitor that is highly selective for human topoisomerase II α over β. *Journal of Medicinal Chemistry* **63,** 12873–12886 (2020).

326.   Sajewicz, W. & Dlugosz, A. Cytotoxicity of some potential DNA intercalators (carbazole, acridine and anthracene derivatives) evaluated through neutrophil chemiluminescence. *Journal of Applied Toxicology* **20,** 305–312 (2000).

327.   Shaikh, M., Karpoormath, R., Thapliyal, N., Rane, R., Palkar, M., Faya, A. M., Patel, H., Alwan, W., Jain, K. & Hampannavar, G. Current perspective of natural alkaloid carbazole and its derivatives as antitumor agents. *Anti-cancer agents in medicinal chemistry* **15,** 1049–1065 (2015).

328.   Das, A., Mohammed, T. P., Kumar, R., Bhunia, S. & Sankaralingam, M. Carbazole appended trans-dicationic pyridinium porphyrin finds supremacy in DNA binding/photocleavage over a non-carbazolyl analogue. *Dalton Transactions* **51,** 12453–12466 (2022).

329.   Denny, W. A. & Baguley, B. C. Dual topoisomerase I/II inhibitors in cancer therapy. *Current Topics in Medicinal Chemistry* **3,** 339–353 (2003).

330.   Salerno, S., Da Settimo, F., Taliani, S., Simorini, F., La Motta, C., Fornaciari, G. & Marini, A. M. Recent advances in the development of dual topoisomerase I and II inhibitors as anticancer drugs. *Current Medicinal Chemistry* **17,** 4270–4290 (2010).

331.   Delord, J.-P., Bennouna, J., Diéras, V., Campone, M., Lefresne, F., Aslanis, V. & Douillard, J.-Y. First-in-man study of tafluposide, a novel inhibitor of topoisomerase I and II. *Molecular Cancer Therapeutics* **6,** 3380 (2007).

332.   Sargent, J. M., Elgie, A. W., Williamson, C. J. & Hill, B. T. Ex vivo effects of the dual topoisomerase inhibitor tafluposide (F 11782) on cells isolated from fresh tumor samples taken from patients with cancer. *Anticancer Drugs* **14,** 467–473 (2003).

333.   Ortega, J. A., Riccardi, L., Minniti, E., Borgogno, M., Arencibia, J. M., Greco, M. L., Minarini, A., Sissi, C. & De Vivo, M. Pharmacophore hybridization to discover novel topoisomerase II poisons with promising antiproliferative activity. *Journal of Medicinal Chemistry* **61,** 1375–1379 (2018).

334.   Schwartz, G. K. & Shah, M. A. Targeting the cell cycle: a new approach to cancer therapy. *Journal of Clinical Oncology* **23,** 9408–9421 (2005).

335.   Jeon, K. H., Park, S., Jang, H. J., Hwang, S. Y., Shrestha, A., Lee, E. S. & Kwon, Y. Ak-i-190, a new catalytic inhibitor of topoisomerase II with anti-proliferative and pro-apoptotic activity on androgen-negative prostate cancer cells. *International Journal of Molecular Sciences* **22,** 11246 (2021).

336.   Bergant Loboda, K., Janežič, M., Štampar, M., Žegura, B., Filipič, M. & Perdih, A. Substituted 4,5′-bithiazoles as catalytic inhibitors of human DNA topoisomerase IIα. *Journal of Chemical Information and Modeling* **60,** 3662–3678 (2020).

337.   Kang, K., Nho, C. W., Kim, N. D., Song, D. G., Park, Y. G., Kim, M., Pan, C. H., Shin, D., Oh, S. H. & Oh, H. S. Daurinol, a catalytic inhibitor of topoisomerase IIα, suppresses SNU-840 ovarian cancer cell proliferation through cell cycle arrest in S phase. *International Journal of Oncology* **45,** 558–566 (2014).

338.   Chen, L., Zhu, X., Zou, Y., Xing, J., Gilson, E., Lu, Y. & Ye, J. The topoisomerase II catalytic inhibitor ICRF-193 preferentially targets telomeres that are capped by TRF2. *American Journal of Physiology - Cell Physiology* **308,** 372–377 (2015).

339.   Liu, J., Geng, G., Liang, G., Wang, L., Luo, K., Yuan, J. & Zhao, S. A novel topoisomerase I inhibitor DIA-001 induces DNA damage mediated cell cycle arrest and apoptosis in cancer cell. *Annals of Translational Medicine* **8,** 89 (2020).

340.   Ferrara, L. & Kmiec, E. B. Camptothecin enhances the frequency of oligonucleotide-directed gene repair in mammalian cells by inducing DNA damage and activating homologous recombination. *Nucleic Acids Research* **32,** 5239–5248 (2004).

341.   Montero, A. J. & Jassem, J. Cellular redox pathways as a therapeutic target in the treatment of cancer. *Drugs* **71,** 1385–1396 (2011).

342.   Ozben, T. Oxidative stress and apoptosis: impact on cancer therapy. *Journal of Pharmaceutical Sciences* **96,** 2181–2196 (2007).

343.   Liou, G. Y. & Storz, P. Reactive oxygen species in cancer. *Free Radical Research* **44,** 479–496 (2010).

344.   Fulda, S. & Debatin, K. M. Extrinsic versus intrinsic apoptosis pathways in anticancer chemotherapy. *Oncogene* **25,** 4798–4811 (2006).

345.   Kolb, R. H., Greer, P. M., Cao, P. T., Cowan, K. H. & Yan, Y. ERK1/2 signaling plays an important role in topoisomerase ii poison-induced G2/M checkpoint activation. *PLoS ONE* **7,** e50281 (2012).

346.   Park, S. H., Lee, J., Kang, M. A., Jang, K. Y. & Kim, J. R. Mitoxantrone induces apoptosis in osteosarcoma cells through regulation of the Akt/FOXO3 pathway. *Oncology Letters* **15,** 9687 (2018).

347.   Khélifa, T. & Beck, W. T. Induction of apoptosis by dexrazoxane (ICRF-187) through caspases in the absence of c-Jun expression and c-Jun NH2-terminal kinase 1 (JNK1) activation in VM-26-resistant CEM cells. *Biochemical pharmacology* **58,** 1247–1257 (1999).

348.   Iguchi, K., Usami, Y., Hirano, K., Hamatake, M., Shibata, M. & Ishida, R. Decreased thymosin beta4 in apoptosis induced by a variety of antitumor drugs. *Biochemical pharmacology* **57,** 1105–1111 (1999).

349.   Alaaeldin, R., Abdel-Rahman, I. M., Ali, F. E. M., Bekhit, A. A., Elhamadany, E. Y., Zhao, Q.-L., Cui, Z.-G. & Fathy, M. Dual topoisomerase I/II inhibition-induced apoptosis and necro-apoptosis in

cancer cells by a novel ciprofloxacin derivative via RIPK1/RIPK3/MLKL activation. *Molecules* **27,** 7993 (2022).

350.   Wang, L. & Eastmond, D. A. Catalytic inhibitors of topoisomerase II are DNA-damaging agents: Induction of chromosomal damage by merbarone and ICRF-187. *Environmental and Molecular Mutagenesis* **39,** 348–356 (2002).

351.   Solier, S. & Pommier, Y. The nuclear γ-H2AX apoptotic ring: Implications for cancers and autoimmune diseases. *Cellular and Molecular Life Sciences* **71,** 2289–2297 (2014).

352.   Solier, S. & Pommier, Y. The apoptotic ring: a novel entity with phosphorylated histones H2AX and H2B and activated DNA damage response kinases. *Cell cycle* **8,** 1853–1859 (2009).

353.   Bhullar, K. S., Lagarón, N. O., McGowan, E. M., Parmar, I., Jha, A., Hubbard, B. P. & Rupasinghe, H. P. V. Kinase-targeted cancer therapies: progress, challenges and future directions. *Molecular Cancer* **17,** 48 (2018).

354.   Cardenas, M. E. & Gasser, S. M. Regulation of topoisomerase II by phosphorylation: a role for casein kinase II. *Journal of Cell Science* **104,** 219–225 (1993).

355.   Ma, Y. C., Wang, Z. X., Jin, S. J., Zhang, Y. X., Hu, G. Q., Cui, D. T., Wang, J. S., Wang, M., Wang, F. Q. & Zhao, Z. J. Dual Inhibition of topoisomerase II and tyrosine kinases by the novel bis-fluoroquinolone chalcone-like derivative HMNE3 in human pancreatic cancer cells. *PLoS ONE* **11,** e0162821 (2016).

PROFESSIONAL EXPERIENCE

October 2022 – November 2022	Instituto Universitario de Bio-Organica Antonio Gonzalez, BioLab Universidad de La Laguna **Research intern** **Project:** Fellowship "PROM" funded by European Union: PPI/PRO/2019/1/00009/U/00001 **Academic fellowship:** "Early pharmacological profiling of small molecules" Identification and evaluation of potential small molecule drugs with anticancer properties, employing advanced methodologies and cellular models.
January 2021 – October 2022	Department of Pharmaceutical Technology and Biochemistry, Faculty of Chemistry Gdansk University of Technology **Research fellow** **Project:** "Propolis and polyphenols derived from this product as potential antifungal agents". A grant from the National Centre of Science: UMO-2020/39/B/NZ7/02901
January 2021 – March 2021	Department of Pharmaceutical Technology and Biochemistry, Faculty of Chemistry Gdansk University of Technology **Research scientist** **Project:** "Technology of extraction of polyphenolic compounds in the production of raw materials for the production of dietary supplements and anticancer medical components". A grant from the National Centre for Research and Development: POIR.01.01.01-00-0353/17-00
April 2019 – April 2022	Department of Pharmaceutical Technology and Biochemistry Faculty of Chemistry Gdansk University of Technology **Research investigator** **Project:** "DNA topoisomerase inhibitors with acridine and acridone scaffold as novel antifungal agents". Grant from "IDUB - Inicjatywa Doskonałości - Uczelnia Badawcza": DEC-24/2020/IDUB/I.3.3
October 2018 – March 2022	Department of Pharmaceutical Technology and Biochemistry Faculty of Chemistry Gdansk University of Technology **Research investigator** **Project:** "New anticancer compounds interfering function of telomeres". Grant from National Centre for Research and Development: STRATEGMED3/306853/9/NCBR/2017

SCIENTIFIC ACHIEVEMENTS

Publication in Journals indexed by Journal Citation Report (list A)

<u>2018</u>

1. Ptaszyńska, N., Gucwa, K., Łęgowska, A., Dębowski, D., Gitlin-Domagalska, A., Lica J., Heldt, M., Martynow, D., **Olszewski, M.**, Milewski, S., Ng, T., Rolka, K. Antimicrobial activity of chimera peptides composed of Human Neutrophil Peptide 1 (HNP-1) truncated analogues and bovine lactoferrampin. Bioconjugate Chemistry 29(9), 3060-3071. (2018) https://doi.org/10.1021/acs.bioconjchem.8b00440. (**IF: 4.349; Q1**)

<u>2020</u>

2. Chylewska, A., Dąbrowska, A., Ramotowska, S., Maciejewska, N., **Olszewski, M.**, Bagiński, M., Makowski, M. The photosensitive and pH-dependent activity of pyrazine-functionalized carbazole derivative as a promising antifungal and imaging agent. Scientific Reports 10, 11767**.** (2020) https://doi.org/10.1038/s41598-020-68758-w (**IF: 4.379; Q1, 140 pkt MNiSW**)

<u>2021</u>

3. Rzad, K., Paluszkiewicz, E., Neubauer, D., **Olszewski, M.**, Kozlowska-Tylingo, K., Kamysz, W., Gabriel, I. The effect of conjugation with octaarginine, a cell-penetrating peptide on antifungal activity of imidazoacridinone derivative. International Journal of Molecular Sciences. 22(24), 13190. (2021) https://doi.org/10.3390/ijms222413190 (**IF: 6.208; Q1, 140 pkt MNiSW**)

<u>2022</u>

4. Maciejewska, N., **Olszewski, M.**, Jurasz, J., Serocki, M., Dzierzynska, M., Cekala, K., Wieczerzak, E., Baginski, M. Novel chalcone-derived pyrazoles as potential therapeutic agents for the treatment of non-small cell lung cancer. Scientific Reports 12, 3703. (2022) https://doi.org/10.1038/s41598-022-07691-6 (**IF: 4.6; Q1, 140 pkt MNiSW**)

5. Marković, S.M, Maciejewska, N., **Olszewski, M.**, Višnjevac, A., Puertad, A., Padrón, J. M., Novaković, I., Kojić, S., Fernandes, H. S., Sousag, S. F., Ramotowska, S., Chylewska, A., Makowski, M., Todorović, T. R., Filipović, N. R. Study of the anticancer potential of Cd complexes of selenazoyl-hydrazones and their sulphur isosters. European Journal of Medicinal Chemistry 238, 114449. (2022) https://doi.org/10.1016/j.ejmech.2022.114449 (**IF: 6.7; Q1, 140 pkt MNiSW**)

6. Witkowska, M., Maciejewska, N., Ryczkowska, M., **Olszewski, M.**, Baginski, M., Makowiec, M. From tryptophan to novel mitochondria-disruptive agent, synthesis and biological evaluation of 1,2,3,6-tetrasubstituted carbazoles. European Journal of Medicinal Chemistry 238, 114453**.** (2022) https://doi.org/10.1016/j.ejmech.2022.114453 (**IF: 6.7; Q1, 140 pkt MNiSW**)

7. Mech-Warda, P., Giełdoń, A., Kawiak, A., Maciejewska, N., **Olszewski, M.**, Makowski, M. Chylewska, A. Low-Molecular Pyrazine-Based DNA Binders: Physicochemical and Antimicrobial Properties. Molecules 27(12), 3704. (2022) https://doi.org/10.3390/molecules27123704 (**IF: 4.6; Q2, 140 pkt MNiSW**)

8. Ryczkowska, M., Maciejewska, N., **Olszewski, M.**, Witkowska, M., Makowiec, M. Design, synthesis, and biological evaluation of tetrahydroquinolinones and tetrahydroquinolines with anticancer activity. Scientific Reports 12, 9985. (2022) https://doi.org/10.1038/s41598-022-13867-x (**IF: 4.6; Q1, 140 pkt MNiSW**)

141

9. Ryczkowska, M., Maciejewska, N., **Olszewski, M.**, Witkowska, M., Makowiec, M. Tetrahydroquinolinone derivatives exert antiproliferative effect on lung cancer cells through apoptosis induction. Scientific Reports 12, 19076. (2022) https://doi.org/10.1038/s41598-022-23640-9 (**IF: 4.6; Q1, 140 pkt MNiSW**)

10. Maciejewska, N., **Olszewski, M.**, Jurasz, J., Baginski, M., Stasevych, M., Zvarych, V., Folini, M., Zaffaroni N. Teloxantron inhibits the processivity of telomerase with preferential DNA damage on telomeres. Cell Death & Disease 13, 1005. (2022) https://doi.org/10.1038/s41419-022-05443-y (**IF: 9; Q1, 140 pkt MNiSW**)

2023

11. Araškov, J. B., Maciejewska, N., **Olszewski, M.**, Višnjevac, A., Blagojević, V., Fernandes, H. S., Sousa, S. F., Puerta, A., Padrón, J. M., Holló, B. B., Monge, M., Rodríguez-Castillo, M., López-De-Luzuriaga, J. M., Uğuz, Özlem, Koca, A., Todorović, T. R., Filipovići, N. R. Structural, physicochemical and anticancer study of Zn complexes with pyridyl-based thiazolyl-hydrazones. Journal of Molecular Structure, 1281, 135157. (2023) https://doi.org/10.1016/j.molstruc.2023.135157 (**IF: 3.8; Q2, 70 pkt MNiSW**)

12. Kallingal, A., **Olszewski, M.**, Maciejewska, N., Brankiewicz, W., Bagiński. M. Cancer immune escape: the role of antigen presentation machinery. Journal of Cancer Research and Clinical Oncology 4, 2023. (2023) https://doi.org/10.1007/s00432-023-04737-8 (**IF: 3.6; Q2, 100 pkt MNiSW**)

13. Rząd, K., Ioannidi, R., Marakos, P., Pouli, N., **Olszewski, M.**, I. Kostakis, K., Gabriel, I. Xanthone synthetic derivatives with high anticandidal activity and positive mycostatic selectivity index values. Scientific Reports 13, 11893. (2023) https://doi.org/10.1038/s41598-023-38963-4 (**IF: 4.6; Q1, 140 pkt MNiSW**)

14. Ćurčić, V., **Olszewski, M.**, Maciejewska, N., Višnjevac, A., Srdić-Rajić, T., Dobričić, V., García-Sosa, A. T., Kokanov, S. B., Araškov, J. B., Silvestri, R., Schüle, R., Jung, M., Nikolić, M., & Filipovići, N. R. Quinoline-based thiazolyl-hydrazones target cancer cells through autophagy inhibition. Archiv Der Pharmazie 357(2) e2300426. (2023). https://doi.org/10.1002/ardp.202300426 (**IF: 5.1; Q2, 70 pkt MNiSW**)

15. **Olszewski, M.**, Stasevych M., Zvarych, V., Maciejewska, N. 9,10-Dioxoanthracenyldithiocarbamates effectively inhibit the proliferation of non-small cell lung cancer by targeting multiple protein tyrosine kinases. Journal of Enzyme Inhibition and Medicinal Chemistry 39(1), 2284113. (2023). https://doi.org/10.1080/14756366.2023.2284113 (**IF: 5.6; Q1, 140 pkt MNiSW**)

2024

16. Kowalik, M., Masternak, J., **Olszewski, M.**, Maciejewska, N., Kazimierczuk, K., Sitkowski, J., Dąbrowska. A., Chylewska, A., Makowski, M. Anticancer study on IrIII and RhIII half-sandwich complexes with bipyridylsulfonamide ligand. Inorganic Chemistry 63(2), 1296-1316. (2024) https://doi.org/10.1021/acs.inorgchem.3c03801(**IF: 4.6; Q1, 140 pkt MNiSW**)

17. **Olszewski, M.**, Maciejewska, N., Kallingal, Chylewska, A., Dąbrowska, A., Biedulska, M., Makowski, M., Padrón, J.M., Baginski, M. Palindromic carbazole derivatives: unveiling their antiproliferative effect via topoisomerase II catalytic inhibition and apoptosis induction. Journal of Enzyme Inhibition and Medicinal Chemistry 39(1), 2302920. (2024). https://doi.org/10.1080/14756366.2024.2302920 (**IF: 5.6; Q1, 140 pkt MNiSW**)

18. Rząd, K., Gabriel, I., Paluszkiewicz, E., Kuplińska, A., **Olszewski, M.**, Chylewska, A., Dąbrowska, A., Kozłowska-Tylingo, K. Targeting yeast topoisomerase II by imidazo and triazoloacridinone derivatives resulting in their antifungal activity. Scientific Reports (accepted 10.02.2024), (2024). (**IF: 4.6; Q1, 140 pkt MNiSW**)

Conference poster presentations

1. **Olszewski, M.**, Maciejewska, N., Serocki M., Jurasz, J., Baginski, M., Stasevych, M., Zvarych, V., Novikov, V., Novel derivatives of anthracenedione as in inhibitors of tyrosine kinase protein. EFMC-YMCS 6th EFMC Young Medicinal Chemist Symposium, Athens, Greece, 05-06.09.2019

2. **Olszewski, M.,** N. Serocki, M., Baginski, M., Stasevych, M., Zvarych, V., Novikov, V., Biological evaluation of new anthraquinone derivatives as anticancer agents. VII EFMC International Symposium on Advances in Synthetic and Medicinal Chemistry, Athens, Greece, 01-04.09.2019

3. **Olszewski, M.**, Maciejewska, N., Baginski, M., Novel symmetric derivatives of carbazole with a dual mechanism of action: inhibition of DNA Topoisomerase IIα and protein tyrosine kinases. Congress - Innovative Cancer Science: Translating Biology to Medicine, Seville, Spain, 20-23.06.2022

Contribution to poster authorship

1. Ptaszyńska, N., Gucwa, K., Łęgowska, A., Dębowski, D., Gitlin-Domagalska, A., Lica J., Heldt, M., Martynow, D., **Olszewski, M**., Milewski, S., Ng, T., Rolka, K. Antimicrobial activity of chimera peptides composed of Human Neutrophil Peptide 1 (HNP-1) truncated analogs and bovine lactoferrampin. 35th European Peptide Symposium, Dublin, Ireland, 26-31.08.2018

2. Maciejewska, N., Serocki M., **Olszewski, M.**, Jurasz, J., Baginski, M., Stasevych, M., Zvarych, V., Novikov, V., New anticancer compounds with dual mechanisms of action as inhibitors of tyrosine kinase protein and telomerase: in silico studies and biological evaluation. EFMC-YMCS 6th EFMC Young Medicinal Chemist Symposium, Athens, Greece, 05-06.09.2019

3. Serbakowska, K., Maciejewska, N., Heldt, M., **Olszewski M.**, Baginski, M., Makowiec, S., In silico design of new carbazole derivatives as a telomerase catalytic subunit inhibitors. Systems approaches in cancer EMBO Workshop, Split, Croatia, 21-26.09.2021

4. Maciejewska, N., **Olszewski, M.**, Baginski, M., Discovery of new pyrazole derivatives disrupting microtubule assembly, Congress - Innovative Cancer Science: Translating Biology to Medicine. Seville, Spain, 20-23.06.2022

5. Rzad, K., Kondaka, K., **Olszewski, M.**, Paluszkiewicz, E., Kozlowska-Tylingo, K., Gabriel, I. Acridines as antifungal agents – topoisomerase II targeting. 4th ISFMS - Biochemistry, Molecular Biology and Druggability of Proteins, Florence, Italy, 06-09.09.2022

6. Brankiewicz, W., Serocki, M., Wojciechowski, W., **Olszewski, M.**, Serbakowska, K., Drab, M., Milewski, S., Baginski, M., Marintsova, N., Polish, N. DNA topoisomerases II-alpha as molecular targets for novel aminopyrazolonaphthoquinones molecules in breast cancer treatment. National network for breast cancer research. Trømso, Norway, 09-11.09.2022